Titre: Title:	The Effects of Intracortical Microstimulation Parameters on Neural Responses
Auteur: Author:	Meghan Chelsea Watson
Date:	2015
Type:	Mémoire ou thèse / Dissertation or Thesis
Référence: Citation:	Watson, M. C. (2015). The Effects of Intracortical Microstimulation Parameters on Neural Responses [Ph.D. thesis, École Polytechnique de Montréal]. PolyPublie. https://publications.polymtl.ca/1878/

UNIVERSITÉ DE MONTRÉAL

THE EFFECTS OF INTRACORTICAL MICROSTIMULATION PARAMETERS ON NEURAL RESPONSES

MEGHAN CHELSEA WATSON

INSTITUT DE GÉNIE BIOMÉDICAL

ÉCOLE POLYTECHNIQUE DE MONTRÉAL

THÈSE PRÉSENTÉE EN VUE DE L'OBTENTION

DU DIPLÔME DE PHILOSOPHIAE DOCTOR

(GÉNIE BIOMÉDICAL)

SEPTEMBRE 2015

UNIVERSITÉ DE MONTRÉAL

ÉCOLE POLYTECHNIQUE DE MONTRÉAL

Cette thèse intitulée :

THE EFFECTS OF INTRACORTICAL MICROSTIMULATION PARAMETERS ON NEURAL RESPONSES

présentée par : WATSON Meghan Chelsea

en vue de l'obtention du diplôme de : Philosophiae Doctor

a été dûment acceptée par le jury d'examen constitué de :

M. SAVARD Pierre, Ph. D., président

M. SAWAN Mohamad, Ph. D., membre et directeur de recherche

M. DANCAUSE Numa, Ph. D., membre et codirecteur de recherche

M. MATHIEU Pierre-A., D.Sc.A., membre

M. CHAPMAN Andrew C., Ph. D., membre externe

ACKNOWLEDGEMENTS

I would like to thank my supervisor Mohamad Sawan and co-supervisor Numa Dancause for their guidance and support during this PhD program, and Dr. Mathieu, Dr. Savard and Dr. Chapman for evaluating this thesis.

I would also like to express my gratitude to all the individuals who facilitated my research and training and contributed to my experience as a graduate student. I am especially grateful to those individuals who helped teach me the skills I have learned in this position which I will carry with me for a lifetime. In particular, I would like to thank Boris Touvykine for helping me with my surgeries, Eleonore Serrano, Ian Moreau Debord and Stephan Quessy for their support during my training, Kelsey Dancause and Guillaume Elgbeilli for consulting on statistical analysis, Philippe Drapeau for his assistance programming the stimulation equipment, and my family and friends for supporting me in my efforts.

This work was supported by the Canada Research Chair in Smart Medical Devices to Mohamad Sawan, and the National Sciences and Engineering Research Council of Canada Discovery grant to Numa Dancause. Additionally, I held a doctoral research scholarship from the Fonds de Recherche du Québec - Nature et Technologies (FRQNT) (2013-2014).

RÉSUMÉ

Les microstimulations de tissues nerveux du cerveau sont utilisés dans un grand nombre de prothèses sensorielles, de thérapies cliniques et autres activités de recherche se servant de la stimulation électrique. Actuellement, les paramètres de stimulation sont adaptés à chaque application via des tests itératifs. Les méthodes d'optimisation cherchent à améliorer les stimuli développés pour des objectifs spécifiques de stimulation, mais la compréhension fondamentale de la façon dont les paramètres de stimulation influencent les circuits neuronaux qu'ils activent reste largement incomplète. Ce déficit retarde l'optimisation de protocoles existants et rend le développement de nouvelles applications de stimulation difficile. À ce jour, un certain nombre de dispositifs prothétiques validés dès les années 1970 restent en développement, principalement en raison de l'incapacité de ces dispositifs à communiquer efficacement avec le cerveau. Pour utiliser la stimulation électrique afin de transmettre des messages au système nerveux central, une meilleure conception du patron du signal de stimulation est nécessaire. Dans cette thèse, nous étudions l'influence que chaque paramètre du signal (un courant constant, symétrique carré biphasique) exerce sur les réponses qu'il évoquées au travers des microstimulations de la zone intracorticale caudale du membre antérieur dans le cortex moteur chez le rat. Les paramètres de ce signal sont l'amplitude du courant, la fréquence et la durée d'impulsion, l'intervalle d'interphase et la durée du train. Leurs effets ont été évalués par un examen des réponses électromyographiques évoquées dans les muscles des membres antérieurs du rat en réponse à chaque stimulus. Les principaux résultats décrivent comment chaque paramètre de stimulation influence l'amplitude, la latence d'apparition et la durée de la réponse. Une composante jusque-là inexplorée du signal de la réponse (que nous appelons 'activation résiduelle') est aussi analysée pour la première fois. Les théories quant à l'origine et le mécanisme neuronal sous-jacent de ce phénomène sont proposés et les paramètres de stimulation touchant son apparition, la prévalence et la durée sont décrits. La fiabilité des signaux de stimulation pour évoquer des réponses cohérentes est également évaluée par rapport aux variations de paramètres. Une méthodologie pour la conception optimisée des signaux de stimulation est proposée en utilisant un modèle de calcul simple, représentant les relations d'entrée-sortie entre les paramètres de stimulation et les réponses qu'ils évoquent. Ce modèle utilise une approche de réseau neuronal artificiel et peut être utilisé pour prédire les propriétés de la réponse lorsque les paramètres du stimulus sont connus. Compte tenu de la prévalence de la stimulation cérébrale dans les applications cliniques, de

recherche et thérapeutiques, les procédures méthodologiques et de modélisation proposées ont des implications importantes dans l'optimisation des paradigmes de stimulation actuels et le développement de protocoles de stimulation pour de nouvelles applications.

ABSTRACT

Microstimulation of brain tissue plays a key role in a variety of sensory prosthetics, clinical therapies and research applications. At present, stimulus parameters are tailored to each application via iterative testing. Computational optimization methods seek to improve tried and tested waveforms developed for specific purposes, however the fundamental understanding of how stimulation parameters influence the neural circuits they activate remains widely unknown. This deficit hinders both the optimization of existing protocols and the development of new stimulation applications. To date, a number of prosthetic devices validated as early as the 1970's linger in the development stages largely due to the inability to effectively interface these devices with the brain. In order to use electrical stimulation to convey messages to the central nervous system, a better understanding of stimulus signal design is required. In this thesis, I investigate the influence that each parameter of the constant-current, symmetric, biphasic square waveform exerts on the responses it evokes through intracortical microstimulation of the caudal forelimb area of the rat motor cortex. The parameters under investigation include the current amplitude, pulse frequency, pulse duration, interphase interval and train duration of the stimulus and effects were assessed by examining the electromyographic responses evoked in the rat forelimb muscles in response to each stimulus. The major findings describe how each parameter of the stimulus signal influences the magnitude, onset latency, and duration of the response. A previously unexplored component of the response signal (which we called 'residual activation') is analyzed for the first time. Hypotheses as to the origin and underlying neural mechanism of this phenomenon are proposed and the stimulus parameters affecting its occurrence, prevalence and duration are described. The reliability of stimulation signals for evoking consistent responses is also assessed with respect to parameter variations. A methodology for the informed design of stimulation signals is proposed and aided by the development of a simple computational model representing the input-output relationships between stimulation parameters and the responses they evoke. This model uses an artificial neural network approach and can be used to predict the properties of the response when the parameters of the stimulus are known. Given the prevalence of brain stimulation in clinical, research and therapeutic applications the proposed methodological and modeling procedures have important implications in the optimization of current stimulation paradigms and the development of stimulation protocols for new applications.

TABLE OF CONTENTS

LIST OF TABLES

LIST OF FIGURES

LIST OF SYMBOLS AND ABBREVIATIONS

AF	Amplitude and frequency pairing
AI	Amplitude and interphase interval pairing
ANN	Artificial neural network
AP	Amplitude and pulse duration pairing
AT	Amplitude and train duration pairing
CFA	Caudal forelimb area
DBS	Deep brain stimulation
EEG	Electroencephalography
EMG	electromyography
FA	Frequency and amplitude pairing
FFN	Feed forward neural network
FI	Frequency and interphase interval pairing
fMRI	Functional magnetic resonance imaging
FP	Frequency and pulse duration pairing
FT	Frequency and train duration pairing
GPi	Globus pallidus interna
HFLD-ICMS	High frequency long duration intracortical microstimulation
HFSD-ICMS	High frequency short duration intracortical microstimulation
ICMS	Intracortical microstimulation
IW	Input weights
LW	Layer weights
M1	Primary motor cortex
MATLAB	Matrix laboratory (software)

MDS-UPDRS	Movement disorder society unified Parkinson's disorder rating scale
MEP	Motor evoked potential
MSE	Mean square error
MT	Middle temporal area of visual cortex
PA	Pulse duration and amplitude pairing
PF	Pulse duration and frequency pairing
PI	Pulse duration and interphase interval pairing
PT	Pulse duration and train duration pairing
IA	Interphase interval and amplitude pairing
IF	Interphase interval and frequency pairing
IP	Interphase interval and pulse duration pairing
IT	Interphase interval and train duration pairing
RNN	Recurrent neural network
SE	Standard error
SPSS	Statistical package for the social sciences (software)
STN	Subthalamic nucleus
TA	Train duration and amplitude pairing
TF	Train duration and frequency pairing
TI	Train duration and interphase interval pairing
TP	Train duration and pulse duration pairing
V1	Primary visual cortex

LIST OF APPENDICES

CHAPTER 1 INTRODUCTION

Electrical stimulation of the brain serves as the foundation for a variety of clinical therapies, sensory prosthetics and research applications. In the clinical setting, brain stimulation is used to alleviate symptoms of Parkinson's disease (Bronstein et al., 2011) and epilepsy (Fisher, 2012) and applications for the treatment of Huntington's disease, cluster headaches, Tourette's syndrome, chronic pain, major depression, schizophrenia, obsessive compulsive disorder, multiple sclerosis, and Alzheimer's disease are currently being explored (Lyons, 2011; Sironi, 2011).

Recently, sensory prosthetics have been developed to restore lost functioning or augment normal perception. Electrical stimulation of the somatosensory cortex produces tactile sensations which can restore a sense of touch to a prosthetic limb user (Berg et al., 2013; Kim, Callier, Tabot, Tenore, & Bensmaia, 2015; Tabot et al., 2013), and it has been postulated that this stimulation could also serve to extend the normal range of perception (Thomson, Carra, & Nicolelis, 2013). Similar efforts have been made to restore sight to the blind by applying electrical stimulation to the visual cortex (Bartlett et al., 2005; Brindley, 1973; Brindley, 1982; Brindley & Lewin, 1968; Dobelle & Mladejovsky, 1974; Penfield & Perot, 1963; Schmidt et al., 1996; Tehovnik, Slocum, Smirnakis, & Tolias, 2009). Stimulation of the visual cortex produces punctate visual percepts which can be activated in patterns to form a representation of the visual field similar to a scoreboard or highly pixelated image.

Countless research applications involving many different regions of the brain use electrical stimulation to explore the function and connectivity of neural circuits or attempt to disrupt or augment normal brain processes. Stimulation delivered to middle temporal area (MT) of the visual cortex can be used to bias motion correlation detection (Murasugi, Salzman, & Newsome, 1993; Salzman, Britten, & Newsome, 1990; Salzman, Murasugi, Britten, & Newsome, 1992) and stimulating the superior colliculus can bias or induce saccadic eye movements (Horwitz & Newsome, 2001; Schiller & Stryker, 1972). Electrical stimulation of the auditory cortex can induce the perception of tones (Otto, Rousche, & Kipke, 2005; Penfield & Perot, 1963), visual cortex stimulation produces visual percepts (Dobelle & Mladejovsky, 1974; Penfield & Perot, 1963; Schmidt et al., 1996), and motor cortex stimulation can evoke muscle contractions or movements (Donoghue & Wise, 1982; Gioanni & Lamarche, 1985; Penfield & Boldrey, 1937).

Despite the prevalence and inherent value of brain stimulation as both a therapeutic method and research tool, little is known about how the electrical stimulus shapes the responses it evokes. Most applications are developed through trial and error and rely heavily on stimulation signals which have proved successful in previous experiments. The work contained in this thesis sought to address this knowledge deficit by exploring the manner in which the parameters of the electrical stimulation signal affect the responses they evoke. The research conducted in this thesis was part of a larger ongoing project of the Polystim Neurotechnologies research group at Ecole Polytechnique de Montreal led by Dr. Mohamad Sawan which seeks to develop an intracortical visual prosthetic device to restore functional vision to the blind. My work aimed to address the issue of interfacing a prosthetic device with the brain by determining how stimulation signals should be designed in order to support effective communication between the device and the brain.

The expertise in neural systems and brain stimulation was provided through a collaborative effort with the laboratory of Dr. Numa Dancause of the Universite de Montreal's Department of Neuroscience. The Dancause laboratory focuses in part on the study of primary motor control of movements in the rat model. This collaboration allowed me to study the influence that each parameter of an electrical stimulus exerts on the responses they evoke while working within a well-documented cortical circuit of moderate complexity.

1.1 Objectives

The main objectives of this thesis were to determine how a stimulation signal shapes the responses it evokes and to uncover the general relationships between stimulation inputs and response outputs for neural systems. This problem was approached by addressing the following specific objectives:

a) Review past stimulation experiments to determine the most prevalent type of stimulus signals, the functional ranges of each signal parameter and previously identified parameter effects.

b) Design experiments to systematically test the effects of each parameter of a stimulus signal on the evoked responses.

c) Propose a stimulus design methodology based on the parameter effects to aid in the optimization of existing stimulation paradigms and facilitate the development of new paradigms.

d) Model the input-output relationship between stimulation parameters (input) and evoked responses (output) to provide a tool for the informed design of stimulation signals.

1.2 Synthesis of content

Chapter 2 of this thesis addresses objectives (a) and (b) through extensive review of past stimulation experiments conducted in a wide variety of species and brain areas for many different applications. Initially, the rat motor cortex system is discussed in terms of its suitability for conducting systematic tests of parameter effects. Once the choice of system and species has been justified, the most prevalent stimulation signals and choice of signal type are described. Following this, the broader technical considerations which must be taken into account when designing a stimulus are covered, then the known effects of stimulation parameters discovered in past studies involving intracortical microstimulation and macrostimulation are reviewed. To conclude chapter 2, a brief summary of the findings is presented to set the stage for the experimental work of the following chapters.

Chapters 3-5 address objectives (b) and (c) through the experimental study of stimulus parameter influence on evoked response properties. Each parameter of the stimulation signal is described in terms of its ability to influence the evoked response's magnitude, onset latency, duration, and reliability. In these chapters, the beginnings of a design methodology are proposed.

Chapter 6 addresses objectives (c) and (d) through the development of a computational model describing the input-output relationship between stimulus parameters and the responses they evoke. The model describes the general relationships between the stimulus parameters and the evoked response metrics and can be used for both the optimization of existing paradigms and the development of new ones. The model serves to consolidate the work of chapters 3-5 and proposes an official methodology for the design of stimulation signals.

1.3 Contributions

The main contributions of this thesis are reported in three articles submitted to peer-reviewed journals and one conference paper. A summary of the major contributions is as follows:

1) Identification of the most commonly used brain stimulation signal parameters in a multitude of clinical and research applications. These parameter ranges were obtained from a comprehensive review of the literature and a subset of these values was selected for testing in the experimental work.

2) Thorough documentation of the specific effects of stimulus parameters on the amplitude, onset latency, duration and reliability of the responses evoked by intracortical microstimulation of the rat motor cortex. This contribution required original research involving systematic experimental testing conducted in animal models and provided specific information about the effects of intracortical microstimulation in the rat motor cortex. These findings were also interpreted generally to describe the effect each stimulus parameter exerted on neural activation in general in order to be extended to other applications.

3) Improved optimization of the standard motor cortex stimulus in the rat model. In the course of our studies we discovered that the commonly accepted signal for movement generation in the caudal forelimb region of the rat could be further optimized.

4) Quantification and assessment of a previously undocumented component of the evoked response signal. We observed that certain stimuli produced responses with activity that persists after the termination of the main response component. We named this persistent activity “residual activation”, and to our knowledge, this component has not been systematically analyzed previously. We documented its characteristics and occurrence with respect to the stimulus parameters that induce it and provided possible interpretations of its origin and neural underpinnings.

5) Methodology for stimulus design. We proposed a shift in the approach to stimulus design in which we seek to avoid conventional trial and error approaches and instead employ a two step process based on insights gained during experimentation pertaining to the general effects of stimulus parameters on neural activation. In this process we first consider the neural

activation required to achieve a specific goal of stimulation and then determine the stimulation parameters required to induce the necessary neural activation.

6) Artificial neural network (ANN) model of the input-output relationships between stimulation parameters and the responses they evoke. We provide a model for predicting the effects of stimulation parameters on evoked responses as a tool for designing stimulation signals. This model can be used directly in the rat motor cortex system and we also detail its extension to a number of applications. To our knowledge this is the first application of ANN modeling applied to the input-output relationships of brain stimulation.

CHAPTER 2 LITERATURE REVIEW

This review contains a theoretical study of past brain stimulation experiments and was conducted for the purposes of developing a series of experiments to systematically test the effects of stimulus parameters on the responses they evoke. This survey led to the discovery of a number of discrepancies and knowledge deficits to be addressed in order to develop a methodology for stimulation design. To overcome these knowledge deficits it was deemed prudent to first establish the general effects of stimulation parameters using a neural circuit of moderate complexity in as low of a mammal species as possible. In this chapter, the neural system, species and stimulus signal selected for the series of experiments are described and their selection is justified. Following this, the broader technical considerations for stimulus signal design are outlined and the known effects of stimulation parameters in a variety of different applications, species and brain regions are reviewed. The outcomes of this survey are the identification of prevalent stimulation signals and the definition of ranges for each stimulus parameter encompassing the values used for a wide variety of stimulation applications.

2.1 Rat motor cortex system

One of the earliest and most documented uses of brain stimulation involves the activation of motor cortex regions to evoke muscle contractions or movements (Penfield & Boldrey, 1937; Penfield & Welch, 1951; Sironi, 2011). Stimulation applied to specific regions of the motor cortex has been shown to evoke movements in humans (Penfield & Welch, 1951), primates (Asanuma, Arnold, & Zarzecki, 1976), cats (Armstrong & Drew, 1984) and rodents (Donoghue & Wise, 1982; Sanderson, Welker, & Shambes, 1984). The motor cortex exhibits a somatotopic organization in which a specific cortical region corresponds to a specific area of the body. Much study has been devoted to mapping the correlation between regions of the motor cortex and the areas of the body they control (Gioanni & Lamarche, 1985; Neafsey et al., 1986; Penfield & Boldrey, 1937; Rouiller, Moret, & Liang, 1993; Schieber, 2001). Of the systems described, the rodent motor system has the simplest structure and the rat forelimb region in particular has been studied extensively to probe function, connectivity and motor deficits.

For the purposes of our study, a system was required that produced clearly defined and measurable outputs in response to stimulation in an extensively documented neural circuit that was responsive to the parameter ranges most commonly used in clinical and research applications. The rat forelimb system proved to be a system which met all of these requirements. When electrical stimulation is applied to the forelimb region of the rat motor cortex, it activates corticospinal neurons which project from the cortex to the spinal cord. Within the spinal cord these efferent neurons are indirectly connected to the motor neurons which innervate the forelimb muscle fibers. When these fibers are activated they produces muscle contractions or limb movements and the corresponding electromyographic (EMG) responses can be recorded directly from the muscles of the forelimb (Figure 2-1 parts (a) and (b)). Working within this system allowed me to deliver a variety of stimulation signals to the cortex and record the evoked EMG responses. Analysis of the properties of the EMG signals provided quantitative measurements of the influence that stimulation parameters exert on the responses they evoke. Figure 2-1c depicts basic examples of the EMG response variations that occurred for different stimulation signals.

2.2 Stimulation signals

Historically, two basic types of stimulation signal have been proven to stimulate the brain in a safe and efficacious manner (Hill, 1936; Lilly, 1961; Lilly, Hughes, Alvord, & Galkin, 1955; Merrill, Bikson, & Jefferys, 2005). These signals are all variations of the square pulse waveform and are depicted in Figure 2-2. The biphasic waveforms depicted in parts (a) and (b) are the most commonly used in clinical and therapeutic applications of intracortical microstimulation because they employ charge balancing to avoid damaging the tissues. The monophasic waveforms depicted in parts (c) and (d) are more prevalently used in research applications (particularly terminal acute experiments) in which tissue damage is not a primary concern since these signals are more effective at evoking responses (Merrill et al., 2005). The parameters of interest in these signals include pulse polarity (anodic, cathodic, anode-leading, cathode-leading), amplitude, frequency, duration and train duration, as well as the duration of the delay between pulses of opposite phases (interphase interval) in the case of biphasic stimulation.

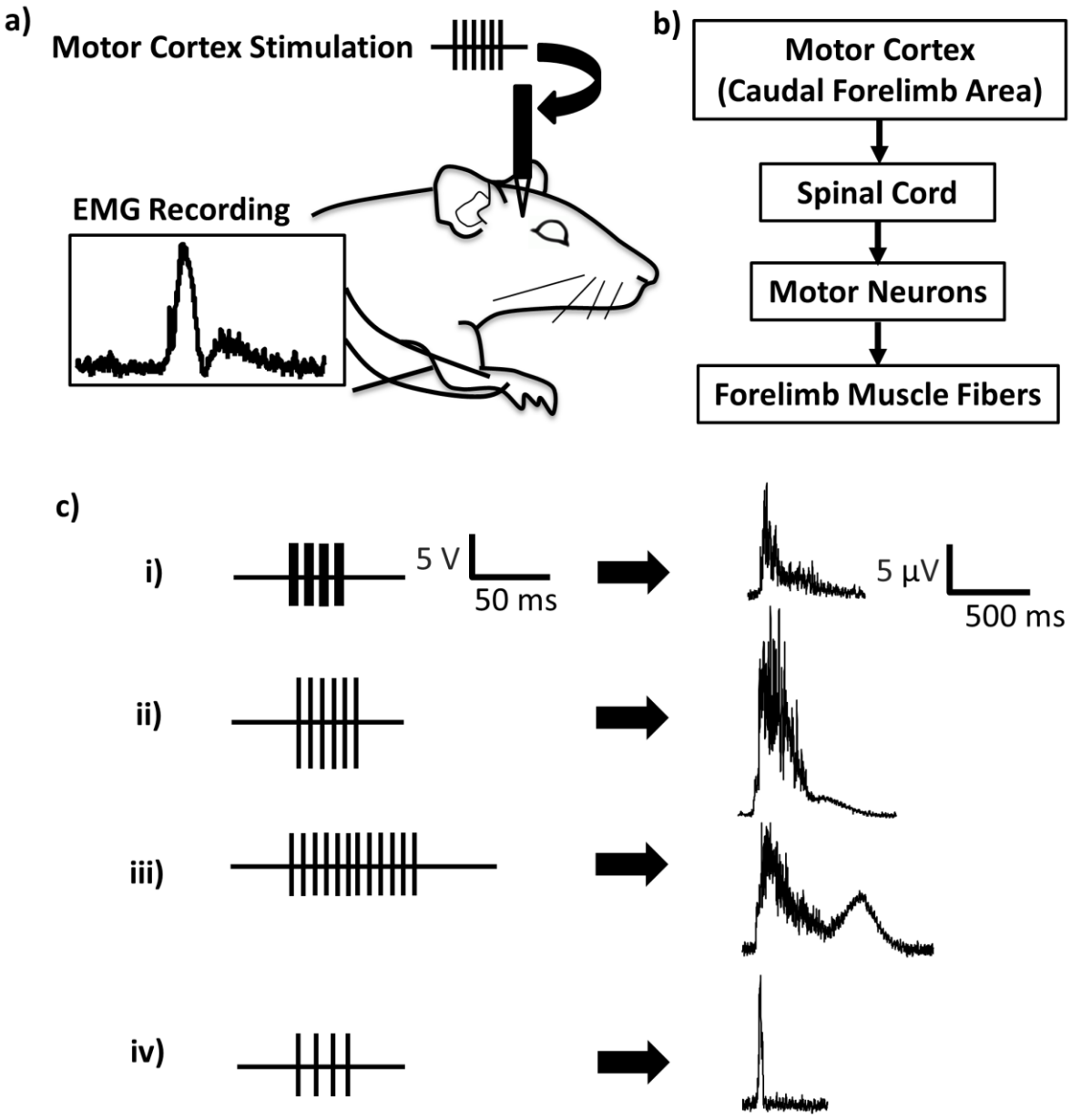

Figure 2-1: Experimental design: rat motor cortex circuitry, system inputs and outputs. Part (a) depicts the experimental paradigm in which stimulation is applied to the forelimb region of the motor cortex producing muscle contractions from which the EMG responses are recorded. Part (b) details the transmission of the electrical stimulus from the cortex to the forelimb. Part (c) shows the variability in EMG responses that occur when the stimulation parameters are varied by

(i), increasing the pulse duration (ii), increasing the amplitude (iii) increasing the train duration, or (iv) reducing the frequency of the stimulus.

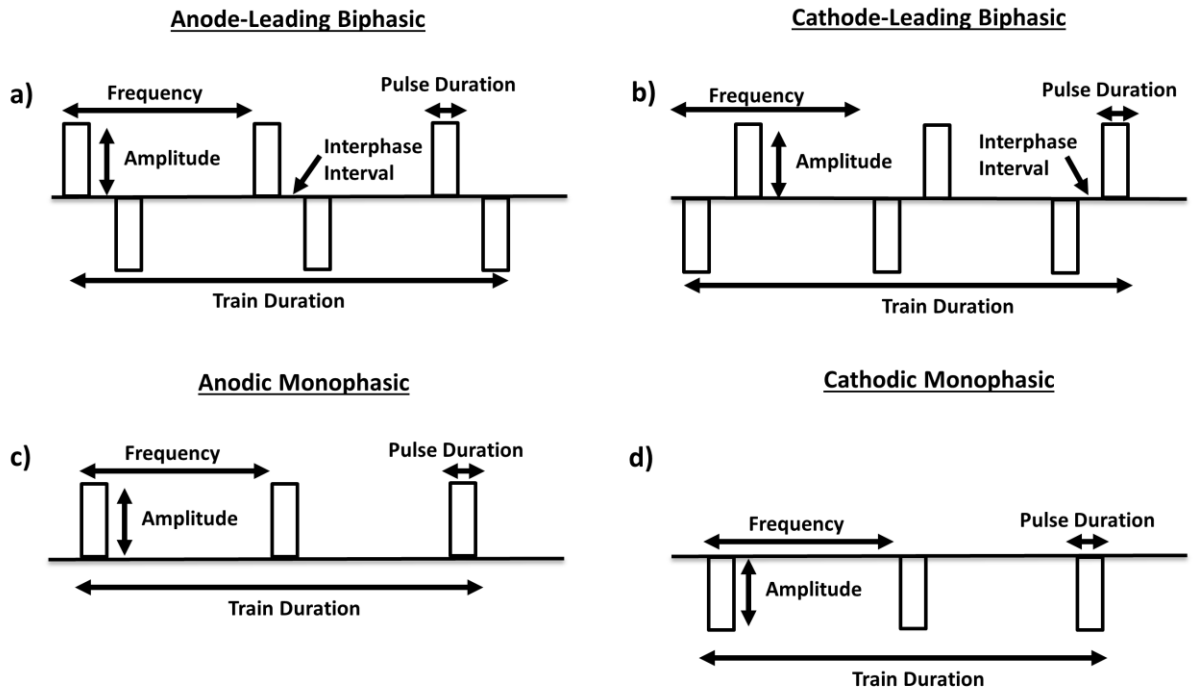

Figure 2-2: Common stimulation signals. The four most common types of stimulation signals are depicted in parts (a)-(d) and their respective parameters are displayed. These signals can be employed with either current or voltage control.

2.2.1 Current vs. voltage controlled waveforms

The choice between current-controlled and voltage-controlled stimulation has long plagued microstimulation experiments and continues to be an issue in prosthetic devices currently undergoing clinical trials such as the retinal and deep brain stimulation (DBS) prosthetics. Current controlled stimulation is more commonly used in microstimulation experiments since it is less sensitive to variations in impedance and allows for greater control over the number of neurons activated. However it also produces long discharge transients after each pulse which exacerbates stimulus artifacts (Gerdle, Karlsson, Day, & Djupsjobacka, 1999). These artifacts prevent recording from the tissues surrounding the stimulating electrode, and most likely produce interference between electrodes in the case of multi-electrode stimulation. Provided that our goal is to optimize the stimulation signal, the issue of stimulation artifacts may not be crucial;

however the artifact implies some degree of abnormal neuronal activation. Current clinical trials in DBS have failed to find any appreciable difference between the two modes of stimulation (Del Rio-Oliva et al., 2012) although some believe current-controlled stimulation minimizes the effects of impedance changes (Lempka, Johnson, Miocinovic, Vitek, & McIntyre, 2010). A study conducted in dissociated cultures found cathode-leading biphasic voltage controlled pulses to be the most effective stimuli (Wagenaar, Pine, & Potter, 2004), however the applicability of these findings to in-vivo experiments remains uncertain. A number of modeling studies have recently been conducted to evaluate the performance differences between the two types of stimulation (Savage & Halpern, 2011; Stecker, 2004) however this remains an unresolved issue. In order to avoid sensitivity to the impedance variations which occur during repetitive stimulation and to ensure highly localized activation I chose to use current controlled waveforms.

2.2.2 Pulse polarity

Cathodal pulses have significantly lower thresholds for nerve excitation (Reilly, 2011b). They have been shown to be more effective than anodal pulses for producing phosphenes with microstimulation (Ranck, 1975; Schmidt et al., 1996), and are more effective for evoking forelimb movements in the rat (Nudo, Jenkins, & Merzenich, 1990). When negative current is injected into the tissue, the negative internal charge of the neuronal cell becomes positive in relation to its surroundings. This shift in membrane potential, known as depolarization, induces action potentials and allows for signal transmission. Anodal pulses are thought to be more effective for delivering surface stimulation (Ranck, 1975), despite inconclusive results (Dobelle & Mladejovsky, 1974). When positive current is injected into the tissue, the negative internal charge of the neuronal cell becomes more negative in relation to its surroundings. This shift in membrane potential, known as hyperpolarization, inhibits action potentials. Cathodal pulses however are known to produce a larger volume of exited tissue which is not always desirable (Reilly, 2011b). For the purposes of this study cathodal or cathode-leading signals were chosen due to their greater ability to evoke neural excitation at cortical depths.

2.2.3 Monophasic vs. biphasic waveforms

Monophasic stimulation (stimulation of only one pulse polarity) has been shown to produce a charge buildup at the electrode/tissue interface leading to electrode corrosion, tissue damage and

eventually cortical lesions (Hanson, Fitzsimmons, & O'Doherty, 2008; Merrill et al., 2005). These effects can be avoided by using biphasic stimulation to prevent electrode polarization through charge balancing in order to avoid electrochemical reactions (Reilly, 2011a; Tehovnik, Slocum, Carvey, & Schiller, 2005). While the alternating polarity of the biphasic signal does avoid tissue and electrode damage it also impairs tissue excitation making stimulation less effective and tends to activate a greater volume of tissue (Kombos et al., 1999; Reilly, 2011a). Reduced excitation and larger current spread are both undesirable properties of biphasic stimulation; however these effects are preferable to the induction of tissue damage which occurs in the monophasic case. The most effective biphasic waveforms tend to use a cathodal pulse to evoke the desired excitation followed by an anodal pulse designed to reverse any Faradic processes occurring at the electrode tip by providing and equal and opposite charge (Lilly et al., 1955; Merrill et al., 2005). Leading with the more efficacious cathodal pulse helps to achieve the desired activation with lower amplitudes of stimulation, and the anodal counterpart serves to implement charge reversal. As our study was designed to explore the effects of stimulation parameters commonly used in clinical and therapeutic applications which require the use of biphasic waveforms to avoid tissue damage, the cathode-leading biphasic square waveform was chosen.

2.2.4 Alternative waveforms

Several studies have been conducted that explore modifications to the biphasic square waveform structure. The chopped pulse is a biphasic waveform which splits each phase into a series of smaller pulses. This waveform was previously investigated for stimulation of the auditory nerve (Shepherd & Javel, 1999) revealing much lower thresholds for chopped waveforms than their biphasic equivalents. Similarly, the triphasic pulse waveform is designed to have an extra phase which serves to produce an overall charge balance while reducing the negative effect of phase reversal. This approach has been examined for stimulation of the auditory nerve within a cochlear implant system (Bahmer & Baumann, 2012; Bahmer, Peter, & Baumann, 2010; Schoesser, H., Zierhofer, C., & Hochmair, E.S., 2001; Shepherd & Javel, 1999) and this configuration was shown to effectively reduce the stimulus artifact typically generated after electrical stimulation with a biphasic waveform. Asymmetric pulse waveforms maintain the biphasic shape while varying the duration and amplitude of each phase. The principal of operation is similar to the

triphasic in that the overall charge balance is maintained while mitigating the effect of phase reversal. Neural stimulation models (McIntyre & Grill, 2000, 2002), and cochlear implant research (Macherey, van Wieringen, Carlyon, Deeks, & Wouters, 2006; van Wieringen, Macherey, Carlyon, Deeks, & Wouters, 2008) have shown that asymmetric waveforms might serve to lower detection threshold levels. The effect of waveform asymmetry has also been explored in auditory cortex by varying the lead phase direction, level of asymmetry and phase duration while maintaining charge balance (Koivuniemi & Otto, 2011). Cathode phase duration was found to be the most important factor in predicting threshold level, and phase asymmetry did not have a significant effect.

Several alternatives to the standard square waveform have been suggested in the literature but have not yet been thoroughly explored. These include triangular, sinusoidal, exponential, and energy efficient waveforms. A computer model of both intracellular and extracellular stimulation was developed to evaluate different types of waveforms for use in deep brain stimulation (Foutz & McIntyre, 2010). They compared a range of charge balanced biphasic waveforms with rectangular, exponential, triangular, Gaussian and sinusoidal stimulus pulse shapes and discovered that in some cases the triangular pulse decreases energy consumption, and pointed to the necessity of optimizing non-rectangular pulses. A similar study (Wongsarnpigoon & Grill, 2010) used a genetic algorithm coupled to a computational model of extracellular stimulation of a mammalian myelinated axon to determine the energy-optimal waveform shape for neural stimulation. With no constraints, the algorithm produced waveforms resembling truncated Gaussian curves. When evaluating the best shape of a monophasic cathodic waveform the algorithm suggested waves that were symmetric. When considering rectangular charge-balanced biphasic pulses, the order of occurrence of the pulses (cathode first/anode first) and sharpness of the cathodic peak varied according to the duration and timing of the anodic phase. While these alternative stimulation waveforms are valid and deserve further study, they are not suitable to the present study whose goals are to explore the general parameter effects of commonly used stimulation signals.

2.2.5 Signal selected for present study

Since very little work has been conducted to define the input-output relationships between stimulus parameters and the responses they evoke it was important to keep the complexity of the

signal to a minimum. For the purposes of this study the parameters of the cathode-leading, constant-current, symmetric biphasic square pulse waveform were examined. This signal is the most commonly used waveform in therapeutic and clinical applications and it is effective in the rat motor cortex system as well. The choice of current control avoids impedance variation sensitivity and ensures highly localized activation at the electrode site. The biphasic structure avoids tissue damage through charge balancing as is required for clinical applications, while the cathode-leading design ensures adequate activation and serves to lower the threshold levels.

2.3 Technical considerations of stimulus design

This section details a number of issues related to stimulation of the cortex which deserve special consideration during the process of stimulus design. These issues include: stimulation induced tissue damage, electrode interactions, electrode configuration and current spread. The various parameters which influence these factors are described.

2.3.1 Stimulation induced tissue damage

For a stimulation device to function properly we must preserve the integrity of the interfacing surfaces. The electrode and its surrounding cortical tissue can be damaged by the reactions that occur at the electrode-electrolyte interface. The saline environment of the brain has a corrosive effect on the electrode surface and the stimulation current can subject the electrode to further degradation through oxidation (Crist & Lebedev, 2008; McCarthy, Otto, & Rao, 2011). These processes can increase the concentration of ions in the surrounding tissue which can be toxic to the tissue or affect the functional properties of the electrode in addition to shortening its lifespan (Neuman, 1998). These reactions can exacerbate the immune response and promote the formation of a glial scar encapsulating the electrode (Polikov, Tresco, & Reichert, 2005). As such, we seek to use non-reactive materials such as noble metals, stainless steel, silicon and polymers as electrode materials to minimize these reactions and employ biocompatible/neurotrophic coatings (Crist & Lebedev, 2008; Hanson et al., 2008). Bio-coatings and insulation in general serve to reduce the immune response and avoid encapsulation.

A change of material is not always sufficient to avoid reactions that can lead to tissue damage. At the electrode tip, high current density can result in electrolysis which produces hydrogen or oxygen gas in the tissue environment inflicting damage by altering the pH (Neuman, 1998;

Tehovnik et al., 2005). Sharp tips easily puncture the cortex and reduce cortical depression during insertion (Hanson et al., 2008), however they reduce surface area at the tip. Reducing tip area reduces the amount of current needed to activate the tissue but also increases the current density at the tip which can lead to tissue damage. However, current density at the electrode tip is responsible for the activation of the neural elements we seek to stimulate and unexcitable neurons require fairly high densities for activation (Tehovnik et al., 2005), thus the effects of current density cannot be mediated by material and shape selection alone.

Stimulation parameters heavily influence the effectiveness and longevity of an implanted electrode. The current threshold for detectable nerve damage was determined to depend on a number of stimulus factors Continuous stimulation of peroneal nerves in cats using 400 μA pulses delivered at 50 Hz caused irreversible neural damage after 48 hours of stimulation. The endoneurial edema resulting from the stimulation progressed to early axonal degeneration 1 week after stimulation. Neural damage could however be mitigated by reducing the duration of stimulation, the frequency of stimulation or using an intermittent duty cycle (Agnew, McCreery, Yuen, & Bullara, 1989).

The threshold for neural injury was determined to result from the combined effects of charge density and charge per phase and work done in the cat parietal cortex determined these parameters interact over the range of 10 to 800 $\mu C/cm^2$ and 0.05 to 5.0 μC respectively (McCreery, Agnew, Yuen, & Bullara, 1990). The threshold for nerve damage in the sciatic nerve of cats was found to be higher for stimuli with short pulse durations (50 μs) and interphase intervals (0 ms), than those with longer pulse durations (100 μs) and interphase intervals (400 μs) (McCreery, Agnew, Yuen, & Bullara, 1992). Further studies in the cat sciatic nerve demonstrated when stimulus frequency is raised from 50 Hz to 100 Hz, the relationship between early axonal degeneration and stimulus amplitude is exaggerated, and the threshold at which degeneration occurs is reduced. At low frequencies (20 Hz) there was no relationship between axonal degeneration which suggests that low frequencies may not induce damage even at high amplitudes (McCreery, Agnew, Yuen, & Bullara, 1995).

Additionally, the length of stimulation time must be considered. Levels which do not produce damage in a single trial can begin to have effects with repeated stimulation at the same site. Despite careful design, parameters commonly used in neurophysiology and neuroprosthetics

research can still cause histological damage after many hours of stimulation, and can lead to cell death in as little as 250 trials of a stimulation experiment (Murasugi et al., 1993). If an implanted array is to survive the environment of the brain and effectively stimulate the tissue, both the physical electrode and stimulation it delivers must be designed in such a way as to reduce or avoid all sources of tissue damage.

2.3.2 Electrode interactions

Electrodes for cortical implants are typically arranged in an array format with equal spacing between electrodes. Standard commercially available devices can contain up to 96 electrodes with standard lengths varying from 0.5-1.5 mm and a standard electrode spacing of 400 μm (Rousche & Normann, 1999). Many applications require highly localized activation focused around the electrode site and spread of the stimulation signal is undesirable. In the case of visual prosthetic devices, each electrode is responsible for eliciting one phosphene, and separations greater than 0.5 mm evoke separate phosphenes when stimulating area V1 with currents less than 30 μA (Schmidt et al., 1996). Stimulation must be designed to ensure a phosphene is separate and distinct from those produced at neighbouring electrodes at close separations. The intention is to activate the neurons in a small area of cortex, particularly the dimensions of the V1 hypercolumn (1 mm x 0.7 mm) which is thought to be the functional unit of phosphene induction (Tehovnik & Slocum, 2007). If the stimulation is stronger than dictated by electrode spacing and hypercolumn width, it will produce phosphenes which overlap causing the percepts to blend into one larger representation. In the case of motor cortex stimulation to evoke movements, if the stimulus signal causes significant spread of activation it can induce movements in multiple muscle groups, particularly if the signal spreads across the borders in the somatotopic representation. Stimulation signals can be designed to activate single muscles with highly localized stimulation (single forelimb muscle), groups of muscles with larger spreading activation (multiple forelimb muscles), and unrelated muscle groups if the stimulus spreads across representations (for example, simultaneous forelimb and whisker movements).

2.3.3 Electrode configuration

The spread of activation can also be controlled by the configuration of the electrodes delivering stimulation. Standard neural stimulation equipment employs monopolar or bipolar electrode

arrangements. The monopolar arrangement uses a stimulating electrode (of either polarity) and a distant reference electrode, whereas the bipolar configuration consists of two electrodes in close proximity of opposite polarity in an attempt to restrict the electric field produced by stimulation (Dokos, Suaning, & Lovell, 2005; Joarder, Dokos, Suaning, & Lovell, 2007). The arrangement focuses the electric field between the electrodes to limit the spatial extent of the activation; however the area of activation is effectively increased since the neurons contacting the return electrode are also stimulated (Lovell, Dokos, Cloherty, Preston, & Suaning, 2005). Auditory physiologists have found the field of activation around the electrode to be more focused going from monopolar to bipolar to tripolar stimulation (Bierer & Middlebrooks, 2002, 2004; Kral, Hartmann, Mortazavi, & Klinke, 1998; Snyder, Bierer, & Middlebrooks, 2004) however the lowest current threshold for neural excitation occurs with monopolar stimulation (Tehovnik & Slocum, 2007).

Recent literature has proposed alternative electrode configurations. The hexpolar configuration surrounds the stimulating electrode with six "guard" electrodes arranged in a hexagonal shape which act as a combined return and localize the tissue activation by "guarding" the spread of current (Habib, Cameron, Suaning, Lovell, & Morley, 2012). The same lab has developed a quasi-monopolar stimulation strategy using this configuration to activate the hex-guard electrodes and the monopolar electrode simultaneously which serves to lower the activation threshold (Matteucci et al., 2012). They have also modeled the response of a retinal ganglion cell to stimulation in this configuration (Abramian, Lovell, Morley, Suaning, & Dokos, 2012). This configuration and its associated stimulation strategies deserve further investigation but will not be addressed here.

2.3.4 Current spread

Confining microstimulation to a specific region helps to focus its effects and limits disruptions to nearby cortical circuitry. When areas outside the region of interest are activated, the effect of the stimulation can be reduced or altered in an often unpredictable manner. Extensive study in motor cortex has led to an equation to describe the relationship between the current required to activate a neuron (I) and the distance (r) between the neuron and the electrode: $I=Kr^2$, where K is a constant (Ranck, 1975; Stoney, Thompson, & Asanuma, 1968). This relationship can be used to predict the area activated by a specific current level, and suggests that confining activity to one

hypercolumn requires current amplitudes less than 100 μA (Hubel & Wiesel, 1977; LeVay, Connolly, Houde, & Van Essen, 1985).

Neurophysiology experiments frequently design a microstimulation stimulus to match a visual stimulus. For example, the electrical stimulus equivalent of a random dot patch visual stimulus is the activation of a middle temporal area (MT) neuron whose preferred direction matches the direction of visual motion (Salzman et al., 1992). The parameters of stimulation are designed so that the behavioral response obtained with the electrical stimulation matches the behavioral response obtained with the visual stimulation. Despite this careful design, neurorecording experiments have shown that the activity produced by microstimulation is very different from that produced by an equivalent visual stimulus (Masse & Cook, 2009). The behavioural results of these experiments have revealed that microstimulation effects are longer lasting with the ability to affect perception for several hundred milliseconds after it stops.

Multiple fMRI studies have shown the calculation of current spread to underestimate the volume of activated tissue for both visual and electrical stimulation; however the discrepancy is much greater for electrical stimulation (Logothetis et al., 2010; Sultan, Augath, & Logothetis, 2007; Tolias et al., 2005). The difference between the calculated and experimental values may be due to the difference in stimulation parameters used defining each, which further emphasizes the need for a common methodology. However, the discrepancy between visual and electrical stimulation is thought to be partially due to the spatiotemporal properties of the stimulus.

The greater variability consistent with visual stimuli is thought to result in asynchronous neural activation, whereas the uniformity of electrical stimulation leads to neural synchrony capable of producing larger responses (Sultan et al., 2007). Current spread may be in part due to the synchrony of activation provided by stimulation, however it is also likely to result from the interconnectivity of cortical tissue which allows for transynaptic activation of neurons nearby those directly stimulated (Tolias et al., 2005). Effective stimulation parameters are necessary to limit these effects and control both the spatial and temporal interference microstimulation imposes on the natural function of cortical circuitry.

2.4 Known effects of intracortical microstimulation parameters

This section details the known effects of intracortical microstimulation parameters documented in past studies in order to gain insight on the general effects of stimulus parameters. To our knowledge, no studies exist which have systematically explored the general effects of stimulation parameters on the responses they evoke; however some efforts have been made to optimize the parameters of stimulation signals for their specific purposes. In the absence of systematic studies, it becomes necessary to review stimulation experiments designed for a variety of different species, systems and applications in order to gain insight pertaining to parameter effects. This review focuses on intracortical microstimulation (ICMS) experiments which use a small electrode (microelectrode) for stimulation of visual, auditory, somatosensory and motor cortical areas. The most commonly used signal is the constant-current, biphasic square waveform. The findings are discussed in terms of the parameters of this signal which include the pulse amplitude, frequency, and duration as well as the interphase interval and train duration. This section concludes with a table (Table 2-1) summarizing the ranges of stimulus parameters used in different regions of the brain for various applications.

2.4.1 Visual cortex

Very few studies have been conducted using intracortical microstimulation of the visual cortex in human subjects. During a brief experiment performed while three awake human subjects were undergoing surgery, the ICMS thresholds for phosphene induction were tested (Bak et al., 1990). Due to time constraints of the surgery, parameters were not examined systematically and these results pertain to a mixture of cathode-leading and anode-leading stimulations. Stimulation was delivered as a constant current, capacitor-coupled waveform of biphasic pulses with 0.2 ms phase duration, delivered at 100 pulses/second, for duration of 1s. Phosphene threshold current amplitudes ranged between 35-300 μA and phosphenes tended to become brighter and smaller as current amplitude increased.

In one of the only long-term studies conducted in the visual cortex of a human subject, 38 microelectrodes were implanted near the pole of the right occipital cortex of a blind woman with no light perception (Schmidt et al., 1996). Visually robust phosphenes were produced using cathodic-first, constant current, biphasic pulses of 200 μs duration delivered at 200 Hz for a total

duration of 125 ms. In accordance with the subject's feedback on the quality of the phosphene, these parameters were adjusted to 500 μs duration pulses delivered at 150 Hz for a total duration of 250 ms. **Amplitude:** Of the 38 electrodes, 25 had thresholds <25 μA (lowest was 1.9 μA) while the other electrodes didn't respond to currents up to 30 μA. Nine of these electrodes had a threshold of 40-77 μA with anode first stimulation. Increasing the current amplitude had mixed effects on size as it could produce no changes, an increase, a decrease or first increase then decreased in size. Current amplitude also affected phosphene colour. Near threshold stimulation typically produced coloured phosphenes, whereas phosphenes at amplitudes >12.5 μA were typically white, yellowish, or grayish. **Frequency:** Increasing the pulse frequency reduced the reaction time for both phosphene onset and offset which plateaued at 150 Hz and 250 Hz respectively. Increases in frequency were also found to increase phosphene brightness. Threshold currents were constant for frequencies between 150-200 Hz however increased by half when frequency was lowered to 75 Hz. **Pulse Duration:** Increasing pulse duration from 200 to 800 μs reduced the threshold from 19.4 μA to 11.7 μA and produced more substantial phosphenes. Increases in pulse duration were found to increase phosphene brightness. **Interpulse Interval:** Long interpulse intervals with short pulse durations reduced thresholds, and increasing the interval from 0 to 100 μs decreased the threshold by 5.4%. **Train Duration:** The thresholds for 250 ms duration trains were 20% lower than those of 125 ms trains, and longer durations produced more easily recognizable phosphenes. Longer train durations produced brighter phosphenes and increasing the train duration from 200-500 ms increased phosphene size. Multiple trains produced separate phosphenes if separated by more than 25 ms. Train durations longer than 250 ms produced an elongated sense of phosphene duration, whereas trains longer than 1000 ms caused the phosphene to extinguish before the stimulation ended.

More extensive work has been conducted in the visual cortex of non-human primates using ICMS threshold detection experiments. In these studies the monkeys indicate the detection of visual percepts in a lever-press task (Bartlett et al., 2005). The stimulus waveform consisted of constant-current, monophasic, cathodal pulses with durations of 0.2 ms delivered at a frequency of 100 Hz in 1s trains. **Amplitude:** The average current threshold for detection ranged from 35-149 μA suggesting large variability among sites. **Frequency:** Fast reaction times were observed for 50-100 Hz stimuli whereas reaction times for 1-10 Hz signals were slow. The detection threshold was found to decrease as frequency increased and these effects were more pronounced in the

range of 10-20 Hz. **Pulse Duration:** Detection threshold was found to decrease as pulse duration increases with the chronaxie (shortest duration of effective stimulation) determined to be 247 μs.

In a similar study, monkeys were trained to perform a 2 choice direction discrimination task in response to stimulation of area MT (Murasugi et al., 1993; Salzman et al., 1990, 1992). The stimulation targeted neurons whose preferred direction was opposite to that of a presented visual motion stimulus with the goal of biasing the monkey's choice of direction. The stimulus waveform consisted of biphasic, cathodal-leading, pulses of 0.2 ms duration with a 0.1 ms interphase interval between the cathodal and anodal pulses. **Amplitude:** While testing the effects of amplitude, the frequency was fixed at 200 Hz and the current values tested were 0, 5,10,20,40 and 80 μA with the threshold identified as 5 μA. The ability to bias behavior improved as current amplitude increased up to 40 μA with large effects seen at 20 and 40 μA. At 80 μA, the monkey could no longer determine the direction of motion. The authors described these effects by stating that lower intensity stimulation added "signal" to the cortex, while higher intensities added "noise". This noise was thought to be caused by the activation of many columns encoding different directions. **Frequency:** While testing the effects of frequency, the amplitude was fixed at 10 μA and the frequency values tested were 0, 25, 50, 100, 200, 500 Hz, with the threshold identified at 25 Hz although weak effects were observed at 12.5 Hz. Variations in the frequency had very little effect on performance.

2.4.2 Auditory cortex

To assess the safety of the Utah Array and the stimulation it provides, a 100 electrode array was implanted into the auditory cortex of three cats (Rousche & Normann, 1999). A two-alternative forced choice task was used to indicate the detection of the stimulus and general trends for parameter variations were examined. The standard stimulus used was a cathodic-leading, constant current signal of 100 μA biphasic pulses with a width of 150 μs and an interphase interval of 100 μs. The stimulation lasted 0.6 s and the pulse pairs were delivered at 250 Hz. **Charge/phase:** With these parameters the charge/phase thresholds varied from 1.5-26 nC/ph. **Frequency:** Stimulus detection was reduced as stimulus frequency decreased. When the charge/phase was less than 1.5 times the threshold, frequencies ranging from 50-2000 Hz produced nearly 100% detection; however 25 Hz stimuli did not produce the same effect even with stimulation an order of magnitude higher than 1.5 times the threshold. **Train Duration:** When the charge per phase

was fixed at 1.5 times the threshold, stimulus detection was reduced to 50% for 0.1 s duration stimuli, whereas durations greater than 0.2 s produced nearly 100% detection.

The effects of interpulse interval and frequency on threshold detection have also been examined in the rat auditory cortex (Koivuniemi, Regele, Brenner, & Otto, 2011). The stimulus waveform was a constant current, biphasic square wave with 205 μs pulses delivered at 150 pulses per second with both cathode-leading and anode-leading stimulation. **Interphase Interval:** Threshold values were found to decrease as the interphase interval increased and anode-leading stimulation had higher thresholds than cathode-leading stimulation for interphase intervals less than 1 ms in duration. **Frequency:** The detection threshold amplitude decreased logarithmically as frequency increased from 16-84 pulses per second; however this trend plateaued between 84-338 pulses per second.

2.4.3 Somatosensory cortex

The effect of stimulus intensity, frequency and duration on detection thresholds has also been explored in the somatosensory cortex of a head-restrained rat (Butovas & Schwarz, 2007). This study focused on the difference between single and repetitive stimuli. A biphasic cathode-leading, constant current square waveform was used in both single pulse and repetitive stimulation trials. **Stimulation Intensity (amplitude x duration):** Using single pulses, at intensities as low as 2 nC, detection probability rose above chance levels, and plateaued at ~80% detection at 4 nC. **Frequency:** Detection threshold levels could be lowered by increasing the stimulus frequency. **Pulse Duration:** Repetitive pulses were found to decrease the detection threshold even when comparing only 2 pulses to a single pulse. Using just 2 pulses, the stimulation threshold could be significantly reduced by increasing the pulse frequency. This effect was more pronounced for short inter-pulse intervals and for stimulations with 5-15 pulses. Additionally, repetitive stimuli boosted performance levels approaching 100% detection, and 2 pulses were found to perform as well as longer trains of stimuli.

In a similar experiment, the effects of stimulus amplitude, frequency and train duration were examined in the somatosensory cortex of an unrestrained rat (Semprini, Bennicelli, & Vato, 2012). The standard stimulus waveform stimulus was 40 current-controlled, biphasic, cathode-leading square pulses with a duration of 160 μs delivered at 200 Hz with an amplitude of 100 μA. **Amplitude:** Varying the amplitude between 5-100 μA with the frequency fixed at 200 Hz

revealed that the ability to detect stimulation at low amplitudes was at chance levels however performance improved greatly (≥70% correctly detected) for amplitudes above 60 μA. **Frequency:** Varying the frequency between 10-200 Hz with amplitude fixed at 80 μA revealed that performance above chance levels was achieved with frequencies as low as 25-50 Hz. After this point performance plateaued at ~70% correct performance. **Train Duration:** Train duration was varied between 5-200 ms with amplitude fixed at 80 μA, and frequency fixed at 200 Hz. Under these conditions performance was above chance levels when duration was greater than 10 ms after which point performance plateaued at ~70% correct.

2.4.4 Motor cortex

An experiment conducted in the rat and mouse motor cortex examined the effects of frequency and train duration on the threshold for producing forelimb movements (Young, Vuong, Flynn, & Teskey, 2011). The standard stimulation signal consisted of 13 monophasic cathodal pulses of 0.2 ms duration delivered at 333 Hz, with trains repeating every second. **Frequency:** In rats, the lowest movement thresholds were found to occur for stimulus frequencies of 181-400 Hz and no difference in threshold was observed between 142- 400 Hz frequencies. In mice, no movements could be evoked using stimulus frequencies of 111, 125 and 500 Hz, however, 333 Hz was effective. **Train Duration:** In rats, movements could be evoked for all train durations longer than 15 ms, and thresholds were not significantly different between durations of 15-60 ms. In mice, movements could be evoked for all train durations longer than 9 ms. Movement thresholds tended to decrease as train duration increased however there were no significant differences between thresholds of 12-39 ms trains.

Table 2-1. List of parameter ranges used in a common brain stimulation applications.

Parameter	**Phosphene Generation (Visual Cortex)**	**Movement Evocation (Motor Cortex)**	**Tone Generation (Auditory Cortex)**	**Tactile Sensation (Somatosensory Cortex)**	**DBS (STN, GPi)**
Amplitude (μA)	2-300	10-200	20-100	5-100	100-3000
Frequency (Hz)	25-5000	100-500	16-350	10-500	130-185
Pulse Duration (ms)	0.01-1	0.1-0.6	0.08-0.5	0.1-0.6	0.06-0.21
Interphase Interval (ms)	0-10	-	0-1	-	-
Train Duration (ms)	80-1000	15-500	30-650	5-200	-

Table 2-1 summarizes the stimulus parameter ranges used in the applications discussed in section 2.4 as well as the ranges used in deep brain stimulation therapies. This table emphasizes the wide variability in parameter values used within and between applications. Within an application, the variability is primarily due to the large range of parameter values which can be used to accomplish a specific stimulation goal, and is partially due to the comparison of studies conducted in a number of different species. The variability between applications suggests that task-specific optimization is valuable since certain parameter ranges appear more effective at accomplishing specific stimulation goals.

The direct comparison of stimulus parameters used in different studies is often of limited value due to differences in the species, regions of the brain and stimulation goals under study. Direct comparison is best limited to studies conducted in the same species and region of the brain for the same purpose. However, even under these restrictions direct comparison may not be effective since different stimulus parameters can be altered to achieve the same effect, resulting in multiple parameter combinations which achieve the same goal. For example, increasing the amplitude or pulse duration of a stimulus signal can have the same effect on phosphene generation. If one study increases the amplitude of a stimulus while another increases the pulse duration they may achieve identical results with different stimuli. A direct comparison of these results may not be beneficial for optimizing an existing stimulus or developing new stimuli.

The major goal of this thesis is to define the general effects exerted by each stimulus parameter on the responses they evoke. To achieve this goal we experimentally tested the effects of each stimulus parameter in a subset of their commonly used ranges. The emphasis is placed on understanding the generalized influence of each parameter rather than focusing on the specific values. This knowledge can be used in the design of new stimulus waveforms and the optimization of existing signals for a specific task. It also provides a basis from which to make indirect comparisons, where we consider the waveform as the sum of the influence of its component parameters. The technical implementation of this approach is detailed in the model described in chapter 6.

CHAPTER 3 ARTICLE 1: INTRACORTICAL MICROSTIMULATION PARAMETERS DICTATE THE AMPLITUDE AND LATENCY OF EVOKED RESPONSES

Meghan Watson[1,2], Numa Dancause[2] and Mohamad Sawan[1]

[1] Polystim Neurotechnologies, Institute of Biomedical Engineering, Polytechnique, Montreal, Quebec, Canada

[2] Département de Neurosciences, Faculté de Médecine, Université de Montréal, Canada

3.1 Presentation of the article

The results of the literature review were used to determine the parameter ranges to test experimentally. These ranges encompassed a wide variety of parameters that are commonly used in brain stimulation applications. A series of experiments (experimental blocks) were designed to systematically test the effects that stimulation parameters exert on the responses they evoke. Each experimental block tested one parameter of the stimulus. The following article describes the effects of stimulus parameters on the amplitude and onset latency of the evoked responses. This article (Watson, Dancause, & Sawan, 2015b) was submitted to the journal of Brain Stimulation on March 27th 2015 and the revised manuscript submitted July 31st 2015 is reproduced here.

3.2 Abstract

***Background*:** Microstimulation of brain tissue plays a key role in a variety of sensory prosthetics, clinical therapies and research applications. However the effects of stimulation parameters on the responses they evoke remain widely unknown.

Objective: We aimed to investigate the contribution of each stimulation parameter to the response and identify interactions existing between parameters.

Methods: Parameters of the constant-current, biphasic square waveform were examined in acute terminal experiments under ketamine anaesthesia. The motor cortex of 7 Sprague-Dawley rats

was stimulated while recording motor evoked potentials (MEP) from the forelimb. Intracortical microstimulation (ICMS) parameters were systematically tested in a pair-wise fashion to observe the influence of each parameter on the amplitude and latency of the MEP.

Results: The amplitude of the MEP increased continually with stimulus amplitude ($p<0.001$) and pulse duration ($p=0.001$) throughout the range tested. Increases were also observed when stimuli were raised from low to moderate values of frequency ($p=0.022$) and train duration ($p=0.045$), after which no further excitation occurs.

The latency of MEP initiation decreased when stimulus amplitude ($p=0.037$) and frequency ($p=0.001$) were raised from low to moderate values, after which the responses plateaued. MEP latencies were further reduced by increasing the pulse duration ($p=0.011$), but train duration had no effect.

Conclusion(s): Our data indicate that MEP amplitude and onset latency can be modulated by alterations to a number of stimulus parameters even in restrictive paradigms and suggest that the parameters of the standard ICMS signal used for evoking movements from the motor cortex can be further optimized.

Key words*:* Intracortical microstimulation, stimulation parameters, motor evoked potentials

3.3 Introduction

Microstimulation of brain tissue has a wide range of applications including visual (Bradley et al., 2005; Davis et al., 2012; Dobelle & Mladejovsky, 1974; Schmidt et al., 1996; Torab et al., 2011) and somatosensory (Berg et al., 2013; Tabot et al., 2013; Thomson et al., 2013) prosthetic devices, deep brain stimulation therapies for Parkinson's (Anderson, Burchiel, Hogarth, Favre, & Hammerstad, 2005; Bronstein et al., 2011; Deuschl et al., 2006; Little et al., 2013; Weaver et al., 2012), and epilepsy (Fisher et al., 2010; Kerrigan et al., 2004; Lee, Jang, & Shon, 2006; Morrell, 2011) and countless research applications involving many different regions of the brain (Bartlett et al., 2005; Brecht, Schneider, Sakmann, & Margrie, 2004; Butovas, 2003; Butovas & Schwarz, 2007; DeYoe, Lewine, & Doty, 2005; Marzullo, Lehmkuhle, Gage, & Kipke, 2010; Murphey & Maunsell, 2007; Salzman et al., 1992; Tehovnik et al., 2005). Although these applications may

involve different electrodes, target sites or specific goals they each seek to replace natural stimuli, correct problems in neural circuitry, or modify behavior using electrical stimulation.

One of the earliest and most documented uses of brain stimulation involves the activation of motor cortex regions to evoke muscle contractions or movements (Penfield & Boldrey, 1937; Penfield & Welch, 1951; Sironi, 2011). Stimulation applied to specific regions of the motor cortex has been shown to evoke movements in humans (Penfield & Welch, 1951), primates (Asanuma et al., 1976), cats (Armstrong & Drew, 1984) and rodents (Donoghue & Wise, 1982; Sanderson, Welker, & Shambes, 1984). The motor cortex exhibits a somatotopic organization in which a specific cortical region corresponds to a specific area of the body. Much study has been devoted to mapping the correlation between regions of the motor cortex and the areas of the body they control (Gioanni & Lamarche, 1985; Neafsey et al., 1986; Penfield & Boldrey, 1937; Rouiller et al., 1993; Schieber, 2001).

When electrical stimulation is applied to the forelimb region of the rat motor cortex, it activates corticospinal neurons which project from the cortex to the spinal cord. Within the spinal cord these efferent neurons are indirectly connected to the motor neurons which innervate the forelimb muscle fibers. When these fibers are activated they produces muscle contractions or limb movements and the corresponding activations can be recorded directly from the muscles of the forelimb.

Short duration stimulus trains (<50 ms) are often used to elicit responses from the motor cortex in anaesthetized animals (Asanuma & Rosen, 1972; Donoghue & Wise, 1982; Gioanni & Lamarche, 1985; Neafsey et al., 1986; Nudo, Jenkins, & Merzenich, 1990; Sanderson et al., 1984). The most commonly used stimulus signals for evoking movements in the rat consists of 13 monophasic cathodal or biphasic cathode-leading pulses, each of 0.2 ms in duration delivered at 333 Hz with trains repeating every second. Although these parameters were determined by trial and error, some general effects of stimulation parameters have been examined. Stimulus current thresholds for eliciting movements can be lowered by extending the train duration beyond 30 ms and increasing the pulse frequency above 300 Hz (Asanuma & Arnold, 1975; Asanuma et al., 1976). The lowest movement thresholds have been shown to occur when stimulating with frequencies between 181-400 Hz for durations of 15-33 ms, with the optimal values being 300 Hz and 39 ms (Young et al., 2011). Stimulus frequency can be used to limit the spread of current

within the cortex. Pulses delivered at frequencies less than 20 Hz localize the activation by preventing the summation of excitatory and inhibitory postsynaptic potentials (Cheney, Griffin, & Van Acker, 2013). While these parameter effects are valuable observations, much remains to be determined.

To accomplish a stimulation goal it is necessary to design each stimulation signal to achieve a specific response. Externally, the response can be viewed as a desirable reaction such as the induction of a visual percept (Tehovnik & Slocum, 2007), the cessation of a tremor (Benabid, Chabardes, Mitrofanis, & Pollak, 2009) or seizure (Fisher, 2012), the generation of a limb movement (Asanuma & Rosen, 1972; Nudo, Jenkins, Merzenich, Prejean, & Grenda, 1992) or the facilitation of a response in a behavioral task (Murasugi et al., 1993; Tehovnik, Slocum, & Schiller, 2003). Internally, the response is characterized by the magnitude of the cortical activation, the speed at which the activation occurs, volume of tissue activated and the duration of this activation. These effects can be controlled by varying the parameters of the microstimulation signal.

We consider one of the most prevalent microstimulation signals: the constant-current, cathode leading, biphasic square waveform, historically suggested to be safe and effective (Lilly et al., 1955). This signal reduces the occurrence of tissue damage by alternating the polarity of the pulse phases to achieve charge balancing. The parameters of this signal include the current amplitude, pulse frequency, pulse duration, interphase interval and pulse train duration (figure 1a). Some of these parameters are known to induce tissue damage within specific ranges (Agnew, McCreery, Yuen, & Bullara, 1989; Asanuma & Arnold, 1975; McCreery, Agnew, Yuen, & Bullara, 1995; McCreery, Pikov, & Troyk, 2010), and most applications have restrictive requirements of the stimulus. As such, many efforts have been made to optimize a signal for its specific purpose, by developing waveforms through iterative testing of parameter combinations shown to be successful from past experience (Koivuniemi & Otto, 2012; Koivuniemi et al., 2011; McIntyre, Frankenmolle, Wu, Noecker, & Alberts, 2009; Motamedi et al., 2002; Rajdev, Ward, & Irazoqui, 2011; Van Acker et al., 2013; Young et al., 2011).

This approach is valuable, yet time consuming and inevitably results in multiple signals addressing the same problem since many effective parameter combinations exist for each application. Extensive variability within a field reduces the power of the collective body of

research and hinders comparisons when stimuli are slightly different, or entirely contradictory. We propose an alternative approach to stimulation design in which the parameters of a waveform are tailored to suit a specific purpose or target area by understanding how each parameter contributes to the response signal. To this end, we systematically explored the influence that parameters and their interactions have on the effectiveness of the biphasic waveform stimulation signal in terms of the amplitude and latency of the response.

3.4 Methods

3.4.1 Experimental design

In many research applications, strong stimuli are used to ensure a response is produced; however this approach is largely unsuitable for clinical and prosthetic applications. We chose to examine parameter ranges typically employed for clinical applications; specifically those developed for visual prosthetic devices which have extremely restrictive stimulation paradigms (Schmidt et al., 1996). These paradigms employ the principle of "minimum effective dose" where a stimulus is just strong enough to produce a visual percept (phosphene), but not strong enough to cause interactions between neighboring electrodes or tissue damage at the electrode interface.

To explore parameters in this range we chose to work in the rat model, stimulating the caudal forelimb area of the primary motor cortex (M1); a region known to produce forelimb movements in anaesthetized animals (Donoghue & Wise, 1982; Gioanni & Lamarche, 1985; Neafsey et al., 1986; Nudo et al., 1992; Sanderson et al., 1984). This model offered high-throughput capabilities and stimulation tasks sensitive to the parameter range of interest. The signal's effectiveness was quantified by recording the response to stimulation in the form of motor evoked potentials (MEP) of forelimb muscles (figure 1b). Using the MEP signal we were able to explore the amplitude of the response and the latency at which it occurred.

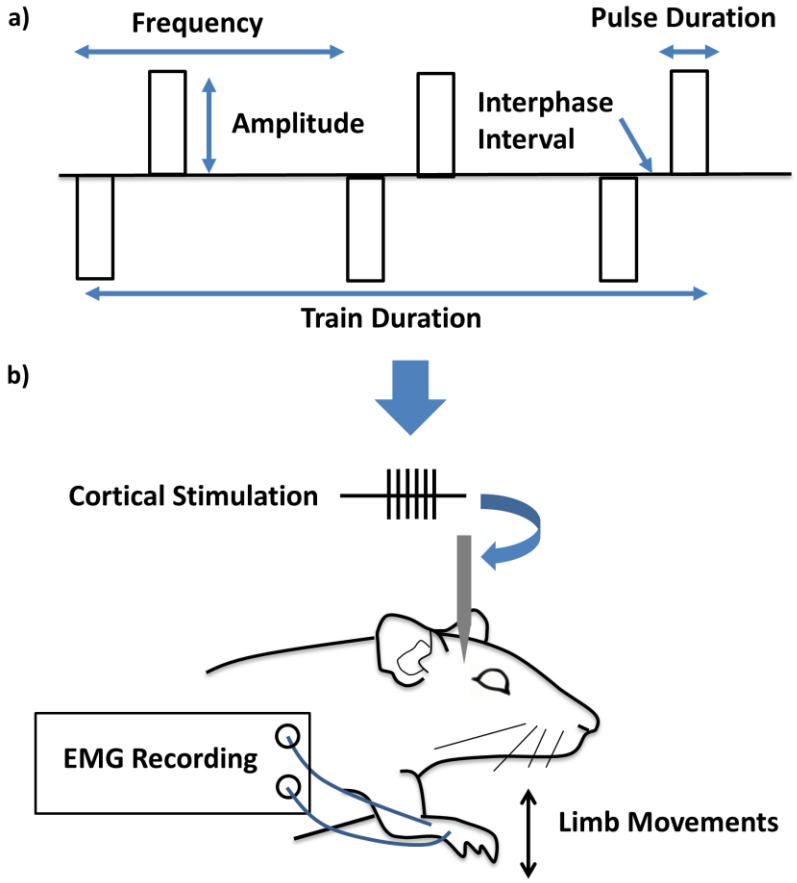

Figure 3-1: Parameters of the constant-current, biphasic square waveform (a), and a schematic representation of the experimental task (b).

3.4.2 Stimulation protocol

Five experiments were conducted to test the specific effects of each constant-current, biphasic square waveform parameter on the MEP signal. The waveform parameters and their ranges are specified in table 1. Each experiment focused on one parameter, testing it against the other four parameters in a pair-wise fashion. Parameters not involved in the comparison were held at a control value derived from the standard stimulation signal proven to be effective in the rat motor cortex (Donoghue & Wise, 1982; Nudo et al., 1990; Young et al., 2011), and the control amplitude was set to 50 µA which was twice the threshold level (Brus-Ramer, Carmel, & Martin, 2009; Chakrabarty, 2005; Marple-Horvat & Armstrong, 1999). The control amplitude level was selected according to the results of preliminary testing. We aimed to ensure the stimulus amplitude was sufficient to produce responses to the majority of stimulus conditions not

explicitly exploring amplitude effects while remaining low enough to avoid masking the influence of other parameters.

In this pair wise testing arrangement, all amplitude levels were tested at 3 frequency levels (low, mid and high values found in the "test levels" column of table 1) with pulse duration, interphase interval and train duration held at the control values. When describing the level of the parameter in question throughout the text, we refer to the smallest value in the test range as "low or short", the middle value as "mid", and the largest value in the test range as "high or long". For instance, in the case of frequency, the low, mid and high values are represented by the first, third and fifth entries of the "test levels" column of table 1, the values of which are 100,300 and 500 Hz respectively. In the case of train duration, the short, mid and long values correspond to 42, 172 and 300 ms respectively. This testing procedure was then repeated until each parameter had been examined in this "pair-wise" arrangement resulting in a total of 300 independent conditions to test all parameters (5 parameters x 5 test values x 4 paired parameters x 3 levels). This arrangement results in identical conditions occurring within different experimental blocks which allows for further comparison. A complete list of all stimulus conditions can be found in the supplementary material. In addition to the parameter of the stimulus signal we also include the number of pulse pairs resulting from each combination of test parameters. The number of pulse pairs is included for instructive purposes only as it has conventionally been detailed in stimulation studies, it is however not an independent parameter of the stimulus but rather a function of the pulse duration, pulse frequency and train duration. Each parameter was tested in a separate experimental block with ten trials for each condition and all trials were pseudo-randomized with 1 second between trials. The maximum duration of MEP responses induced by our experimental conditions was 700 ms, thus a delay of 1 second between trials allowed the MEP response to return to baseline and placed a buffer between the end of the response and the beginning of the next trial. All five blocks were tested in a randomized order at two different sites within the motor cortex of each rat (14 sites in total).

Table 3-1: Parameter test values

Parameter	Unit	Range	Test Levels	Control	Pairings
Amplitude (A)	μA	30-65	30, 39, 48, 56, 65	50	AF, AP, AI, AT
Frequency (F)	Hz	100-500	100, 200, 300, 400, 500	303	FA, FP, FI, FT
Pulse Duration (P)	ms	0.18-0.5	0.18, 0.26, 0.34, 0.42, 0.5	0.2	PA, PF, PI, PT
Interphase Interval (I)	ms	0.08-0.5	0.08, 0.19, 0.29, 0.40, 0.5	0	IA, IF, IP, IT
Train Duration (T)	ms	43-300	43, 107, 172, 236, 300	43	TA, TF, TI, TP

3.4.3 Surgical procedures

Seven female Sprague-Dawley rats (Charles River, QC, CA) weighing 273-450 g were used in terminal acute experiments. Anaesthesia was induced with intraperitoneal ketamine injection (80 mg/kg) and maintained with isofluorane (~2% in 100% oxygen). Subcutaneous injection of mannitol (4 g/kg) and intramuscular injection of dexamethasone (1 mg/kg) were given prior to the craniotomy to prevent swelling and oedema inflammation. A self-regulating heating pad maintained body temperature which, along with pulse rate and oxygen saturation, was monitored continuously. Insulated, multi-stranded wires (Cooner Wire, Chatsworth CA, USA) were implanted in the extensor digitorum communis muscle of the forelimb contralateral to the stimulating electrode to record MEP signals.

The animal was placed in a stereotaxic frame for both the surgical and stimulation procedures; positioned to allow free movement of the forelimb. A small craniotomy (8 mm x 5 mm) exposed the motor cortex (left hemisphere), the dura was removed and mineral oil applied to the cortex. Anaesthesia was switched to ketamine (~10 mg/kg/10 minutes) administered through intraperitoneal injections as needed for the duration of the stimulation procedure.

Stimulation was delivered with a digital stimulator (TDT IZ2 Stimulator and RZ5 BioAmp processor), through a glass insulated tungsten microelectrode (FHC Bowdoin, ME USA, UEWSDESGBN4G, 110-175 kΩ) manipulated by a microdrive (David Kopf Instruments Model 2662, Tujunga, CA). Appropriate sites were located using standard intracortical microstimulation (ICMS) trains: 13 monophasic, cathodic, square pulses of 0.2 ms duration with 3.3 ms between the pulses delivered at 1 Hz. MEPs were monitored and recorded at 5 kHz (RZ5 BioAmp Processor). Sites were chosen within the caudal forelimb region of the motor cortex which produced MEP responses as recorded from the extensor digitorum communisis muscle of the

forelimb. MEP threshold levels were determined by increasing the stimulus amplitude (up to 50 μA) until a MEP response was observed. We then lowered the stimulus amplitude until the response disappeared. The lowest stimulus amplitude at which the MEP response could be evoked was defined as the threshold amplitude. We sought stimulation sites which had MEP threshold amplitudes of 25-35 μA. Electrode depth varied from 1534-2104 μm (mean 1792 μm) between sites within the caudal forelimb area (0-4 μm anterior, 2.0-3.7 μm lateral to bregma). When choosing a site, the response was first tested at 1500 μm targeting output layer V, which is known to contain pyramidal neurons which project to lower motor neurons to produce movements (Wang & Kurata, 1998). If a threshold MEP response was produced in the extensor digitorum communisis muscle this depth was selected, if not, the electrode was advanced to find a suitably responsive site and only one depth was used within an electrode tract.

All experimental blocks were tested in 2 sites per rat. All procedures followed the guidelines of the Canadian Council on Animal Care and were approved by the Comité de Déontologie de l'Expérimentation sur les Animaux of the Université de Montréal.

3.4.4 Statistical analysis

A maximum of two trials per condition were excluded if they contained excessive equipment noise. The stimulus artifact was very small due to the low amplitudes of stimulation and was easily removed with a 5-point moving average filter. For each of the 14 stimulation sites, trials were averaged to produce a mean signal for each condition. The mean amplitude and onset latency were derived from these averages (figure 2). Response onset was computationally detected as the first instance where the response signal remained three standard deviations above baseline for more than ten sample points and all responses and onset times were visually inspected to confirm the accuracy of detection. Certain combinations of parameter pairs near the threshold amplitude did not cause sufficient excitation to evoke MEP responses and will be referred to as absent responses. Specifically, 30-39 μA stimuli delivered at 100 Hz, or 30 μA stimuli delivered by 43 ms duration trains were ineffective. A condition was included in the statistical analysis if responses were obtained from a minimum of 5 stimulation sites. Conditions evoking a response from less than 5 sites will be referred to as infrequent responses and typically occurred for stimuli composed of low amplitude short pulses delivered at low frequencies. To differentiate between absent and infrequent responses, data obtained from infrequent responding

conditions (<5 sites) are included in graphical representations differentiated by marker type. Further detail on the absent and infrequent responses can be found in the rightmost column of the appended supplementary material.

To evaluate the effects of each parameter on the response metrics we used a repeated measures linear mixed model, with random slope and intercept, followed by Bonferroni posthoc analyses to test the effects of main and paired parameters on outcomes. Main and paired parameters were entered as fixed factors, followed by the interaction between the two. The interaction term was significant only in the frequency and pulse duration pairings of the mean response ($p=0.003$). For all other outcomes, it was not significant ($p=0.05$ - $p=0.99$) and was trimmed from the model. Analyses were conducted with SPSS 22.0 (SPSS, Inc.) software using the mixed procedure with a factorial design and a significance level of $\alpha<0.05$. We report only statistically significant findings. If a value is absent it indicates that the particular condition either did not produce significant trends or was excluded from the analysis due to infrequent responses (<5 sites). In the text we indicate if a result is excluded due to infrequent responses, and the reader can also view the number of responding sites in the supplementary material as well.

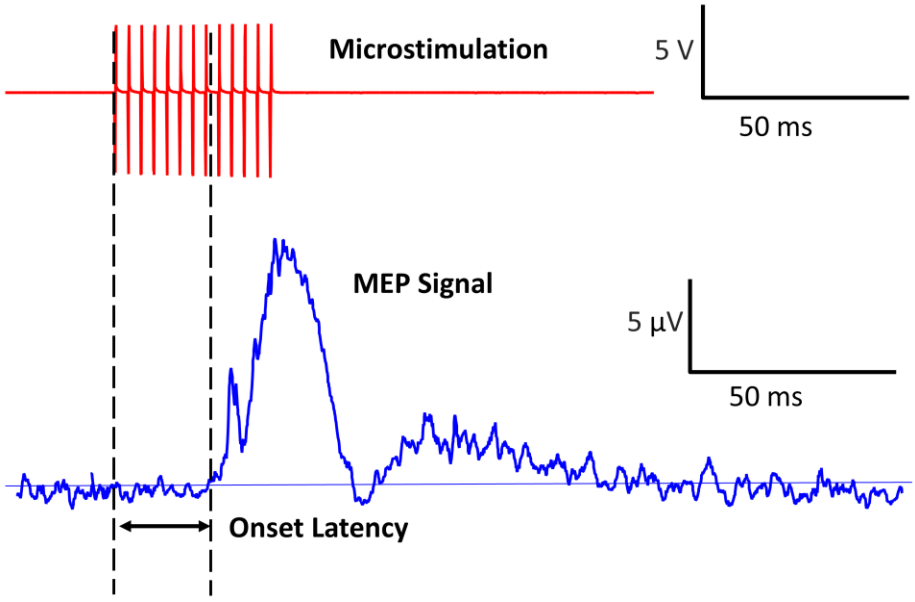

Figure 3-2: Illustration of performance measurements of the MEP signal. Onset latency is the delay between the onset of stimulation and the initiation of the MEP. Onset time is the first instance where the MEP signal remains above baseline levels for a minimum of 10 samples of the recorded voltage signal.

3.5 Results

Four of the five experiments showed significant trends demonstrating the effects that the main and paired parameters exerted on the performance metrics as well as the influence of interactions between parameters. The interphase interval experiment however yielded no significant results and does not appear to have any influence over the MEP signal as both a main and a paired parameter in the range tested, therefore will not be described here however its lack of influence is depicted in figure 7. Parameter pairings will be denoted by abbreviations of table 1 in which the main parameter appears first and paired parameter second (e.g. AF represents amplitude paired with frequency).

3.5.1 MEP response amplitude

The mean amplitude of the MEP response increased with stimulus amplitude for all paired parameters (AF: $p<0.001$; AP: $p<0.001$; AT: $p<0.001$) as shown in figure 3. As a paired parameter, increases in the stimulus amplitude could boost the response up to 43% when raised from low to mid levels (PA: 43% increase, $p<0.001$) and between 20-37% when raised from mid to high levels (FA: 34%, $p<0.001$; PA: 20%, $p=0.011$; TA: 37%, $p<0.001$). When high amplitude (56-65 μA) stimuli were delivered by mid/long duration trains or at high frequencies the response amplitude began to plateau suggesting an upper limit to these parameter pairings after which no further excitation can be induced. Conversely, the excitation induced by low amplitude stimuli can be effectively augmented by extending the duration of the stimulus pulse. At low amplitudes, the longest pulse durations produced larger responses than those of the longest train (36%) and highest frequency (76%) stimuli.

The mean amplitude of the MEP increased with stimulus frequency between 100-200 Hz (FA: $p=0.022$; FP: $p=0.014$) as shown in figure 4. Above this frequency the response plateaued at a maximum whose magnitude was dictated by the paired parameter; pairwise comparisons of values at 200 Hz with higher frequencies were non-significant. Frequency did not exert a significant influence on mid and long train duration stimuli which achieved large responses at all frequencies. As such, extending the duration of the stimulus train may be the most effective method to boost low frequency stimulation. At low frequencies, the longest trains produced larger responses than those of the longest pulse (87%) and highest amplitude (70%) stimuli.

As a paired parameter, mid and high frequency stimuli induced similar responses but low frequency responses were smaller when paired with pulse duration (PF: 48% decrease, $p<0.001$).

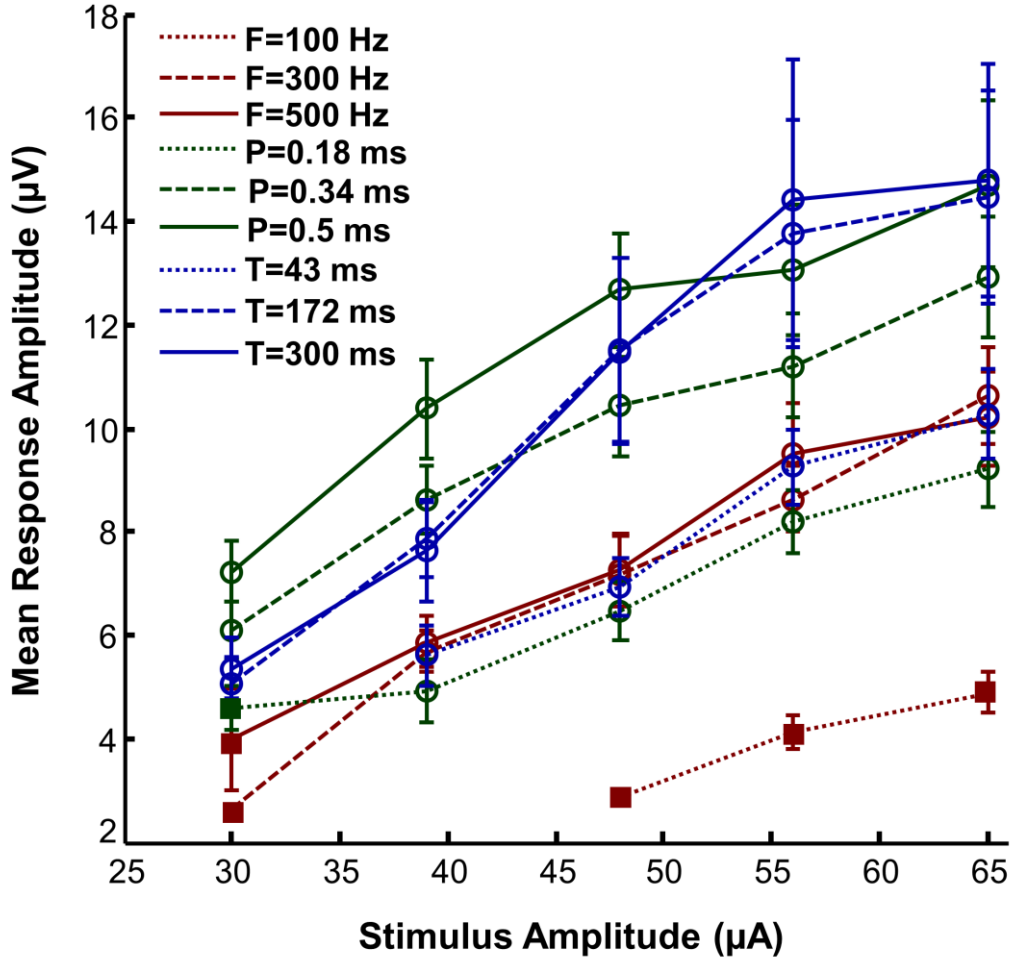

Figure 3-3: Representation of the MEP amplitude (mean ± SE) as a function of stimulus amplitude for all parameter pairings. Square symbols represent conditions with an insufficient number of responding sites ($n<5$) and were not included in statistical analysis. Circular symbols represent conditions with reliable responses ($n=5$-14). F=frequency, P=pulse duration, T=train duration, SE=standard error.

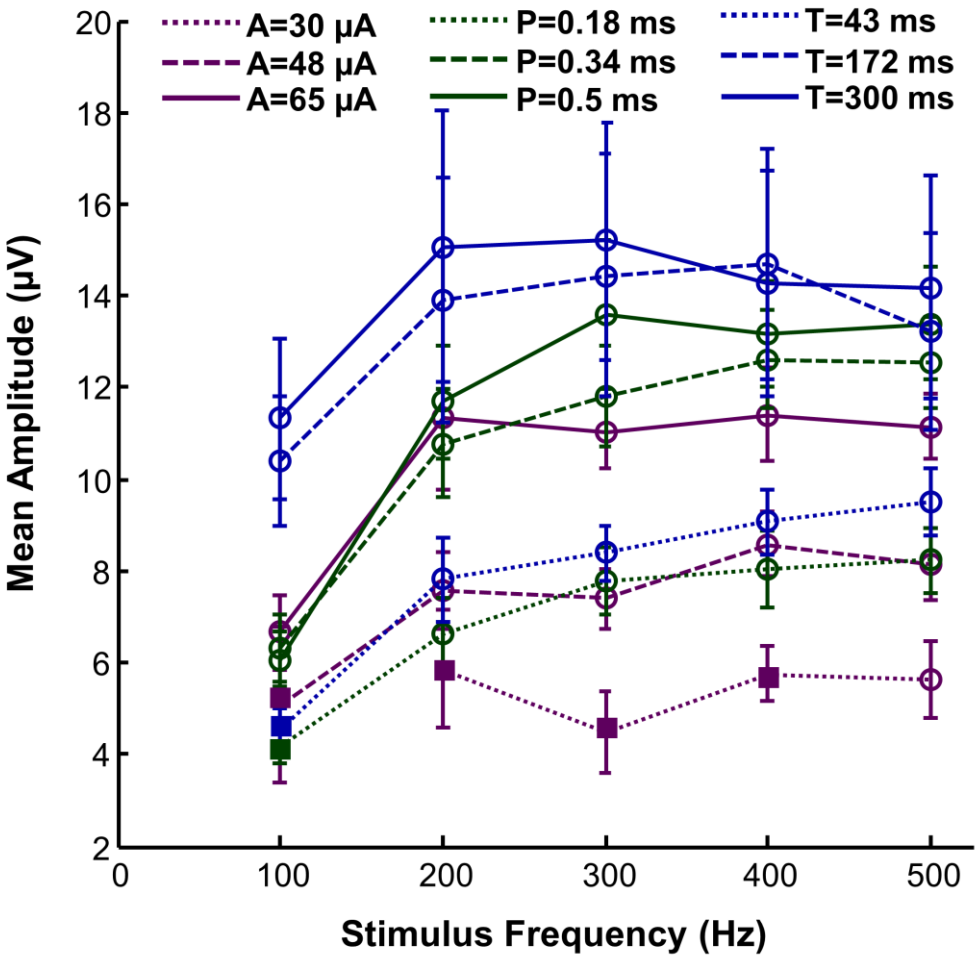

Figure 3-4: Representation of the MEP amplitude (mean ± SE) as a function of stimulus frequency for all parameter pairings. Square symbols: infrequent responses n<5, circular symbols: reliable responses (n=5-14), A=amplitude, P=pulse duration, T=train duration, SE=standard error.

The mean amplitude of the MEP increased with the pulse duration of the stimulus for all paired parameters (PA: $p<0.001$; PF: $p<0.001$; PT: $p=0.001$). As a paired parameter, the stimulus pulse duration boosted the response between 44-74% when raised from short to long duration pulses (AP: 74%, $p<0.001$; FP: 51%, $p<0.001$; TP: 44%, $p<0.001$). The response to short pulse stimuli was most effectively increased by raising the amplitude or extending the train duration. Using short pulses, the longest trains produced larger responses than those of the highest amplitude (22%) and frequency (68%) stimuli.

The mean amplitude of the MEP increased with stimulus train duration between 43-172 ms (TA: $p=0.045$). Above this duration the response plateaued at a maximum; pairwise comparisons of values at 172 ms with longer trains were all non-significant. As a paired parameter, responses to mid and long duration trains were similar, while responses to short duration trains were ~20-36% smaller (AT: 27%, $p<0.001$; FT: 36%, $p<0.001$; PT: 20-22%, $p<0.021$). These findings suggest the plateau occurring between short (43 ms) and mid duration trains (172 ms) is likely to occur between 107- 172 ms. Train duration did not exert a significant influence on mid and long pulse duration stimuli since large responses were achieved for all durations of train containing these pulse lengths. The increase in response amplitude between 43-172 ms did however exist to a lesser extent for short pulse duration stimuli and frequencies of all levels, however an insufficient number of sites responded to 43 ms train durations preventing their inclusion in the statistical analysis. The lack of response to short trains within the train duration experiment suggests an adaptation exists which renders short trains less effective when presented amidst long trains and is detailed in our previous work (Watson, Dancause, & Sawan, 2015a). The response to short train stimuli was most effectively increased by extending the pulse duration or raising the amplitude. Using short trains, the longest pulses produced larger responses than those of the highest amplitude (16%) and frequency (68%) stimuli.

3.5.2 MEP onset latency

The onset latency of the MEP decreased as stimulus amplitude increased from low to mid levels (AF: 39-48 μA, $p=0.037$; AT: 30-48 μA, $p=0.037$) as depicted in figure 5. Above this amplitude, latency plateaued at a minimum whose magnitude was dictated by the paired parameter; pairwise comparisons of values at 48 μA with higher amplitudes were non-significant. Response latencies decreased continually as amplitude increased when paired with pulse duration ($AP<0.001$). As a paired parameter, stimulus amplitude increases could reduce the latencies up to 26% when raised from low to mid levels (PA: 26%, $p=0.003$) and 19-34% when raised from mid to high levels (FA: 29%, $p<0.001$; PA: 19%, $p=0.007$; TA: 34%, $p<0.001$). At low amplitudes of stimulation the response onset was most effectively expedited by increasing the duration of the stimulus pulse. At low amplitudes, the longest pulses produced faster responses than those of the highest frequency (37%) and longest train (49%) stimuli.

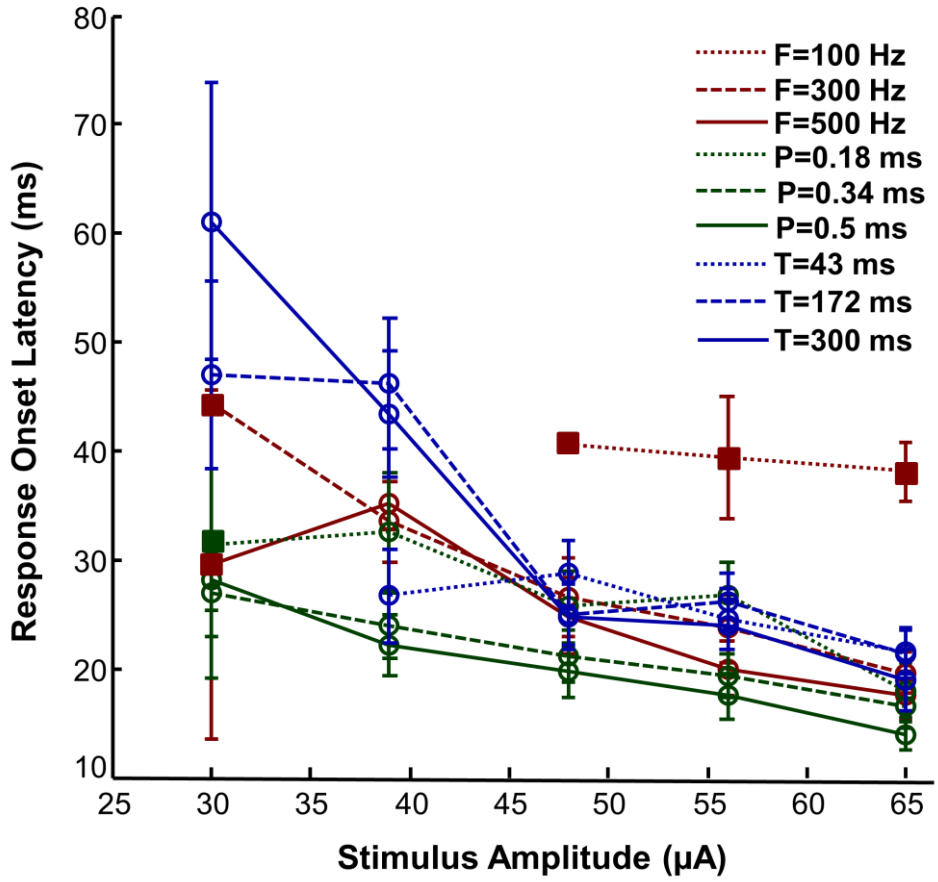

Figure 3-5: Representation of the MEP onset latency (mean ± SE) as a function of stimulus amplitude for all parameter pairings. Square symbols: infrequent responses n<5, circular symbols: reliable responses (n=5-14), F=frequency, P=pulse duration, T=train duration, SE=standard error.

The response onset latency decreased as stimulus frequency was raised from 100-200 Hz when paired with amplitude (FA: p=0.001) and 100-300 Hz when paired with train duration (FT: p<0.001). Above these frequencies the response plateaued at a minimum; pairwise comparisons were not significant between higher frequencies and values of 200 Hz or 300 Hz as shown in figure 6. Response speeds increased continually with frequency when paired with pulse duration (FP: p<0.001). As paired parameters, mid and high frequency stimuli had similar latencies, but latencies of low frequency stimuli were much longer (PF: 73-85%, p<0.001; TF: 82-105%, p<0.001). At low frequencies of stimulation the response onset was most effectively expedited by extending the duration of the stimulus pulse or increasing the stimulus amplitude. At low frequencies, the longest pulses produced faster responses than those of the highest amplitude

(11%) and longest train (62%) stimuli. The fastest response times were achieved with a combination of high frequency (400-500 Hz) and long pulse duration (0.5 ms) stimulation.

Onset latency decreased as the duration of the stimulus pulse increased for all paired parameters (PA: p=0.001; PF: p=0.006; PT: p=0.011). As a paired parameter, pulse duration increases could reduce the latencies by up to 54% when raised from short to long duration pulses (AP: 24%, p=0.003; FP: 36%, p<0.001; TP: 54%, p<0.001). Stimulus train duration had no effect on the response latency as a main or paired parameter.

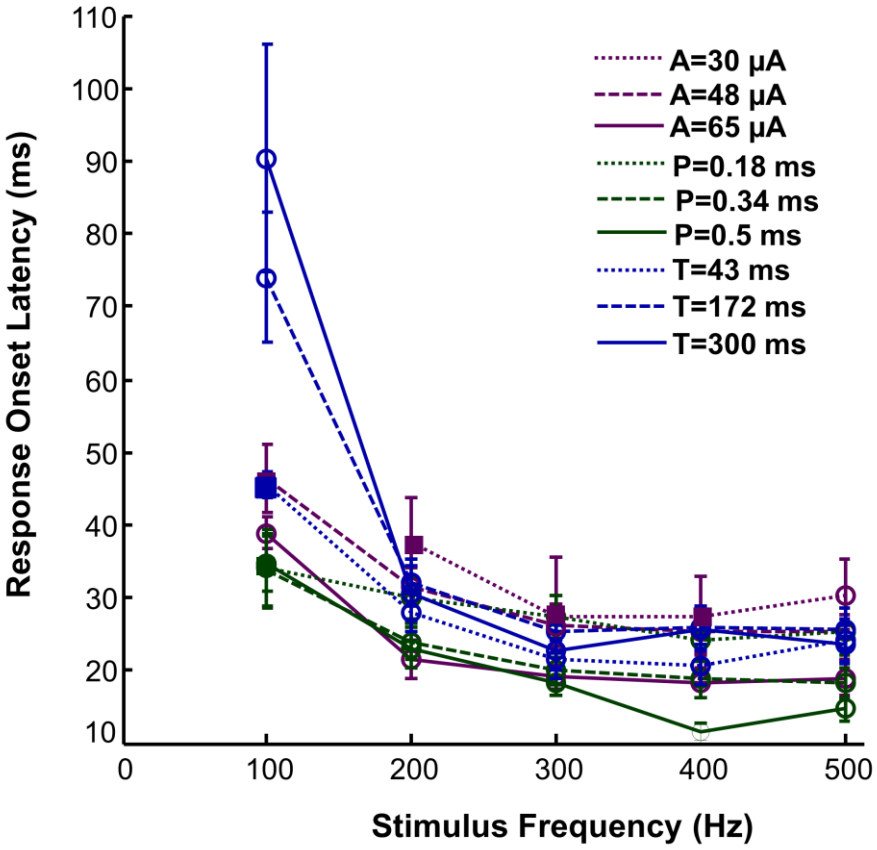

Figure 3-6: Representation of the MEP onset latency (mean ± SE) as a function of stimulus frequency for all parameter pairings. Square symbols: infrequent responses n<5, circular symbols: reliable responses (n=5-14), A=amplitude, P=pulse duration, T=train duration, SE=standard error.

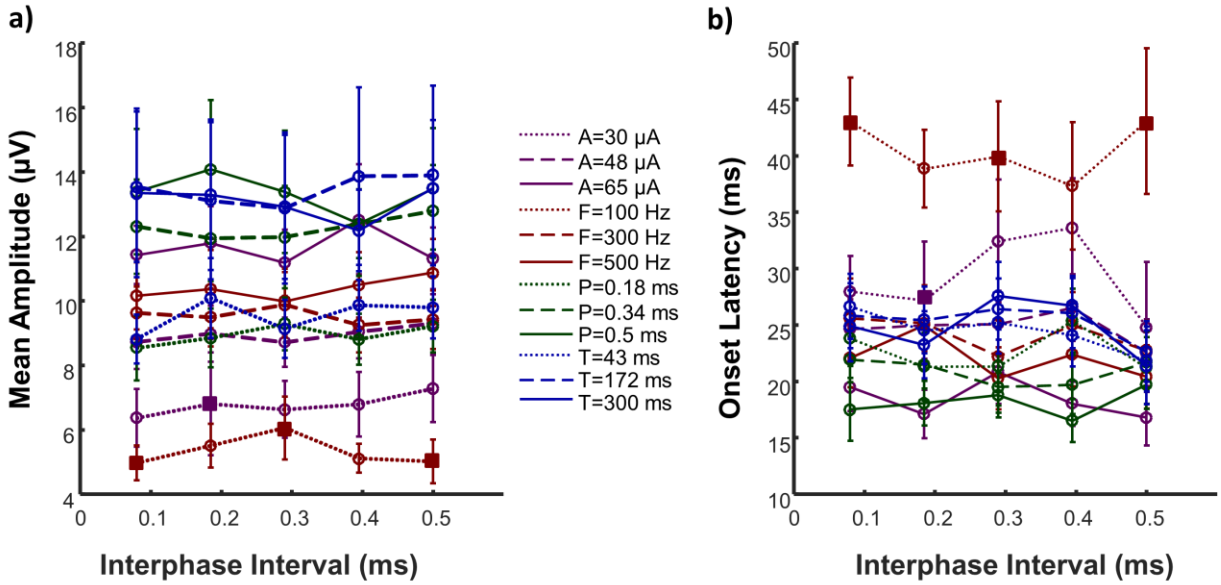

Figure 3-7 Representation of the MEP onset latency (mean ± SE) as a function of interphase interval. The null effect of interphase interval is demonstrated for all parameter pairings. Square symbols: infrequent responses n<5, circular symbols: reliable responses (n=5-14), A=amplitude, F=frequency, P=pulse duration, T=train duration, SE=standard error.

3.6 Discussion

This study demonstrated the general effect that each parameter exerted on the MEP signal and emphasized several major points. The mean amplitude of the MEP response increased with all stimulus parameters. The increase was continual for the parameters of stimulus amplitude and pulse duration however for stimulus frequency and train duration, no further increases were observed beyond the range of 100-200 Hz and 43-172 ms respectively. Previous studies reported no significant difference in movement thresholds for frequencies between 142-400 Hz (Young et al., 2011), which when combined with our findings suggests that the limit to the influence of frequency occurs in the range of 100-142 Hz.

Studies exploring long duration stimulation (LD-ICMS) tend to use 500-2000 ms trains (Brown & Teskey, 2014; Graziano, Taylor, & Moore, 2002; Griffin, Hudson, Belhaj-Saïf, & Cheney, 2014; Van Acker et al., 2013), however our findings suggest that the influence of train duration on MEP amplitude reaches its limit at much shorter durations (107-172 ms). The MEP amplitudes resulting from 172 ms trains and 300 ms trains are not significantly different which

suggests that the complex, multi-joint movements produced by very long duration stimuli (500-2000 ms) do not rely on increased levels of activation for particular muscles. Long duration stimuli may result in greater spread of current within the cortex via multi-synaptic projection serving to innervate a larger number of muscle groups whose coordinated activation produces complex movements. The present study cannot however lend direct support to either theory regarding the functional organization of the motor cortex as either muscle-based (Andersen, Hagan, Phillips, & Powell, 1975; Asanuma & Rosen, 1972; Donoghue, Leibovic, & Sanes, 1992; Donoghue & Wise, 1982; Ebrahimi, Pochet, & Roger, 1992; Gioanni & Lamarche, 1985; Hall & Lindholm, 1974; Neafsey et al., 1986; Sanderson et al., 1984) , or movement-based (Bonazzi et al., 2013; Brown & Teskey, 2014; Gharbawie, Stepniewska, & Kaas, 2011; Graziano et al., 2002; Haiss & Schwarz, 2005).

The onset latency of the MEP response decreased as the parameters of stimulus amplitude, frequency and pulse duration increased. The decrease was continual with increases in pulse duration, however for stimulus amplitude and frequency, no further decrease in onset latencies were observed beyond the ranges of 30-48 μA and 100-200 Hz respectively. Train duration exerted no influence on MEP onset latency.

This study also identified parameter combinations which serve to overcome specific restrictions on the stimulus signal, and described how to modulate the MEP amplitude and onset latency by altering unrestricted stimulus parameters. Applications which must restrict the stimulus amplitude to low levels can increase the MEP amplitude by extending the duration of the stimulus pulse, which also serves to expedite the onset of the response in this condition. These findings are in agreement with threshold current studies which have previously demonstrated that extending stimulus pulse duration lowers threshold current levels (Bartlett et al., 2005; Schmidt et al., 1996). Applications which require low stimulus frequencies can increase the MEP response amplitude by extending the duration of the stimulus train, and response onset can be expedited by extending the duration of the stimulus pulse or increasing the stimulus amplitude. Similarly, raising the stimulus amplitude or extending the train duration serve to increase the amplitude of MEP responses produced by short pulse duration stimuli, whereas extending the pulse duration or raising the amplitude serve to increase the MEP response amplitudes produced by short stimulus trains.

We have used the MEP response metrics to quantify the influence exerted by each stimulus parameter on the motor system. The intensity of the muscle contraction reflects the relative quantity of innervating motor neurons activated by the stimulation and the number of action potentials they produce. This gives us an estimate of the volume of tissue activated and the level of activation achieved, whereas the onset speed measures how quickly this activation occurs. We propose that these physiological outcomes are common measures for all stimulation paradigms and should be the focus of a stimulation design methodology.

At present, when a new stimulation therapy is developed, the waveform is typically based on the results of similar therapies or iterative testing is conducted for the first time until the desired outcome is achieved. This task-specific optimization focuses on the external response only, while ignoring the cortical effects. Instead we propose the stimulus be designed considering the known effects that each stimulation parameter exerts on the tissue and the physiological goals of the particular application.

For example, visual prosthetic devices aim to simulate vision by generating patterns with the visual percepts (phosphenes) that are produced by stimulating the visual cortex. Stimulation is typically delivered through an electrode array where the individual electrode pins are separated by 500 μm and each produce a separate phosphene. From a physiological stand point, the goal is to activate a very small region of the cortex and prevent neighbouring electrodes from interacting with each other. Neighbouring pins do not necessarily produce neighbouring phosphenes due to the topographic organization of the visual cortex, and the spread of the signal between pins could produce oddly placed phosphenes disrupting the intended representation. Based on these restrictions, we might design a stimulus with very low amplitude and frequency to limit spread and extend either pulse or train duration to improve the strength of the signal. In practice, this combination was determined to be the most effective through iterative testing (Schmidt et al., 1996).

Stimulus parameter relationships can also be used to transform effective paradigms into optimized or energy efficient strategies. Often a range of stimulation paradigms are used to accomplish the same task which creates unnecessary variability. Identifying the functional limitations of each parameter in the range can help develop standardized stimulation protocols for each task. In the case of motor cortex stimulation to produce forelimb movements, we observed

that the effect of frequency plateaued at maximum after 200 Hz, however many stimulation experiments use a higher frequency. In our experience, higher frequencies did not prove to be more effective or more reliable which suggests that there is room for further optimization of the parameters within the paradigm.

3.7 Conclusion

Using standard ICMS procedures to evoke MEP responses from the rat motor system we found that response amplitude and onset latency can be modulated by altering stimulus waveform parameters. In particular, we described the role each stimulus parameter exerts on the MEP metrics and identified parameters which can be altered to overcome performance deficits introduced by restrictions placed on each parameter of the stimulus. Understanding how the parameters of electrical stimuli shape the responses they evoke has implications for the development and optimization of clinical and research applications of brain stimulation. We propose a shift away from iterative testing approaches, replacing them with a design methodology in which we consider the desired physiological response and the neural activations necessary to achieve it. Our future work aims to quantify the effects of stimulation parameters on the duration and spread of the response and provide a model of parameter interactions.

3.8 Acknowledgements

The authors thank Boris Touvykine and Ian Moreau Debord for their contribution to data collection, Guillaume Elgbeili and Kelsey N. Dancause for consulting on statistical analysis procedures, Philippe Drapeau for assistance with programming, and Stephan Quessy for his input to this project.

CHAPTER 4 ARTICLE 2: INTRACORTICAL MICROSTIMULATION PARAMETERS DICTATE THE DURATION OF EVOKED RESPONSES

Meghan Watson[1,2], Mohamad Sawan[1], and Numa Dancause[2-3]

[1] Polystim Neurotechnologies, Institute of Biomedical Engineering, Polytechnique, Montreal, Quebec, Canada

[2] Département de Neurosciences, Faculté de Médecine, Université de Montréal, Canada

[3] Groupe de Recherche sur le Système Nerveux Central (GRSNC)

4.1 Presentation of the article

The data obtained from the experiments described in chapter 3 also provided information pertaining to the influence of stimulation parameters on the duration of the responses they evoke. The following article describes how stimulus signals can be shaped to extend or shorten the duration of the response. This article (Watson, Sawan, & Dancause, 2015) was submitted to the Journal of Neurophysiology on June 18th 2015 and is reproduced here in an updated version.

4.2 Abstract

. Microstimulation of brain tissue plays a key role in a variety of sensory prosthetics, clinical therapies and research applications; however the effects of stimulation parameters on the responses they evoke remain widely unknown. We aimed to investigate the contribution of each stimulation parameter to the motor evoked potential (MEP) duration. Additionally we sought to address the previously unexplored phenomenon of residual activation, which we defined as activation that lingers after the main response ends. We used constant-current, biphasic square waveforms in acute terminal experiments under ketamine anaesthesia. Stimulation parameters were systematically tested in a pair-wise fashion in the motor cortex of 7 Sprague-Dawley rats while MEP recordings from the forelimb were used to quantify the influence of each parameter. Stimulus amplitude and train duration were shown to be the dominant parameters responsible for increasing the MEP main response and residual activation durations, and interphase interval had no effect. Increasing stimulus frequency from 100-200 Hz or pulse duration from 0.18-0.34 ms extended the duration of the main response. Moderate and long pulse and train duration stimuli

produced longer residual durations. Stimuli involving moderate and long trains produced the highest occurrence and widest range of residual responses. Stimuli involving low amplitudes, low frequencies, short pulse durations, short train durations were less likely to induce residual activations. Our results show that the parameters of an ICMS stimulus exert significant influence on the spatial and temporal properties of the MEP responses they evoke, and as such can be tuned to modulate cortical activation.

***Key words**:* Intracortical microstimulation, stimulation parameters, neuroprostheses, rat, motor cortex, motor evoked potentials, EMG

4.3 Introduction

Since its advent in the early 19th century, stimulation of the brain has been used in a wide variety of clinical and therapeutic applications, many of which involve novel treatments for diseases and disorders such as visual (Dobelle, Mladejovsky, & Girvin, 1974; Schmidt et al., 1996; Tehovnik et al., 2009; Torab et al., 2011) and somatosensory (Berg et al., 2013; Tabot et al., 2013; Thomson et al., 2013) prosthetic devices, and deep brain stimulation therapies for Parkinson's Disease (Anderson et al., 2005; Deuschl et al., 2006; Little et al., 2013; Weaver et al., 2012) and epilepsy (Fisher et al., 2010; Lee et al., 2006; Morrell, 2011). These applications inject an electrical stimulus into neural circuitry in order to modify activity or produce sensations or behaviors. While brain stimulation plays a crucial role in countless therapies and research areas, little is known about how the parameters of the stimulation signal influence neural activity or how they shape the outputs produced.

Many types of stimulation signal have been explored but the most prevalent is the constant-current, cathode leading, biphasic square waveform (Lilly et al., 1955). The parameters of this signal include the current amplitude, pulse frequency, pulse duration, interphase interval and pulse train duration. Studies of the motor system have historically used short duration (<50 ms) stimulus trains composed of parameters proven to effectively elicit responses from the motor cortex (Asanuma et al., 1976). These high frequency short duration trains of intracortical microstimulation (HFSD-ICMS) are typically used to map motor areas of the brain by observing the brief movements or recording the evoked muscle activity they produce in anesthetized

animals (Asanuma & Rosen, 1972; Donoghue & Wise, 1982; Gioanni & Lamarche, 1985; Neafsey et al., 1986; Nudo et al., 1990; Sanderson et al., 1984).

Some general effects of stimulation parameters have been explored using these short trains. Stimulus frequency and train duration exert a combined influence on threshold levels by facilitating muscle contractions when excitation is hindered by low current intensity. Thresholds can be lowered by extending the train duration beyond 30 ms and increasing the pulse frequency above 300 Hz (Asanuma & Arnold, 1975; Asanuma et al., 1976), and the lowest movement thresholds occur when stimulating with frequencies between 181-400 Hz for durations of 15-33 ms (Young et al., 2011). Independently, the parameter of stimulus frequency can be used to limit the spread of the ICMS signal within the cortex. Pulses delivered at frequencies less than 20 Hz prevent the summation of excitatory and inhibitory postsynaptic potentials which localizes the activation (Cheney et al., 2013). Stimulus train duration is the dominant parameter influencing the accuracy of forelimb movement trajectories. Stimuli which last for 500-1000 ms are known to generate forelimb movements to stable, predictable end points regardless of initial limb position (Graziano et al., 2002).

To better understand the mechanism of microstimulation, it is essential to determine the exact effect exerted by each stimulus parameter on the resulting cortical activation and consequently, the outputs driven by this activity. The study of corticomotoneuronal cell activity can be used to predict electromyographic (EMG) activity (Griffin, Hudson, Belhaj-Saïf, McKiernan, & Cheney, 2008). Likewise, EMG activity recorded while stimulating the motor cortex provides insight into the relationship between the activity of cortical neurons and motor outputs (Hyland, 1998). Some studies have examined the effects of certain parameters on threshold levels (Koivuniemi & Otto, 2011; Koivuniemi & Otto, 2012; Murasugi, Salzman, & Newsome, 1993; Schiller, Slocum, Kwak, Kendall, & Tehovnik, 2011; Tehovnik & Slocum, 2007; Van Acker et al., 2013), however the duration of the EMG signal has been widely ignored. To our knowledge, these temporal components of the response have never been classified and independently assessed.

Here we systematically explore the effect of each parameter of a stimulation signal on the duration of the motor evoked potentials (MEP) elicited by microstimulation of the caudal forelimb area (CFA) of the rat primary motor cortex (M1). We assess the duration of the response by separating it into two components: 1) the main response, consisting of the initial Gaussian

shaped curve containing the signal's peak, and 2) the residual activation which we define as the activity which persists after the main response. We describe potential sources and interpretations of each component and discuss the implications of response duration as an assessment parameter.

4.4 Methods

4.4.1 Surgical procedures and data collection

Seven female Sprague-Dawley rats (Charles River, QC, CA) weighing 273-450 g were used in terminal acute experiments. All procedures followed the guidelines of the Canadian Council on Animal Care and were approved by the Comité de Déontologie de l'Expérimentation sur les Animaux of the Université de Montréal.

Anaesthesia was induced with intraperitoneal ketamine injection (80 mg/kg) and maintained with isofluorane (~2% in 100% oxygen). Subcutaneous injection of mannitol (4 g/kg) and intramuscular injection of dexamethasone (1 mg/kg) were given prior to the craniotomy to prevent swelling and oedema. A self-regulating heating pad maintained body temperature which, along with pulse rate and oxygen saturation, was monitored continuously throughout the surgery. Insulated, multi-stranded wires (Cooner Wire, Chatsworth CA, USA) were implanted in the extensor digitorum communis muscle of the forelimb contralateral to the stimulating electrode to detect MEP signals which were monitored and recorded at 5 kHz (RZ5 BioAmp Processor) and analyzed offline.

The animal was placed in a stereotaxic frame for both the surgical and stimulation procedures; positioned to allow free movement of the forelimb. A small craniotomy (8 mm x 5 mm) exposed the motor cortex (left hemisphere), the dura was removed and mineral oil applied to protect the cortex. Anaesthesia was switched to ketamine (~10 mg/kg/10 minutes) administered through intraperitoneal injections as needed for the duration of the stimulation procedure.

In order to control for the effects of stimulus current amplitude and ensure a consistent level of excitability across all test sites, we set selection criteria. Sites were chosen within the caudal forelimb region of the motor cortex which produced MEP responses as recorded from the extensor digitorum communisis muscle of the forelimb. MEP threshold levels were determined by increasing the stimulus amplitude (up to 50 μA) until a MEP response was observed. We then

lowered the stimulus amplitude until the response disappeared. The lowest stimulus amplitude at which the MEP response could be evoked was defined as the threshold amplitude. We sought stimulation sites which had MEP threshold amplitudes of 25-35 μA to ensure that all test sites had similar levels of excitability and to set a control value for amplitude within the stimulation protocol. The control value for amplitude (Table 1) was set to 50 μA in order to be twice as strong as the site's threshold level.

Sites within the CFA were tested for the selection criteria using a standard ICMS train: 13 monophasic square pulses of 0.2 ms duration with 3.3 ms between the pulses delivered at 1 Hz (Donoghue & Wise, 1982; Nudo et al., 1990; Stowe et al., 2007; Touvykine et al., 2015). The response was first tested at 1500 μm targeting output layer V, which is known to contain pyramidal neurons which project to lower motor neurons to produce movements (Wang & Kurata, 1998). If a threshold MEP response was produced in the extensor digitorum communisis muscle this depth was selected, if not, the electrode was advanced to find a suitably responsive site. Electrode depth varied from 1534-2104 μm (mean 1792 μm) between sites and only one depth was used within an electrode tract. All experimental blocks were tested in 2 sites per rat.

Stimulation was delivered with a digital stimulator (TDT IZ2 Stimulator and RZ5 BioAmp processor), through a glass insulated tungsten microelectrode (FHC Bowdoin, ME USA, UEWSDESGBN4G, 110-175 kΩ) manipulated by a microdrive (David Kopf Instruments Model 2662, Tujunga, CA). At the end of the data collection, the animal was euthanized with a lethal dose of sodium pentobarbital.

4.4.2 Stimulation protocol

We designed a stimulation protocol to systematically test the influence that each parameter of an ICMS signal exerted on the MEP it produced when delivered to the CFA of the rat motor cortex. The constant-current, cathode leading, biphasic square waveform was chosen since it is the most prevalent in both research and therapeutic applications of ICMS. The parameters of this signal include the current amplitude, pulse frequency, pulse duration, interphase interval and pulse train duration (Figure 1). We selected the test ranges of each stimulation parameter so that they included the typical values used in common prosthetic devices and therapeutic applications of brain stimulation. In particular, the ranges reflect the most restrictive stimulation paradigm among the applications: visual prosthetic devices (Schmidt et al., 1996).

The test range of each parameter was divided evenly into five levels (low, low-mid, mid, mid-high, and high) and a control value was set which was derived from the standard stimulation signal proven to be effective in the rat motor cortex (Donoghue & Wise, 1982; Nudo et al., 1990; Stowe et al., 2007; Touvykine et al., 2015). The control value for amplitude was set to 50 µA, which was twice the threshold level since all stimulation sites were deliberately chosen to have thresholds of approximately 25 µA. The ranges, levels and control values selected for each parameter can be found in Table 1.

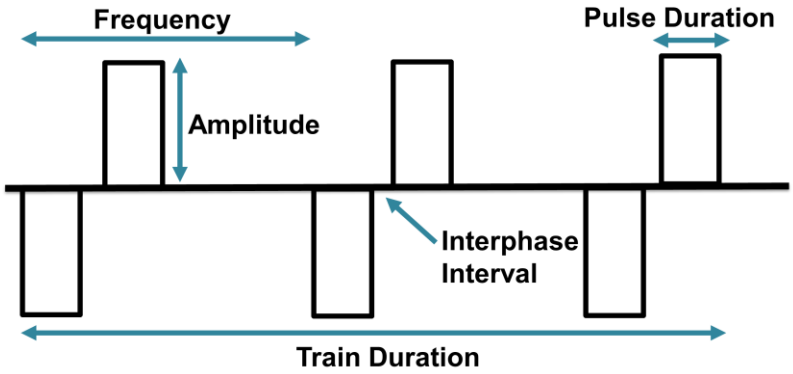

Figure 4-1: Parameters of the constant-current, biphasic square waveform.

Table 4-1: Parameter test values.

Parameter	Unit	Range	Test Levels	Control	Parameter Pairs
Amplitude (A)	µA	30-65	30, 39, 48, 56, 65	50	AF, AP, AI, AT
Frequency (F)	Hz	100-500	100, 200, 300, 400, 500	303	FA, FP, FI, FT
Pulse Duration (P)	ms	0.18-0.5	0.18, 0.26, 0.34, 0.42, 0.5	0.2	PA, PF, PI, PT
Interphase Interval (I)	ms	0.08-0.5	0.08, 0.19, 0.29, 0.40, 0.5	0	IA, IF, IP, IT
Train Duration (T)	ms	43-300	43, 107, 172, 236, 300	43	TA, TF, TI, TP

The stimulation protocol was composed of five experimental blocks designed to test the specific influence that each of the five parameters of the stimulation signal exerted on the MEP signal. Each block focused on one parameter, systematically testing it against the other four parameters in a pair-wise fashion. The parameter of focus was called the primary parameter and each parameter tested against it was referred to as the paired parameter. The primary parameter was tested at all five levels in the range (low, low-mid, mid, mid-high, and high) against three levels of a paired parameter (low, mid, high) while all other parameters were held at their control values (see Table 1). This allowed us to observe how the MEP signal changed in response to changes in the primary parameter and identified interactions occurring between the primary and paired parameters.

To test the effects of current amplitude for example, all five values in the amplitude range (30, 39, 48, 56, 65 μA) were tested at 3 frequency levels (low-100 Hz, mid-300 Hz, and high-500 Hz) with pulse duration, interphase interval and train duration held at the control values (0.2 ms, 0 ms and 43 ms respectively). Similarly, all five values in the amplitude range (30, 39, 48, 56, 65 μA) were tested at 3 pulse duration levels (low-0.18 ms, mid-0.34 ms, and high-0.5 ms) with frequency, interphase interval and train duration held at the control values (303 ms, 0 ms and 43 ms respectively). This procedure was then repeated until each parameter had been tested against amplitude in this "pair-wise" arrangement representing all the conditions contained in the amplitude test block. All "parameter pairs" are listed in the far right column of Table 1.

Each pair-wise condition within a block was tested with ten trials, and all trials within a block were pseudo-randomized with 1 second between trials. The trial order within a block was preserved, however to ensure that there were no adverse effects of conducting the trials of a block in a fixed order we compared results from overlapping conditions between blocks. These comparisons were also used to determine if the primary parameter of the block had an overall effect on the MEP signals produced within it. The five experimental blocks resulted in a total of 300 independent test conditions (5 parameters x 5 test levels x 4 paired parameters x 3 test levels). To control for fatigue of the preparation, all five blocks were tested in a randomized order at two different sites within the CFA of each rat for a total of 14 sites.

4.4.3 Classification of MEP response components

We observed that many MEP responses consisted of two main components: an initial Gaussian shaped curve containing the signal's peak and a secondary component of lesser amplitude which can take the shape of a Gaussian curve (Figure 2c,e,h, i), exponential decay (Figure 2f), or inverse exponential decay (Figure 2g). We labeled these two components the "main response" and "residual activation" respectively (Figure 2c). It is important to note that the residual activation is not present in all MEP responses and is largely dependent upon the parameters of the stimulation signal. While the majority of MEP responses are replicas of Figure 2c with a distinct baseline crossing, a wide variety of signal envelopes were encountered (Figure 2d-i), and the residual can be entirely absent (Figure 2d) or endure for hundreds of milliseconds. Despite these variations, the demarcation between the two regions of the response is always discernible both computationally and visually.

From a computational standpoint, a number of criteria were developed to automate the designation between the main response and residual activation. The MEP response's baseline was defined as the average of the recorded signal taken 10 ms prior to stimulation. Averaging the first 50 sample points of the recording provided the baseline for each individual trial. The main response began shortly after the onset of stimulation, and was detected as the first instance where ten sequential sample points of the MEP signal remained above the trial's baseline level. If residual activation occurred in a trial, it began at the offset of the main response and continued until the signal returned to baseline for 10 sample points.

In the case of Gaussian shaped residuals, the main response offset was computed as the first instance after the main response peak in which the signal falls within 3 standard deviations of baseline for 10 sample points. If a baseline crossing was not achieved, the main response offset was taken as the point of lowest signal amplitude between the peaks of the main and residual responses. In the case of exponential decay and inverse exponential decay shaped residuals (i.e. no secondary peaks), the main response offset was taken as the first instance where the signal amplitude fell below 1/8th of the peak value. All responses were classified computationally and their accuracy was confirmed with visual inspection.

4.4.4 Statistical analysis

A maximum of two trials per condition were excluded if they were contaminated by noise. The stimulus artifact was small due to the low amplitudes of stimulation and was removed with a 5-point moving average filter. For each of the 14 stimulation sites, trials were averaged to produce a mean response for each condition. The means of the main response duration and residual activation duration were derived from these averages (Figure 2) and values are reported as mean ± standard deviation.

Certain combinations of parameter pairs using current amplitudes near threshold levels did not cause sufficient excitation to evoke any MEP responses. Specifically, 30-39 μA stimuli delivered at 100 Hz, or 30 μA stimuli delivered by 43 ms duration trains were ineffective. A condition was included in the statistical analysis if responses were obtained from a minimum of 5 stimulation sites. Conditions evoking a response from less than 5 sites will be referred to as infrequent responses and typically occurred for stimuli composed of low amplitude short pulses delivered at low frequencies. To differentiate between absent and infrequent responses, data obtained from infrequent responding conditions (<5 sites) are included in graphical representations differentiated by marker type.

To evaluate the effects of each parameter on the response metrics we used a repeated measures linear mixed model, with random slope and intercept, followed by Bonferroni posthoc analyses to test the effects of main and paired parameters on outcomes. Main and paired parameters were entered as fixed factors, followed by the interaction between the two. The interaction term was significant only when amplitude was the primary parameter paired with train duration, for all other outcomes it was not significant and was trimmed from the model.

Analyses were conducted with SPSS 22.0 (SPSS, Inc.) software using the mixed procedure with a factorial design and a significance level of $\alpha<0.05$. We report only statistically significant findings. If a value is absent it indicates that the particular condition either did not produce significant trends or was excluded from the analysis due to infrequent responses (<5 sites). In the text we indicate which results are excluded due to infrequent responses. Correlation analyses between the duration of the MEP and other characteristics of the response were conducted with Pearson's correlations. A t statistic was used to establish if the correlation was statistically

significant. The residual activation occurred inconsistently, and as such was described in terms of its frequency of occurrence, mean and range of duration.

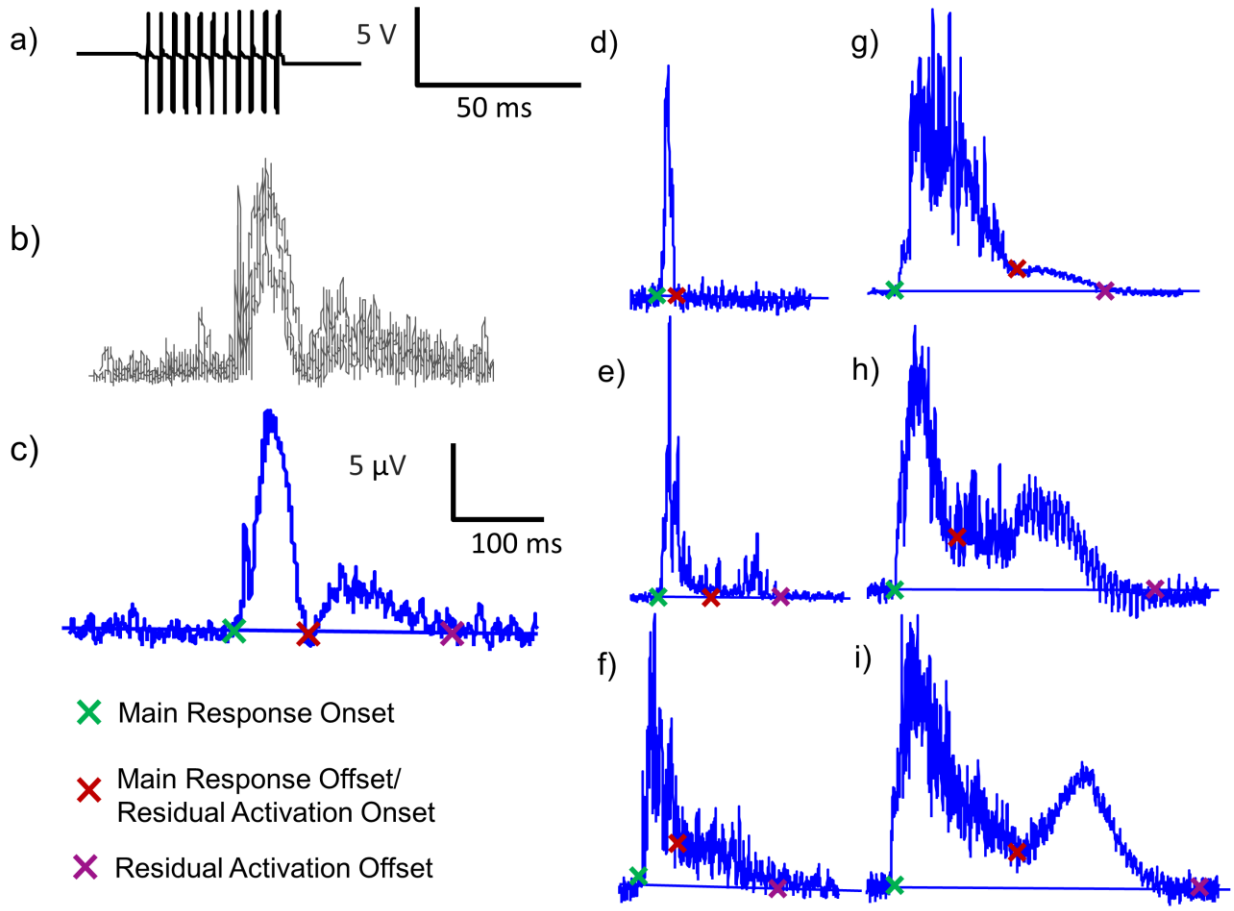

Figure 4-2: Classification of MEP Signal Components. Each MEP response was separated into two components: 1) the main response, defined as the large component of the signal containing the MEP's peak, and the 2) residual activation defined as the region of lesser activation which persisted after the main response (a-c). Components c-i depict the shape of a variety of signal envelopes and their respective component classifications.

4.5 Results

Four of the five experimental blocks showed significant trends demonstrating the effects that each parameter exerted on the MEP response duration. The interphase interval parameter did not exert an influence on the MEP response duration within the range tested (0.08-0.5 ms). When describing the results, all parameter pairs will be denoted by abbreviations of Table 1 in which the primary parameter appears first and paired parameter second (ex. AF represents amplitude paired with frequency).

4.5.1 MEP main response duration

The MEP main response duration increased with stimulus amplitude for all parameter pairings (AF: $p<0.001$; AP: $p<0.001$; AT: $p=0.004$) as shown in Figure 3. As a paired parameter, increases in stimulus amplitude could extend the response duration up to 19% when its value was raised from its mid (48 μA) to high (65 μA) levels (FA: 19% increase, $p=0.048$; TA: 16% increase, $p=0.003$) and 33% when raised from low (30 μA) to high (65 μA) levels (PA: 33%, $p=0.009$). When high amplitude (48-65 μA) stimuli were delivered by long duration trains the main response duration plateaued suggesting an upper limit for this parameter pairing after which the duration of the main response cannot be extended. Conversely, when low amplitude stimuli are used, the duration of main response is most effectively extended by increasing the stimulus pulse duration or train duration. Under these conditions, the responses evoked by the longest pulse durations (0.5 ms) were 41% longer than those evoked by the highest frequency (500 Hz) stimuli, however the longest train duration (300 ms) evoked responses 3.3 times longer yet still.

The MEP's main response duration increased with stimulus frequency for all parameter pairings (FA: $p=0.046$; FP: $p=0.015$; FT: $p=0.005$), most noticeably between 100-200 Hz (Figure 3a). When stimulating with frequencies above 200 Hz, the response plateaued at a maximum whose magnitude was dictated by the paired parameter. Increasing the frequency from low (100 Hz) to high (500 Hz) levels could extend the main response duration (PF: 39%, $p=0.02$), however mid (300 Hz) and high (500 Hz) frequency stimuli evoked similar durations (AF: $p=0.43$; PF: $p=0.49$; TF: $p=0.69$). When stimulation frequency was low, extending the duration of the stimulus train was the most effective method of increasing the main response duration. Under these conditions,

the longest trains (300 ms) produced responses 4-4.2 times longer than those of the longest pulse (0.5 ms) and highest amplitude (65 µA) stimuli respectively.

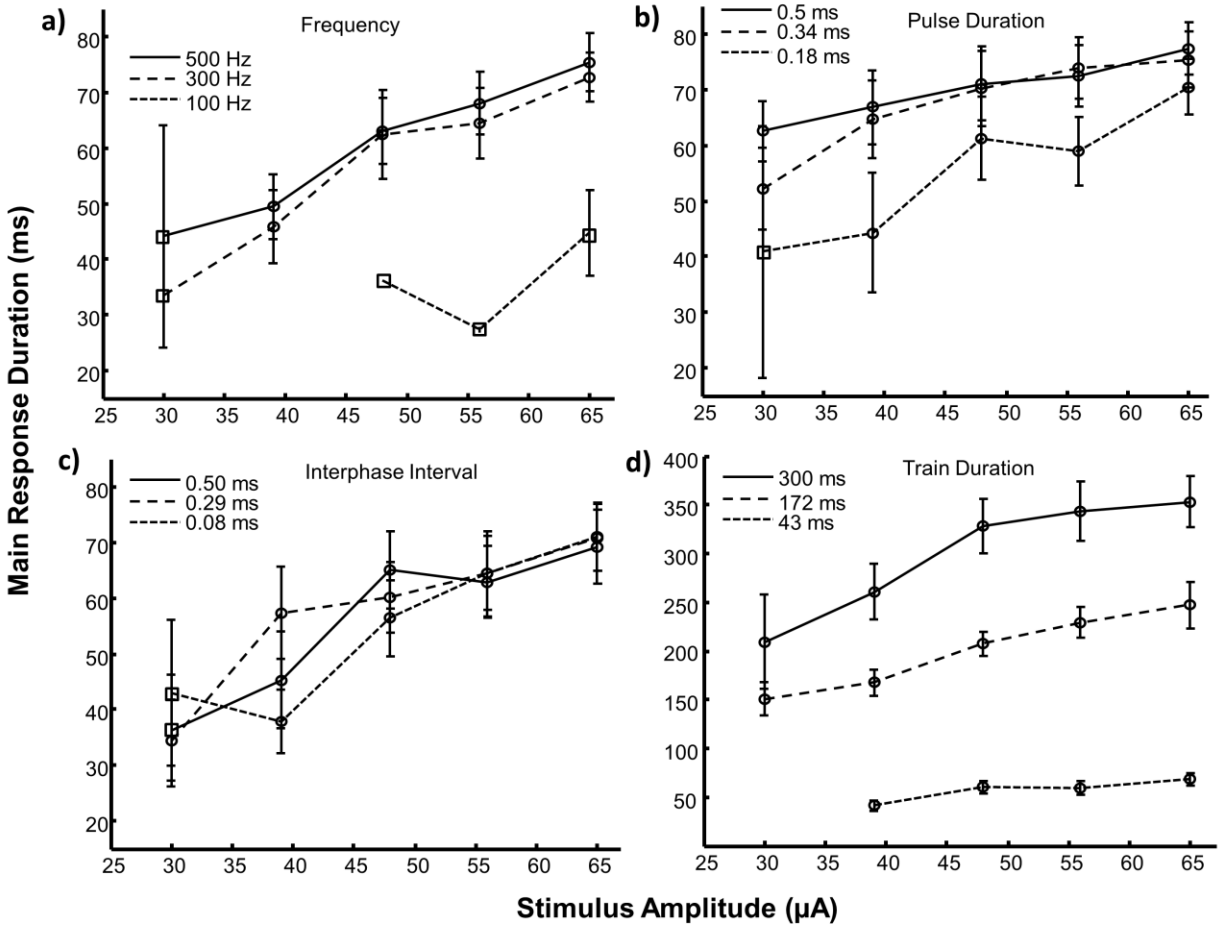

Figure 4-3: Representation of the MEP main response duration (mean ± SE) as a function of stimulus amplitude. The effects of amplitude paired with three frequency levels (a), pulse durations (b), interphase intervals (c) and train durations (d) are depicted. Note the difference in scale for trials involving train duration (part d).Square symbols represent conditions with an insufficient number of responding sites (n<5) and were not included in statistical analysis. Circular symbols represent conditions with reliable responses (n=5-14). Control values for each parameter were: A=50 µA, F=303 Hz, P=0.2 ms, I=0 ms, T=43 ms. F=frequency, P=pulse duration, I=interphase interval, T=train duration, SE=standard error.

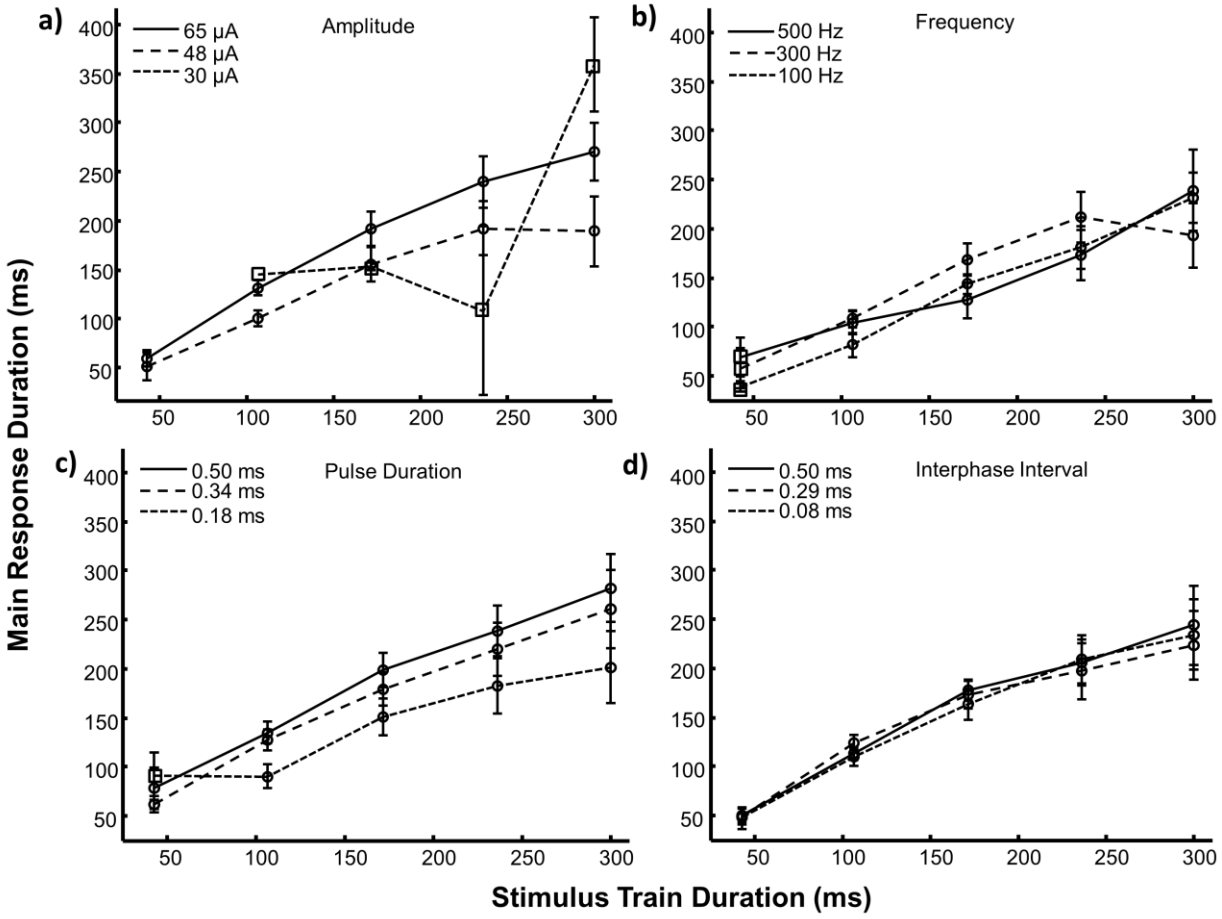

Figure 4-4: Representation of the MEP main response duration (mean ± SE) as a function of stimulus train duration. The effects of train duration paired with three current amplitudes (a), frequencies (b), pulse durations (c) and interphase intervals (d) are depicted. Square symbols represent conditions with an insufficient number of responding sites (n<5) and were not included in statistical analysis. Circular symbols represent conditions with reliable responses (n=5-14). Control values for each parameter were: A=50 µA, F=303 Hz, P=0.2 ms, I=0 ms, T=43 ms. F=frequency, P=pulse duration, I=interphase interval, T=train duration, SE=standard error.

The MEP main response duration increased with stimulus pulse duration only when paired with frequency (PA: p=0.085; PF: p=0.04; PT: p=0.06). Increasing stimulus pulse duration from short (0.18 ms) to mid (0.34 ms) levels extended the duration however pulses longer than 0.34 ms had no further effect. As a paired parameter, increasing the pulse duration from short (0.18 ms) to long (0.5 ms) could extend the main response duration between 20-32% (AP: 20%, p=0.021; FP: 24%, p=0.011; TP: 32%, p=0.001). When short pulse durations were used, the main response

duration was most effectively extended by increasing the train duration. Under these conditions, the longest trains (300 ms) evoked responses 4.25-4.45 times longer than highest amplitude (65 μA) and frequency (500 Hz) stimuli respectively.

The MEP main response duration increased with stimulus train duration for all parameter pairings (TA: $p<0.001$; TF: $p<0.001$; TP: $p<0.001$). These effects were less pronounced once the train duration reached 172 ms and do not observe a direct linear relation (Figure 4). As a paired parameter, increasing stimulus train length from short (43 ms) to mid (172 ms) durations could extend the response duration up to 3.81 times (AT: increase 3.81x, $p<0.001$; FT: increase 3.06x, $p<0.001$; PT: increase 3.19x, $p<0.001$). Similarly, increasing the train length from mid (172 ms) to long (300 ms) durations increased the response duration yet again (AT: increase 1.49x, $p<0.001$; FT: increase 1.39x, $p<0.001$; PT: increase 1.51x, $p<0.001$). For all durations of the stimulus train, increasing the amplitude or pulse duration served to further extend the duration of the MEP's main response however pulse duration had less effect on short duration trains (43 ms).

4.5.2 MEP residual activation occurrence and duration

Figure 5 shows how often residual activations occur (top panel) and demonstrates the mean and range of durations associated with them as a function of the stimulus parameters (bottom panel). We observed that the occurrence of residual activations increases with stimulus amplitude for all parameter pairings. The stimuli involving moderate and long trains tended to produce the highest percentage of residual occurrences. These long trains produced residual activations in more than 80 % of the trials representing these conditions and were also shown to produce substantial main response durations.

Certain parameter ranges are less likely to induce residual activation, including low amplitudes, low frequencies, short pulse durations, short train durations and combinations thereof. In particular, we observe the absence of residual responses when stimuli combine low amplitudes (30-39 μA) with low frequency (100 Hz), or short pulse duration (0.18 ms). These conditions were also shown to produce short main response durations suggesting that these conditions evoked smaller levels of activity overall.

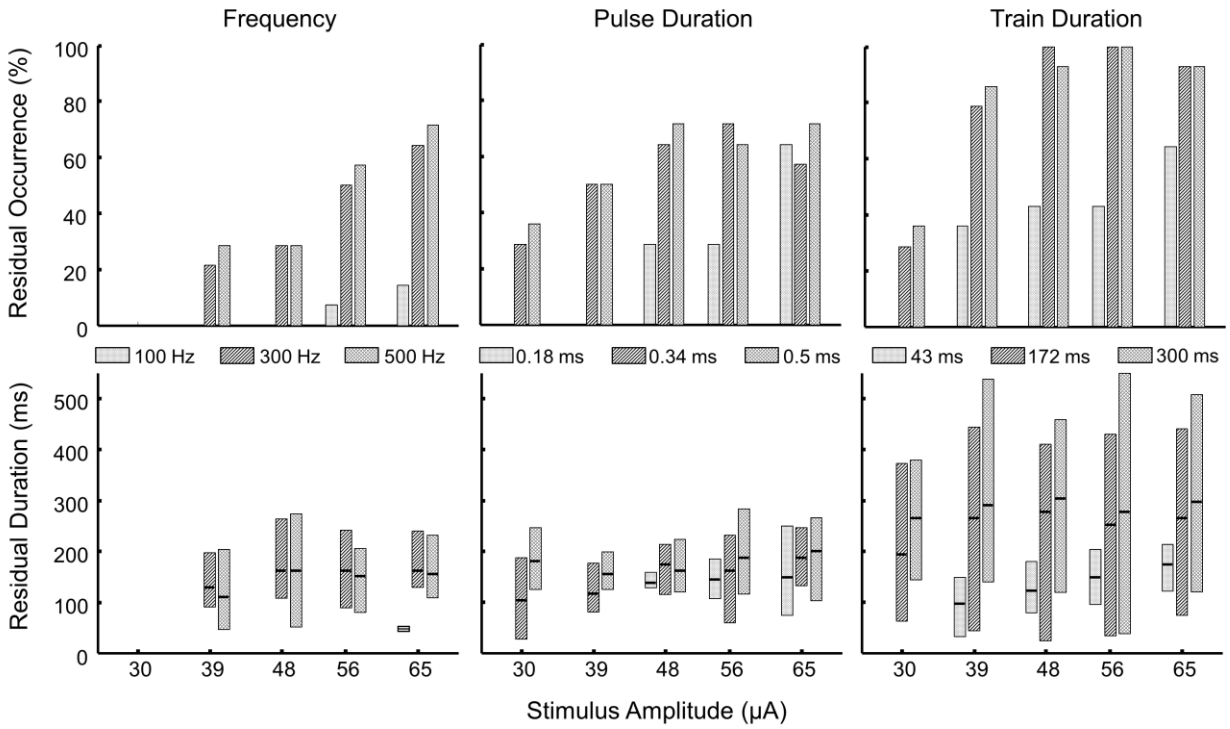

Figure 4-5: Comparison of MEP residual activation duration occurrence, mean and range as a function of stimulus amplitude. The top panel shows how frequently a residual response was produced for a given stimulus condition. Percentage occurrence was calculated as the number of times a residual response occurred out of the total number of trials for the particular stimulus condition. The bottom panel shows the range in residual durations as well as the mean residual duration for a given stimulus condition. Residual duration ranges were determined as the maximum and minimum durations observed in trials which produced a residual response. The mean was calculated from the trials which produced a residual response per given stimulus condition and is represented by the white horizontal line within each range bar. F=frequency, P=pulse duration, T=train duration.

We observed that the mean value of the residual duration tended to increase with stimulus amplitude. Similarly, the long pulse durations and long train durations tended to produce higher mean values of residual duration. The variability of the ranges appeared to be primarily tied to the influence of the paired parameter levels. These ranges tended to increase as the paired parameter's value was increased, particularly for the parameter of train duration. The long stimulus trains tended to produce a wider range of residual durations than their shorter counterparts.

4.5.3 Correlation between durations and other MEP parameters

Certain metrics of the MEP response were valid predictors of the main response and residual activation durations. A total of four metrics in addition to the main and residual durations served to quantify the MEP response. Onset latency was defined as the delay between the onset of stimulation and the initiation of the MEP. The mean was computed as the average of the main response component, whereas peak amplitude was the signal's maximum during the main response component. Peak time specifies the time instance of the peak amplitude occurrence. Pearson's correlation coefficient was computed for each block of trials to provide a quantitative measure of the strength and direction of the relationships between the response metrics (Evans JD, 1996).

The correlation with onset latency was negligible for the residual activation duration ($r=-0.03$, $p=0.62$) but was however correlated to the main response duration ($r=0.15$, $p<0.01$). Peak amplitude was strongly correlated with the main duration ($r=0.36$, $p<0.001$), and with the residual activation duration ($r=0.58$, $p<0.001$). Similarly, the mean amplitude was strongly correlated with the main duration ($r=0.43$, $p<0.001$) and with the residual activation duration ($r=0.64$, $p<0.001$). Peak was strongly correlated with both the main ($r=0.70$, $p<0.001$) and residual durations ($r=0.55$, $p<0.001$). Finally, as mentioned previously, the durations of the residual activation and main response are very strongly correlated ($r=0.91$, $p<0.001$). These findings suggest that stimuli that produce large or delayed peaks also result in longer main responses and residual activations. Similarly, responses that produce long main durations tend to produce longer residual activations.

4.6 Discussion

This study examined the factors influencing the duration of the MEP response, and for the first time, separated this signal into two key components. Until now, the residual activation component has largely been ignored, either excluded from the response entirely or lumped together with the main response. Procedures for defining MEP offsets vary in their methodology, and common practices either place the offset at the time of baseline crossing or truncate the response at the time when the signal amplitude returns to a certain percentage of the peak. Our findings demonstrated that the shape of the MEP response signal envelope varies greatly and is heavily dependent on the stimulation parameters. As such, neither of the commonly used offset

definition procedures are adequate on their own as they do not independently account for variability in signal shape. Whether the residual takes the shape of a Gaussian, exponential decay or inverse exponential decay curve, this component is markedly different from the main response and deserves careful classification and demarcation from the main component.

Certain temporal and spatial metrics of the MEP response could be used to predict the main and residual activation durations. Of the temporal metrics, peak time was strongly correlated to both response durations, whereas onset latency was only a predictor for the main response duration. The durations of the residual and main response are strongly correlated, and stimuli that induced long main durations also produced long residual activations. Of the spatial metrics, the peak and mean amplitudes were correlated to both main and residual response durations. These findings suggest that the spatial and temporal metrics of the MEP response are directly linked and their interactions must be considered when designing a stimulus signal.

We demonstrated that the duration of the MEP response main and residual can be modulated through alterations to stimulation parameters. The MEP main response duration increased with all stimulus parameters and this increase was continual for the parameters of stimulus amplitude and train duration although the effects were less pronounced for trains longer than 172 ms. Notably, the MEP durations did not scale directly with the duration of the stimulus train and responses as short as 25 ms could be evoked with a 43 ms stimulus. For the parameters of frequency and pulse duration, no further increases in response duration were observed beyond the range of 100-200 Hz and 0.18-0.34 ms respectively.

Previous studies reported the lowest movement thresholds to occur when stimulating with frequencies between 181-400 Hz, with no significant difference in thresholds for frequencies between 142-400 Hz (Young et al., 2011), and our previous work demonstrated the limit to frequency influence on MEP reliability to occur between 100-200 Hz (Watson et al., 2015a). Combined with our present results we suggest that the rat forelimb system is sensitive to frequencies below 142 Hz and no further excitation is produced by the higher frequency stimulation which is commonly used in this system. Similarly, studies exploring long duration stimulation (HFLD-ICMS) typically use 500 ms trains (Brown & Teskey, 2014; Graziano et al., 2002; Griffin, Hudson, Belhaj-Saïf, & Cheney, 2014; Van Acker et al., 2013), which are nearly 3 times the maximum level we observed to be effective at increasing response duration and nearly

5 times the level we observed to influence MEP reliability, amplitude and latency. These results could suggest that multi-synaptic projection induced by the current spread from these sustained stimuli may be responsible for producing the complex movements of HFLD-ICMS and that limited spread is observed within our parameter range.

Microstimulation and natural stimulation have vastly different mechanisms of action and as such, produce vastly different responses within the cortex. The spike response to visual stimulation, for example involves a short delay period after the stimulus followed by a period of excitation lasting up to several hundred milliseconds (Wurtz & Mohler, 1976). The spike response to electrical stimulation however has an initial excitation component occurring shortly after the stimulus is applied, followed by a period of inhibition lasting up to 100 ms, which was sometimes followed by a rebound period of activation (Butovas, 2003). This rebound activation was described as intermittent in occurrence and as presenting a variety of shapes and durations. Although no firm conclusions can be drawn with the present data set, it is possible that the main duration is the physical manifestation of the initial excitation period, which falls to baseline during the inhibitory period only to return as the residual response during the rebound activation period. Alternatively, the main response could reflect the direct activation of neurons surrounding the stimulation site, while the residual activation could reflect indirect activation at sites farther from the electrode caused by post-synaptic transmission. It is also possible that the residual activation is simply an after effect due to sustained activation of neurons in the cortex or the tissues they innervate in the forelimb.

An inherent weakness of this study is that it was conducted under anaesthesia and at present we cannot ascertain the presence and shape of the residual in awake, behaving animals. We hypothesize that the factors which influenced the MEP durations will preserve their general trends; however different limits are likely to be observed specific to the species and muscle group under study. Additionally, our study addressed evoked movements only, and whether or not the residual component of the MEP response is present in volitional movements remains to be determined.

To our knowledge, the phenomenon of residual activation has not been previously assessed; however it may have significant implications in the design of a stimulation signal. In applications where a brief, localized stimulus is desired, the residual activation may not be

desirable. In these instances, stimuli involving combinations of low amplitude, low frequency, short pulse durations and short train durations could be used to limit both main and residual durations. Conversely, when restriction are placed on certain stimulus parameters and longer response durations are desired, both the main and residual durations can be increased most effectively by extending the stimulus train duration and to a lesser extent by increasing the pulse duration and amplitude. In particular, residual activation was strongly linked to the stimulus amplitude and train duration suggesting that these parameters dominate its prevalence, duration and magnitude. Similarly, if the residual activation component is determined to be absent from volitional movements it would suggest that this component is a by-product of stimulation. Properties of the evoked response can however be modulated via alterations to the stimulation signal parameters to evoke responses which mimic those produced naturally.

4.7 Conclusion

Despite some unresolved issues regarding the underlying mechanism of the main and residual response durations, our data shows that the traditional ICMS signal used for study of the motor cortex could be improved. Frequencies above 200 Hz do not improve the reliability or extend the duration of MEPs. Similarly, stimulating with trains longer than 172 ms does not substantially extend the response duration. Responses without residual activations may suggest more localized stimulation and can be achieved by limiting the parameters of a stimulus. As such, it is essential to consider the desired physiological response and appropriate parameter combinations necessary to achieve it when designing a stimulus, and both the properties and underlying cause of the response components (main and residual) deserve further study.

4.8 Acknowledgements

The authors thank Boris Touvykine and Ian Moreau Debord for their contribution to data collection, Guillaume Elgbeili and Kelsey Dancause for consulting on statistical analysis procedures, Stephan Quessy for comments on experimental design and data processing, and Philippe Drapeau for assistance with programming the stimulation equipment.

CHAPTER 5 ARTICLE 3: EFFICIENT MICROSTIMULATION OF THE BRAIN: A PARAMETRIC APPROACH

Meghan Watson[1,2], Numa Dancause[2] and Mohamad Sawan[1]

[1] Polystim Neurotechnologies, Institute of Biomedical Engineering, Polytechnique, Montreal, Quebec, Canada

[2] Département de Neurosciences, Faculté de Médecine, Université de Montréal, Canada

5.1 Presentation of the article

In the preceding chapters, we have shown that stimulus parameters exert considerable influence on the properties of the responses they evoke. These parameters also determine the reliability of a stimulus signal and certain parameter combinations are more effective for response evocation. The following article describes which parameter combinations are most effective for eliciting responses and details strategies to boost reliability in the case of application-dependent restrictions on the stimulus signal. This article (Watson, Dancause & Sawan 2015a) is reproduced here as it was published in the Proceedings of the 37th Annual International Conference of the IEEE Engineering in Medicine and Biology Society on August 28th, 2015.

5.2 Abstract

Microstimulation of brain tissue plays a key role in a variety of sensory prosthetics, clinical therapies and research applications. At present, tailoring the parameters of a stimulation signal to a specific goal relies heavily on parameters from literature. Optimization methods seek to improve tried and tested waveforms developed for specific purposes, however the fundamental understanding of how stimulation parameters interact and the effects these interactions have on brain tissue remains widely unknown. This study explores the interactions between parameters of the constant-current, biphasic square waveform with the intention of developing a stimulation efficient strategy. We find that, the traditional premise of a waveform's effectiveness being dominated by its amplitude does apply, however exceptions are noted which may be of essential importance to the development of electrical stimuli in restrictive paradigms.

Index Terms—Microstimulation, neuroprosthesis, stimulation parameters

5.3 Introduction

Microstimulation of brain tissues has a wide range of applications including visual (Dobelle & Mladejovsky, 1974; Schmidt et al., 1996) and somatosensory prosthetic devices (Thomson et al., 2013), deep brain stimulation therapies for Parkinson's disease (Anderson et al., 2005), and epilepsy (Lee et al., 2006; Morrell, 2011) and countless research applications involving many different regions of the brain. Despite the different purposes of the stimulation and variability in the type of electrodes used, the overall goal is to produce an effective stimulus. An effective stimulus is one which accomplishes the goal of the stimulation reliably and consistently without damaging the surrounding tissues or causing adverse effects.

One of the most prevalent microstimulation signals is the constant-current, cathode leading, biphasic square waveform. This waveform is used extensively in clinical and research applications as it is historically suggested to be safe and effective (Lilly et al., 1955). The parameters of this signal include the current amplitude, pulse frequency, pulse duration, and train duration (Figure 5-1). Some of these parameters are known to induce tissue damage within specific ranges (McCreery et al., 1995), and most applications have restrictive requirements of the stimulus.

Many efforts have been made to optimize a signal for its specific purpose, by developing waveforms through modeling (McIntyre et al., 2009), or iterative testing (Koivuniemi & Otto, 2012; Rajdev et al., 2011; Young et al., 2011) of parameter combinations shown to be successful from past experience. This approach inevitably results in multiple signals addressing the same problem since many effective parameter combinations exist for each application. Although many combinations can produce the desired outcomes, certain combinations are less reliable than others and this reliability should be considered in the stimulus design. To this end, we systematically explored the influence that signal parameters and their interactions have on the effectiveness of the biphasic waveform stimulation signal in terms of its ability to consistently evoke a response. Signals were classified based on their contribution to responsiveness, and parameters that can be used to improve responsiveness in restrictive paradigms were identified.

5.4 Methods

In many sensory and motor research experiments, strong stimuli are used to ensure a response is produced, however this approach is largely unsuitable for clinical and prosthetic applications. We chose to examine clinically relevant parameter ranges; specifically those developed for visual prosthetic devices which have extremely restrictive stimulation paradigms (Schmidt et al., 1996). These paradigms employ the principle of "minimum effective dose" in which a stimulus is just strong enough to produce a visual percept (phosphene), but not strong enough to cause interactions between neighboring electrodes or tissue damage at the electrode interface.

5.4.1 Experimental design

We chose to work in the rat model, stimulating the caudal forelimb area of M1 in motor cortex; a region which is known to produce forelimb movements in anaesthetized animals (Donoghue & Wise, 1982). The signal's reliability was quantified by recording the electromyographic (EMG) signals of forelimb muscles to determine if a response was produced.

5.4.2 Stimulation protocol

Four experiments were conducted to test the specific effects of each constant-current, biphasic square waveform parameter on the production of an EMG response. The waveform parameters and their ranges are specified in Table 5-1. Each experiment focused on one parameter, testing it against all other parameters in a pair-wise fashion. Parameters not involved in the comparison were held at a control value derived from the standard stimulation signal proven to be effective in the rat motor cortex (Donoghue & Wise, 1982), and the control amplitude was set to 50 μA which was double the threshold level of each stimulation site.

For example, all amplitude levels were tested at 3 frequency levels (low, mid and high) with pulse duration and train duration held at the control values. This procedure was then repeated until each parameter had been tested in this "pair-wise" arrangement resulting in a total of 180 independent conditions to test all parameters (4 parameters x 5 test values x 3 paired parameters x 3 levels). Each parameter was tested in a separate experimental block with ten trials for each condition and all trials were pseudo-randomized with 1 second between trials. The four

experiments were conducted in a randomized order at two different stimulation sites within the motor cortex of each rat (14 sites in total).

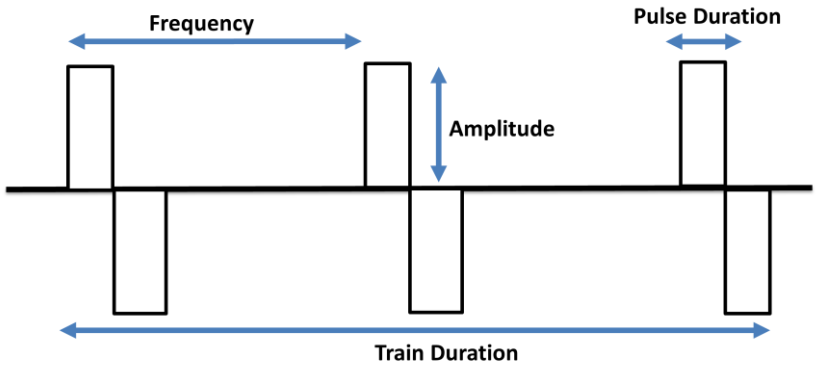

Figure 5-1: Parameters of the constant-current, biphasic square waveform.

Table 5-1: Parameter test values

Parameter	Unit	Test Levels	Control
Amplitude (A)	µA	30, 39, 48, 56, 65	50
Frequency (F)	Hz	100, 200, 300, 400, 500	303
Pulse Duration (P)	ms	0.18, 0.26, 0.34, 0.42, 0.5	0.2
Train Duration (T)	ms	43, 107, 172, 236, 300	43

5.4.3 Surgical procedures

Seven female Sprague-Dawley rats (Charles River, QC, CA) weighing between 273-450 g were used in terminal acute experiments. Anaesthesia was induced with intraperitoneal ketamine injection (80 mg/kg) and maintained with isofluorane (~2% in 100% oxygen). Subcutaneous injection of mannitol (4 g/kg) and intramuscular injection of dexamethasone (1 mg/kg) were given prior to the craniotomy to prevent inflammation. A self-regulating heating pad maintained body temperature which, along with pulse rate and oxygen saturation, was monitored continuously. Insulated, multi-stranded wires (Cooner Wire, Chatsworth CA, USA) were implanted in the extensor digitorum communis muscle of the contralateral forelimb to record EMG signals.

The animal was placed in a stereotaxic frame for both the surgical and stimulation procedures; positioned to allow free movement of the forelimb. A small craniotomy (8 mm x 5 mm) exposed the motor cortex (left hemisphere), the dura was removed and mineral oil applied to the cortex. Anaesthesia was switched to ketamine (~10 mg/kg/10 minutes) administered through intraperitoneal injections as needed for the duration of the stimulation procedure.

Stimulation was delivered with a digitally based stimulator (TDT IZ2 Stimulator and RZ5 BioAmp processor), through a glass insulated tungsten microelectrode (FHC Bowdoin, ME USA, UEWSDESGBN4G, 110-175 kΩ) manipulated by a microdrive (David Kopf Instruments Model 2662, Tujunga, CA). Appropriate sites were located using a standard motor cortex activation signal: 13 monophasic, cathodic square pulses of 0.2 ms duration with 3.3 ms between the pulses delivered at 1 Hz (Donoghue & Wise, 1982). EMG responses were monitored and recorded at 5 kHz (RZ5 BioAmp Processor). All procedures followed the guidelines of the Canadian Council on Animal Care and were approved by the Comité de Déontologie de l'Expérimentation sur les Animaux of the Université de Montréal.

5.5 Results

The reliability of a stimulus signal was based on the number of stimulation sites which responded to that particular signal. Response rates were pooled across all stimulation sites tested (n=14). This analysis allowed for the classification of stimulus parameter combinations as: 1) ineffective, 2) inconsistent, or 3) reliable, based on their ability to produce a response. We also identified

parameters which can be adjusted to improve the reliability of a response, shedding light on the role each parameter plays when generating a response.

5.5.1 Ineffective stimuli

Certain combinations of parameter pairs were entirely unable to evoke EMG responses. Figure 5-2 shows that 30-39 µA stimuli delivered at 100 Hz were incapable of producing a response due to insufficient levels of excitation. Stimulation at low amplitudes was however successful if the stimulus frequency was raised. Conversely, in the train duration experiment, 30 µA stimuli delivered by 43 ms trains were shown to be ineffective despite sufficiently high stimulation frequencies. This effect is likely due to an adaptation effect and will be detailed in section 5.5.6 below.

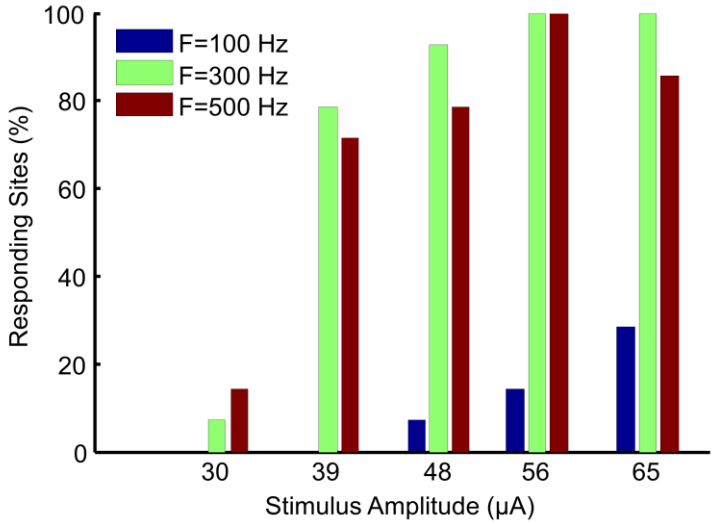

Figure 5-2: Influence of stimulus frequency and amplitude on signal reliability. Signals combining low amplitude and frequency were less effective at evoking responses. Reliability improved when frequencies were raised from 100 to 300 Hz and could be boosted by raising stimulus amplitude.

5.5.2 Inconsistent stimuli

Stimulus signals which elicited a response from less than 50% of the stimulation sites tested were classified as inconsistent. These stimuli typically involved low amplitudes (<48 µA), low frequencies (<200 Hz), short pulse durations (<0.2 ms) or combinations thereof. Short pulse durations were only problematic when paired with either low amplitude or low frequency parameters.

Stimulus amplitudes at threshold levels (30 µA) produced inconsistent responses which could however, be boosted into reliable ranges (>80% of sites responding) when pulse duration was extended to a minimum of 0.34 ms (Figure 5-3). Increasing frequency or train duration were less effective means of boosting the signal, resulting in a maximum of 15% or 55% increase in responding sites respectively.

Frequencies lower than 200 Hz were significantly detrimental (Figure 5-2); however these stimuli could be vastly improved by extending the train duration which placed them in reliable ranges. Longer pulse durations also provided substantial improvements (up to 85%), but raising the stimulus amplitude has only slight effects (up to 50%).

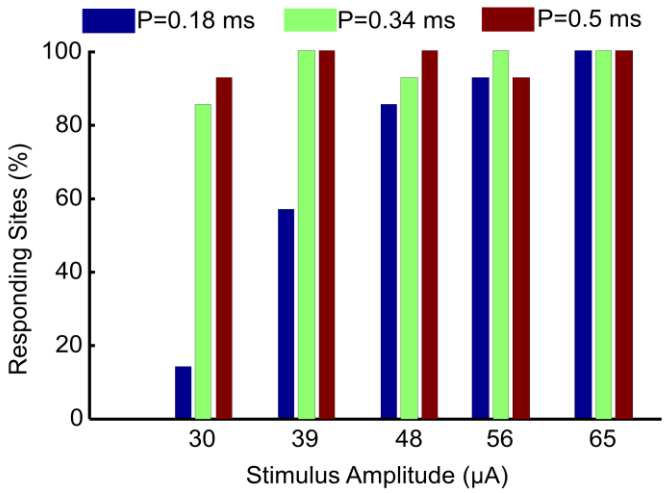

Figure 5-3: Influence of stimulus pulse duration and amplitude on signal reliability. Signals combining low amplitude and short pulse durations were less effective at evoking responses. Reliability improved when pulses were extended from 0.18 to 0.34 ms and weak responses could be boosted by raising stimulus amplitude.

5.5.3 Reliable stimuli

Stimulus signals which elicited a response from more than 80% of the sites tested were classified as reliable. Reliability improved with increases to the stimulus amplitude, frequency, pulse duration and train duration. In general, high levels of success were achieved with amplitudes of at least 48 μA (1.5 x threshold), frequencies at or above 200 Hz and pulse durations longer than 0.18 ms for all train durations.

5.5.4 Improving reliability in restrictive paradigms

In many cases, particularly in the clinical setting, there are restrictions placed upon a stimulation signal. Particular therapies are most effective within certain parameter ranges or rely on the effects of specific parameters. Additionally, physiological constraints are imposed in order to avoid damage to the tissue especially in the case of long-term stimulation. It is necessary to understand the influence of each signal parameter on the responses they evoke in order to overcome these restrictions. For instance, deep brain stimulation therapies often use frequencies less than 200 Hz; a level described here as providing inconsistent or ineffective stimulation when applied to the cortex. Despite the differing stimulation target areas, it may be possible to improve the reliability of the signal while respecting the frequency limitation by increasing the train duration, pulse duration and/or amplitude. An intracortical visual prosthetic device requires low amplitudes of stimulation to prevent phosphenes from blurring together, however many signals with low amplitudes tested here were classified as ineffective. To improve reliability while respecting the amplitude limit we can extend the pulse duration, train duration and/or increase the frequency (Schmidt et al., 1996).

5.5.5 Functional limits

While many parameters can be used to augment a weak signal in order to improve its reliability, there appear to be functional limitations. Little difference is noted between the performance of 300 and 500 Hz stimuli (Figure 5-2). Likewise, all amplitudes above 1.5 x threshold values (48 μA) have similar performance. All pulse durations above 0.2 ms exhibit similar reliability levels (Figure 5-3), as do trains longer than 107 ms (Figure 5-4). These limitations suggest that each parameter has an upper limit after which increases provide no further excitation. This upper limit is likely specific to the application and species in question; however we expect the general effects

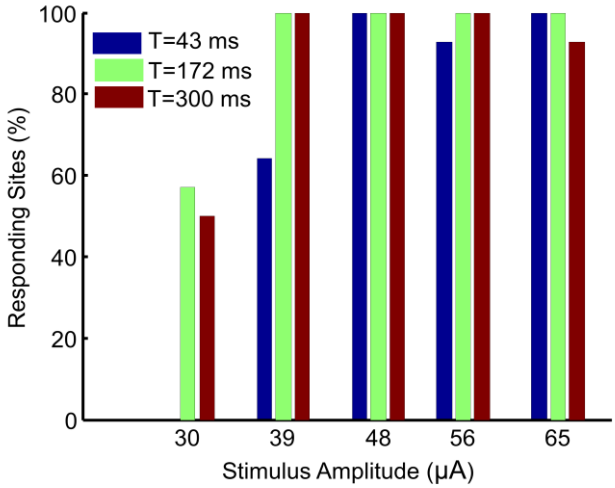

Figure 5-4: Influence of stimulus train duration and amplitude on signal reliability. Signals combining low amplitude and short train durations were less effective at evoking responses, likely due to adaptation effects. Reliability improved when pulses were extended from 43 to 172 ms and weak responses could be boosted by raising stimulus amplitude.

of each parameter to be preserved. In order to avoid adverse effects of stimulation, the signal should be designed to employ the lowest value of each parameter which achieves the highest reliability. This study identified specific parameter combinations which improve the reliability of the signal, suggesting that when designing a stimulus it is necessary to consider not only the independent effects of each component, but also their interactions.

5.5.6 Parameters which cause neural adaptation

When a system is presented with repetitive stimuli the responsiveness of the system can change. Stimuli which previously produced a specific response may elicit different responses over the course of time as a result of neural adaptation. Evidence of this phenomenon can be observed by comparing the responses from the train duration experiment to matching conditions within the amplitude, frequency and pulse duration experiments. When longer duration trains were more prevalent in an experimental session, responsiveness to short duration trains was reduced. The number of sites responding to short trains delivered with amplitudes of 48 μA was 64% lower for the train duration experiment than the amplitude experiment. Similarly, 77% fewer sites responded to short trains delivered at 500 Hz in the train duration experiment than under identical conditions in the frequency experiment. Finally, the number of sites responding to short trains

delivered with 0.18 ms pulses was 80% lower for the train duration experiment than the pulse duration experiment.

A similar effect is observed in the amplitude experiment, where the number of sites responding to low amplitude stimuli can be up to 75% lower in the amplitude experiment than under identical conditions in the other experiments.

These comparisons examine identical stimulus conditions occurring in separate experiments, and we would expect them to have similar results. We postulate that the results are influenced by the other trials occurring within each experiment. For example, the train duration experiment contains the largest number of long duration trains whose repeated application at the stimulation site appears to make the site less receptive to short train duration stimuli. Similarly, the amplitude experiment contains the largest number of high amplitude stimuli whose repeated application at the stimulation site appears to make the site less receptive to low amplitude stimuli. These findings emphasize that it is necessary to not only consider the parameters of the current signal, but also those of the preceding stimulations when designing an effective stimulus.

5.6 Conclusion

This study identified a number of parameter combinations which serve to overcome specific restrictions on the stimulus signal and demonstrated the general role that each parameter played in evoking a response. Additionally, we provided evidence in support of considering the effects of the preceding stimulation on the reliability of the current stimulus. Our future work aims to quantify the effects of stimulation parameters on the amplitude, latency, duration and spread of the response and provide a model of parameter interactions. This approach will not only allow for the optimization of existing paradigms but will facilitate the developments of new applications.

5.7 Acknowledgements

The authors thank Boris Touvykine and Ian Moreau Debord for their contribution to data collection, Philippe Drapeau for programming assistance, Guillaume Elgbeili and Kelsey N. Dancause for consulting on statistical analysis procedures, and Franco Lepore for his input to this project.

CHAPTER 6 ARTICLE 4: PREDICTION OF RESPONSES EVOKED BY INTRACORTICAL MICROSTIMULATION USING AN ARTIFICIAL NEURAL NETWORK MODEL

Meghan Watson[1,2], Numa Dancause[2] and Mohamad Sawan[1]

[1] Polystim Neurotechnologies, Institute of Biomedical Engineering, Polytechnique, Montreal, Quebec, Canada

[2] Département de Neurosciences, Faculté de Médecine, Université de Montréal, Canada

6.1 Presentation of the article

In the preceding chapters, we have shown that stimulus parameters can be used to shape the responses they evoke. The following article presents a methodology for the design of stimulation signals and provides a model of the input-output relationship between stimulus parameters and the responses they evoke. This methodology can be used to aid in the optimization of existing stimuli as well as the design of new stimulation applications. The model proposed here can be used to predict properties of the responses evoked by stimulation and to computationally explore parameter effects. This article (Watson, Dancause, & Sawan, 2015c) was submitted to the Journal of Neural Engineering on June 18th 2015 and is reproduced here in an updated version.

6.2 Abstract

Objective. Microstimulation of the brain has a wide variety of clinical and research applications which employ an extensive range of stimulation parameters. The manner in which the parameters of a stimulus influence the responses they evoke is not always known and as such, most stimulation paradigms are determined by trial-and-error approaches. Our goal was to provide a simple method for modeling the input-output relationship between stimulation parameters and the responses they evoke. *Approach.* A two layer feed-forward artificial neural network was implemented to model the relationship between the parameters of an intracortical microstimulation signal delivered to the rat motor cortex and the EMG responses they evoked. The parameters of the constant-current, biphasic square waveform (amplitude, frequency, pulse

duration, and train duration) were examined in relation to their influence on the EMG metrics (onset latency, peak amplitude, peak time, mean amplitude, main response duration, and residual activation duration).*Main results*. Single target neural networks were able to accurately predict the EMG response metrics and were an effective method of modeling the input-output relationships between the parameters of a stimulation signal and the metrics of the evoked EMG responses. *Significance.* In addition to providing a directly applicable model for EMG prediction in rat motor cortex studies, we also describe the extension of this approach to other applications. Our findings suggest this approach may be essential to both the development of new stimulation protocols and the optimization of existing paradigms.

Key words: Intracortical microstimulation, stimulation parameters, neuroprostheses

6.3 Introduction

Electrical stimulation of the brain has a number of applications including visual (Bradley et al., 2005; Davis et al., 2012; Dobelle & Mladejovsky, 1974; Schmidt et al., 1996; Torab et al., 2011) and somatosensory (Berg et al., 2013; Tabot et al., 2013; Thomson et al., 2013) prosthetic devices, deep brain stimulation therapies for Parkinson's (Anderson et al., 2005; Bronstein et al., 2011; Deuschl et al., 2006; Little et al., 2013; Weaver et al., 2012) and epilepsy (Fisher et al., 2010; Kerrigan et al., 2004; Lee et al., 2006; Morrell, 2011) and countless research applications involving many different regions of the brain (Bartlett et al., 2005; Brecht et al., 2004; Butovas, 2003; Butovas & Schwarz, 2007; Dancause, Barbay, Frost, Mahnken, & Nudo, 2007; DeYoe et al., 2005; Marzullo et al., 2010; Murphey & Maunsell, 2007; Salzman et al., 1992; Tehovnik et al., 2005; Touvykine et al., 2015). These applications use a wide variety of stimulation signals, the parameters of which are most commonly determined by trial and error or based on successful studies found in the literature. Alternatively, efforts have been made to model the effects of stimulation on the brain (Foutz & McIntyre, 2010; Joucla, Branchereau, Cattaert, & Yvert, 2012; Joucla & Yvert, 2009; McIntyre et al., 2009; McIntyre & Grill, 2001; Overstreet, Klein, & Helms Tillery, 2013; Reich et al., 2015). While these approaches have been effective, there is room for improvement in terms of efficiency particularly for optimizing existing protocols and developing new ones. Recently, considerable effort has been focused on optimizing existing protocols for both clinical (Birdno et al., 2012; Birdno, Cooper, Rezai, & Grill, 2007; Foutz & McIntyre, 2010; Rajdev et al., 2011; Reich et al., 2015; Shigeto et al., 2013; Van Nieuwenhuyse et al., 2015) and

research applications (Koivuniemi & Otto, 2011, 2012; Murasugi et al., 1993; Schiller et al., 2011; Tehovnik & Slocum, 2007; Van Acker et al., 2013). While these approaches are valuable and have made many improvements, they are time consuming and do not aid the development of protocols for new applications.

We propose a shift away from the conventional trial and error development of stimulus protocols, towards the development of a design methodology. In order to determine a set of rules or guidelines for the design of stimulation signals we must first understand the influence that each signal parameter exerts on the responses they evoke. Since the brain is an incredibly complex system, a bottom-up approach in which we determine the complete functioning from cell to system is unreasonable at present. Instead, we favor a top-down design in which we formulate an overview of a complete system containing three components: the stimulation signal, the brain it is applied to and the response evoked by the stimulus. Since two of the three components are known and measurable, we are able to take a "black box" approach to model the unknown component. The stimulation signal is used as the input, while the brain is treated as the black box, and the evoked response is used as the output. The functionality of the black box can then be simulated by an artificial neural network.

Our approach was inspired by recent novel applications of input-output modeling to neural systems using artificial neural networks. This type of modeling has been used to predict neural responses to auditory stimuli by training a network with neural spike responses of frequency modulation-sensitive neurons in the auditory midbrain when exposed to different tones (Chang, Chiu, Sun, & Poon, 2012). Artificial neural networks have also been used in computational models of brain stimulation, particularly to model the spread of activation evoked around a deep brain stimulation probe. These ANN models predicted the volume of tissue activated by deep brain stimulation based on the parameters of stimulation signals and the configuration of the electrodes delivering the stimulation (Chaturvedi, Luján, & McIntyre, 2013). ANN models have also successfully predicted nonlinear responses from the primary visual cortex resulting from exposure to visual stimuli (Lau, Stanley, & Dan, 2002; Prenger, Wu, David, & Gallant, 2004). Similarly, the parameters of optic nerve stimulation have been linked to features of the visual percepts they induced (Archambeau, Delbeke, Veraart, & Verleysen, 2004).

Here we describe the use of an artificial neural network to model the input-output relationship between electrical stimuli applied to the brain and the responses they evoke. Our data set was derived from work in the rat model, where we applied intracortical microstimulation (ICMS) to the caudal forelimb area of the motor cortex and recorded the electromyographic (EMG) signals evoked in the forelimb muscles. The model takes the parameters of the stimulus waveform as inputs and metrics of the recorded EMG signals as outputs (or model targets). The artificial neural network was trained, validated and tested on this data set and can be used as a tool for predicting various metrics of the response signal. The intention behind this implementation is twofold. It may be used directly as a tool for researchers studying the motor cortex as they design their stimulation protocols. In this way, parameters of the stimulus can be varied and the response metrics simulated to avoid trial and error testing within an experiment. More importantly however, this model provides a template that can be easily modified and applied to other protocols. Both applications of the model will be detailed in the discussion and a tutorial including MATLAB code and the data set described in this study are appended as supplementary material (Appendices a and b).

6.4 Materials and methods

This model is implemented using a data set collected in the rat model which examined the specific effect of each parameter of a stimulus on the responses they evoked. The data collection procedures, methods and results of this study are detailed extensively in our forthcoming works (Watson et al., 2015a, 2015b; Watson et al., 2015). The present work provides a brief description of the experiment, data collection procedures and analysis while greater emphasis is placed on the implementation of the model and application of the model to future studies.

6.4.1 Surgical procedures and data collection

Experiments were conducted using seven female Sprague-Dawley rats (Charles River, QC, CA) weighing 273-450 g. Anaesthesia was induced with intraperitoneal ketamine injection (80 mg/kg) and maintained with isofluorane (~2% in 100% oxygen) throughout the surgical procedure. Injections of mannitol (4 g/kg subcutaneously) and dexamethasone (1 mg/kg intramuscularly) were given before the craniotomy and temperature was maintained with a self-regulating heating pad. The rat's pulse rate, oxygen saturation, and temperature were monitored continuously. To

record EMG signals, insulated multi-stranded wires (Cooner Wire, Chatsworth CA, USA) were implanted in the extensor digitorum communis muscle of the forelimb contralateral to the stimulating electrode, and recordings were sampled at 5 kHz (RZ5 BioAmp Processor) for offline analysis. All further procedures were conducted with the animal in a stereotaxic frame. A small craniotomy (8 mm x 5 mm) exposed the motor cortex (left hemisphere), the dura was removed and mineral oil was then applied to protect the cortex. For the stimulation procedure, anaesthesia was switched to ketamine (~10 mg/kg/10 minutes) administered through intraperitoneal injections as needed for the duration of the experiment.

All stimulation signals were tested in two separate sites of the caudal forelimb area (CFA) in the motor cortex of each rat specifically: 0-4 μm anterior and 2.0-3.7 μm lateral to bregma at electrode depths of 1534-2104 μm (mean 1792 μm). To locate suitable stimulation sites, we delivered a standard ICMS train: 13 monophasic square pulses of 0.2 ms duration with 3.3 ms between the pulses delivered at 1 Hz which has been shown to be effective in the motor cortex (Donoghue & Wise, 1982; Nudo et al., 1990; Stowe et al., 2007; Touvykine et al., 2015). Sites were selected based on their ability to produce threshold responses to stimulation current amplitudes of 25-35 μA. Choosing sites with a specific threshold level ensured that all test sites had similar levels of excitability and allowed us to set the control value for amplitude within the stimulation protocol. The control value for amplitude (Table 6-1) was set to be twice as strong (50 μA) as the threshold level (25-35 μA).

The stimulation protocol was run sequentially in two different sites within the CFA of each rat. Stimulation was delivered with a digital stimulator (TDT IZ2 Stimulator and RZ5 BioAmp processor), through a glass insulated tungsten microelectrode (FHC Bowdoin, ME USA, UEWSDESGBN4G, 110-175 kΩ) manipulated by a microdrive (David Kopf Instruments Model 2662, Tujunga, CA). Data was collected from a total of 14 sites (2 sites per rat). At the end of the data collection, the animal was euthanized with a lethal dose of sodium pentobarbital. All procedures followed the guidelines of the Canadian Council on Animal Care and were approved by the Comité de Déontologie de l'Expérimentation sur les Animaux of the Université de Montréal.

6.4.2 Stimulation protocol

The stimulation protocol was designed to systematically test the influence that each parameter of a microstimulation signal exerted on the EMG response it evoked when delivered to the rat motor cortex. All stimuli were variants of the constant-current, cathode leading, biphasic square waveform known for its prevalence in both research and therapeutic applications of ICMS. The parameters of this waveform include the current amplitude, pulse frequency, pulse duration and train duration (Figure 1b). The ranges of each parameter were chosen to include typical values used in prosthetic devices and therapeutic applications of brain stimulation. In particular, the ranges reflect the most restrictive stimulation paradigm among the applications: visual prosthetic devices (Schmidt et al., 1996). The test range of each parameter was divided evenly into five levels (low, low-mid, mid, mid-high, and high) and a control value was derived from the standard stimulation signal proven to be effective in the rat motor cortex (Donoghue & Wise, 1982; Nudo et al., 1990; Stowe et al., 2007; Touvykine et al., 2015). The control value for amplitude was set to 50 μA, which was twice the threshold level of each site. The ranges, levels and control values selected for each parameter can be found in Table 6-1.

The stimulation protocol was conducted in four experimental blocks each designed to test the influence of one stimulus parameter against the other three parameters in a pair-wise fashion. Each parameter was tested at all five levels in the range (low, low-mid, mid, mid-high, and high) against three levels (low, mid, high) of a paired parameter while all other parameters were held at their control values (see Table 6-1). Ten trials of each condition were conducted within each experimental block and were pseudo randomized with 1 second between trials. This arrangement resulted in a total of 180 independent test conditions (4 parameters x 5 test levels x 3 paired parameters x 3 test levels) that were tested in a total of 14 sites (2 per rat).

For example, to test the effects of current amplitude, all five values in the amplitude range (30, 39, 48, 56, 65 μA) were tested at 3 frequency levels (low-100 Hz, mid-300 Hz, and high-500 Hz) with pulse and train duration held at the control values (0.2 ms and 43 ms respectively). Similarly, all five values in the amplitude range (30, 39, 48, 56, 65 μA) were tested at 3 pulse duration levels (low-0.18 ms, mid-0.34 ms, and high-0.5 ms) with frequency, and train duration held at the control values (303 ms and 43 ms respectively). Finally, all five values in the amplitude range (30, 39, 48, 56, 65 μA) were tested at 3 train duration levels (low-43 ms, mid-

172 ms, and high-300 ms) with frequency, and pulse duration held at the control values (303 ms and 0.2 ms respectively). This procedure was then repeated for frequency, pulse duration and train duration until each parameter had been tested against amplitude in this "pair-wise" arrangement.

6.4.3 Response metrics

For each of the stimulation sites, trials were averaged to produce a mean response for each condition. In order to quantify the effects of a stimulus parameter on the evoked responses, six features were extracted from each mean EMG signal and classified as response metrics (Table 6-1). For the purposes of this model, the response metrics obtained for each condition were averaged across all 14 sites producing a mean data set.

The signal features chosen to describe the response include: 1) onset latency, 2) mean amplitude, 3) peak amplitude, 4) peak time, 5) main response duration and 6) residual activation duration. The onset latency was defined as the time delay between the onset of the stimulus signal and the initiation of the EMG response (Figure 6-1b right). The mean amplitude was taken as the average of the signal during the component extending from EMG onset to the return of the signal to baseline (denoted as the main response). The peak amplitude was defined as the maximum value of the response and the timing of this occurrence was called the peak time. The main response was defined as the larger component of the signal which contains the EMG's peak, and the residual activation was defined as the intermittently present region of lesser activation which persisted after the main response (Figure 6-1b right). The parameters of main response duration and residual activation duration provide the timescale of these two components. The residual activation is a newly classified phenomenon detailed in our forthcoming work (Watson et al. 2015). It is not present in all EMG responses and is largely dependent upon the parameters of the stimulation signal. These residuals take many shapes, and can be entirely absent or endure for hundreds of milliseconds.

Table 6-1: ANN model input-output parameters

ANN Inputs				**ANN Outputs**
Input Parameters	**Unit**	**Test Range**	**Control**	**Output Parameters**
Amplitude (A)	μA	30, 39, 48, 56, 65	50	Onset Latency
Frequency (F)	Hz	100, 200, 300, 400, 500	303	Mean Response
Pulse Duration (P)	ms	0.18, 0.26, 0.34, 0.42, 0.5	0.2	Peak Response
Train Duration (T)	ms	43, 107, 172, 236, 300	43	Peak Time
				Main Response Duration
				Residual Activation Duration

6.4.4 Artificial neural networks

Artificial neural networks are statistical learning models which can be used to approximate functions and perform computational processes. They are designed to mimic biological neural networks in the sense that they are composed of systems of interconnected components (known as nodes or neurons) which relay signals. An artificial neural network is not intended to be a model which firmly represents a system's performance in the way that a look up table or an equation would. Rather it learns the statistical model of the process generating the data through a training process which makes it able to adapt to new inputs. The network generates weights and biases used to describe the relationship between all connected components and tunes them continually during training to render the network adaptive to new inputs as a form of machine learning. The artificial neural network (ANN) approach allows us to simulate metrics of the EMG responses evoked by stimulation using a black box model (Figure 6-1a). The input is the set of stimulation parameters, and the output is one of the EMG metrics. We represent the motor cortex by the black box, whose response to stimulation is simulated by the ANN (Figure 6-1b).

Neural networks can be implemented with countless topologies in which the connection methods, number of neurons, number of layers, and types of transfer functions are varied; however they can be divided into two broad classifications. Feed-forward neural networks (FNN) have a one directional flow of data and are the simplest to implement. They are typically used for function approximation and nonlinear regression to generalize the relationships between the inputs and outputs of a system or for pattern recognition and classification. Recurrent neural networks (RNN) have feedback pathways which accommodate dynamic temporal behavior and are

inherently more complicated to implement. These networks are better suited to uses involving time series or sequential data. To model our input-output data set, we chose the simplest network architecture possible and all implementation choices were kept as close to the standard guidelines for basic implementation of ANN models.

Our implementation is a 2 layer feed-forward neural network composed of a hidden layer, and an output layer (Figure 6-1c). Our network takes four inputs to accommodate the number of stimulus parameters of interest, which are fed into a hidden layer consisting of 20 hidden neurons (Figure 6-2). A connection exists between each hidden unit and output unit, and the strength of the connection is represented by the weights. If one unit exerts a large influence on another, the weight describing their connection will be large. The nature of the relationship (inhibitory/excitatory) is indicated by the sign of the weight (negative/positive). The inputs are first adjusted by the input weights (IW) and then summed with the input bias weights (b1) generated during training. Before exiting the hidden layer, the resulting sum is scaled by the hyperbolic tangent activation function (implemented via MATLAB's tansig function). The output of the hidden layer is passed through an output layer containing one neuron and is adjusted by output layer weights (LW) before being summed with output bias weights. Before exiting the output layer, the resulting sum is scaled by a linear activation function (implemented via MATLAB's purelin function). The resulting output represents the ANN's response to the particular set of inputs. This process is schematically detailed in Figure 6-2 and is represented by the following equation:

$$y = b2 + LW * \tanh(b1 + IW * x) \qquad (6\text{-}1)$$

where, y represents the network output in response to input vector x. Variables b2 and b1 represent the output and input bias weights respectively, while variables LW and IW represent the layer weight and input weight matrices of the network.

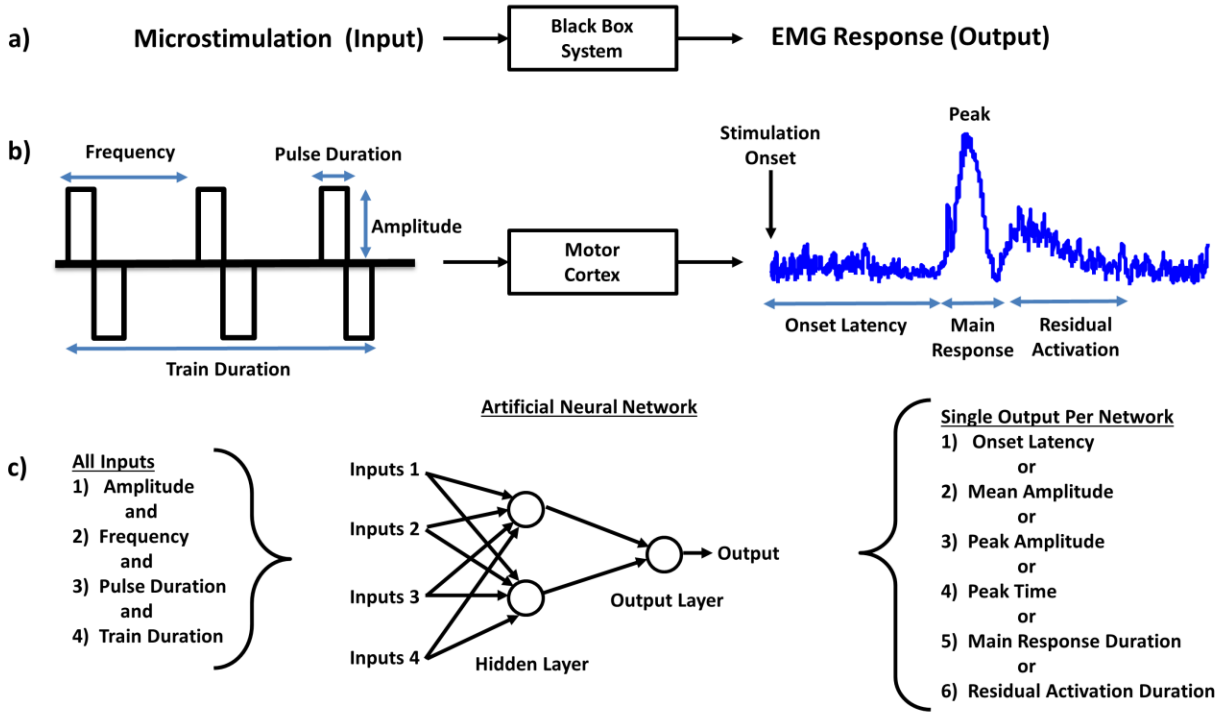

Figure 6-1: ANN model design. Part (a) describes the black box approach to modeling the input-output relationship between intracortical microstimulation signals delivered to the motor cortex and the EMG responses they produced. Part (b) shows the parameters of the constant-current, biphasic square waveform stimulus and the EMG response metrics. Part (c) depicts the ANN structure which simulates the function of the motor cortex. A separate two layer feed-forward network was implemented to simulate a single EMG metric. The system takes four inputs representing the stimulus signal and produces one of six outputs representing EMG metrics. Note: the diagram shows only 2 neurons in the hidden layer for simplicity however 20 are implemented.

6.4.5 ANN simulation in MATLAB

The ANN model was implemented in MATLAB using the Neural Network Toolbox (Mathworks, Natick, MA, USA). For the purpose of simplicity and to demonstrate the ease of reproducibility, the model was developed using the standard (default) settings recommended in this toolbox. No outlier removal was performed and the network was trained only once (no retraining). Data was arranged into an input vector containing the four parameters of each stimulus condition, and a target vector containing the six metrics of the EMG response produced by the stimulus condition.

Both the input and target vectors were preprocessed to scale them for the chosen activation functions and to make them relative to one another via normalization.

Fitting data with the artificial neural network was a three step process involving training, validation and testing. These procedures were implemented following the recommended guidelines found in MATLAB's Neural Network Toolbox. The entire data set was randomly divided into three components allocated to one of the three processes. In this model, 70% of the data (126 trials) was used to train the network which is an iterative process in which the system automatically estimates the weights and biases of possible designs. The training algorithm employed was the Levenberg-Marquardt which is a damped least-squares method for least squares curve fitting. Once the system identifies possible designs, a different 15% of the data (27 trials) was used to iteratively validate the performance error of these designs. When the error ceased to improve, validation process ended and the final 15% of the data was used one time only to test the design with the best performance obtaining an unbiased estimate for the predicted error when the system is exposed to new inputs.

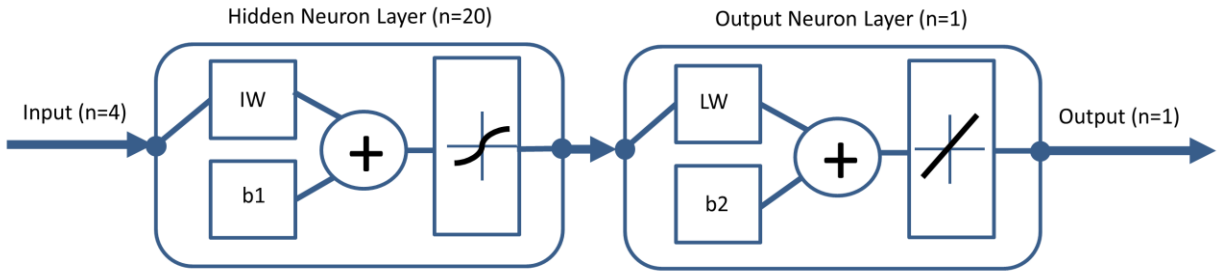

Figure 6-2: Computational implementation of ANN model. A two layer feed forward neural network composed of a hidden layer with 20 hidden neurons and an output layer with one neuron was implemented to model the input-output relationships corresponding to 4 inputs (stimulus parameters) and 6 outputs (EMG metrics). Inputs are adjusted by the input weights (IW) then summed with the input bias weights (b1) and the result is scaled by the hyperbolic tangent activation function (tansig) of the hidden layer. Once the result is transmitted to the output layer it is adjusted by output layer weights (LW) before being summed with output bias weights and the resulting sum is scaled by a linear activation function (purelin).

6.5 Results

A separate model was implemented to simulate each metric of the output EMG signal in a single-target prediction approach. This approach was taken to ensure model simplicity and to avoid assumptions about target dependency. Dependency between targets is typically not known prior to simulation and is learned from the data set. Since dependency is inherent to the data set and derived through training it can be argued that exploiting the relationships between targets provides no additional information at a greater computational expense. In the discussion, we address the possibility of implementing a multi-target prediction approach and its implications. The single-target simulations yielded satisfactory results using the default parameters of the MATLAB Neural Network Toolbox. These findings suggest that ANN implementations may be a simple yet effective approach for modeling input-output data of this type. The model was assessed in terms of its network performance error and goodness of fit and was determined to effectively map the nonlinear relationship between the input stimulation and output EMG metrics.

6.5.1 Network performance

Figure 6-3 quantifies the performance of the network by examining the mean squared error (MSE) representing the difference between the model outputs and targets at each iteration (epoch) in the training, validation and testing phases. Error values close to zero indicate that the ANN estimator predicts outputs which match the targets very closely. The best performance occurs where the horizontal and vertical dotted lines intersect and is highlighted with a green circle. All of the networks perform well, as the validation and testing curves are very similar and no performance issues were identified. There are no indications of under or overtraining in any of the networks. The network simulating onset latency performed best after 4 epochs (MSE=0.03), as did the network simulating mean amplitude (MSE=0.12). The network predicting peak amplitude needed 5 epoch to reach its best performance (MSE=0.11), as did the network simulating the main response duration (MSE=0.07). The peak time network however required only 2 epochs (MSE=0.03), while the residual activation duration network performed best after 3 (MSE=0.05).

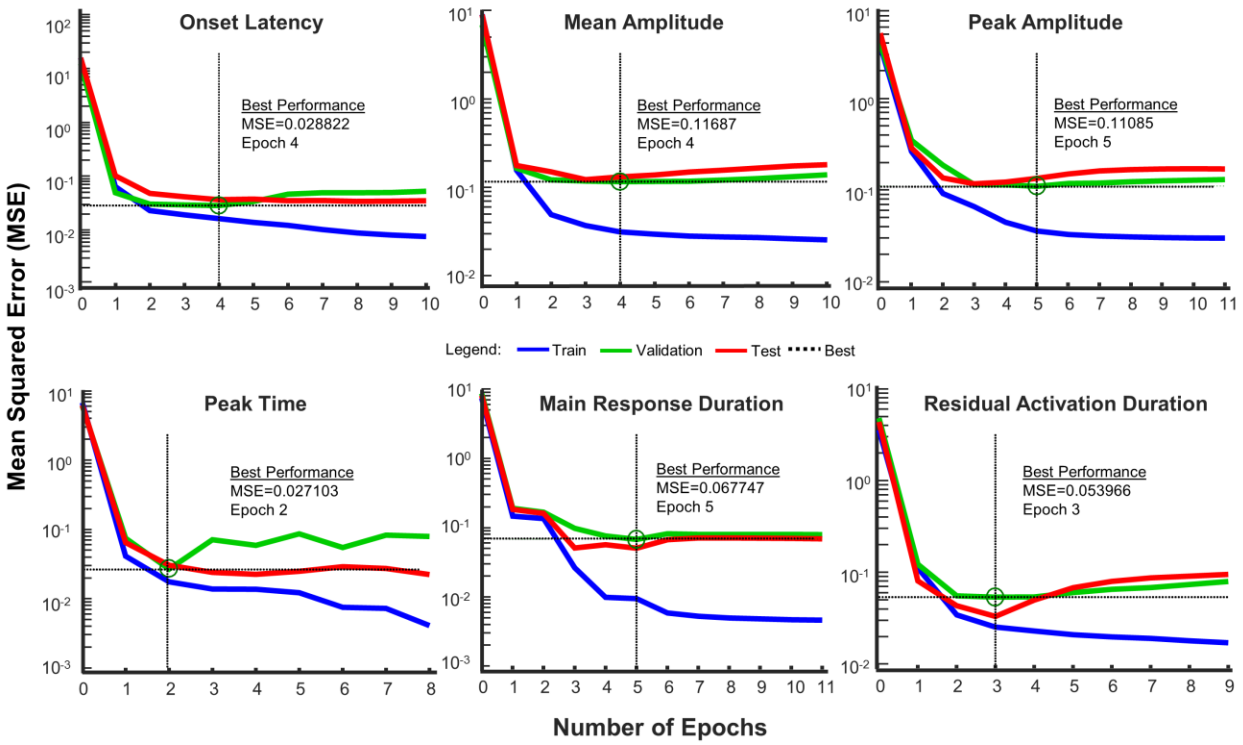

Figure 6-3: Network performance. Each EMG metric was simulated by an independent neural network. The mean square error of the network at each iteration (epoch) is shown with the best performance occurring where the horizontal and vertical dotted lines intersect as highlighted by the green circle. Performance is detailed for the training (blue), validation (green) and testing (red) phases of model implementation.

6.5.2 Goodness of fit

Figure 6-4 quantifies the goodness of fit between the network outputs and target values using the best fit linear regression between the two parameters. The graph allows you to compare the perfect condition in which the outputs match the targets and the correlation coefficient has a value of 1 (dotted line) and the results of the model simulations (in blue). All of the networks perform well, and exhibit a high degree of correlation between the network outputs and target vectors despite the presence of several outlier data points. The network simulating response durations had the best performance (main response duration: r=0.95; residual activation duration: r=0.94), as did the networks for other temporal parameters (onset latency: r=0.90; peak time: r=0.91). However the fit of the networks responsible for predicting the spatial parameters was slightly lower than desirable (mean amplitude: r=0.88; peak amplitude: r=0.89) but was still

acceptable. Options for improving performance will be detailed in the discussion. Figure 6-5 depicts the goodness of fit between the targets and ANN outputs as error histograms for each network with a bin size of 20. Each network histogram exhibits a roughly Gaussian shape; however the distribution does show evidence of outlying data points particularly in the spatial outputs (mean and peak amplitude).

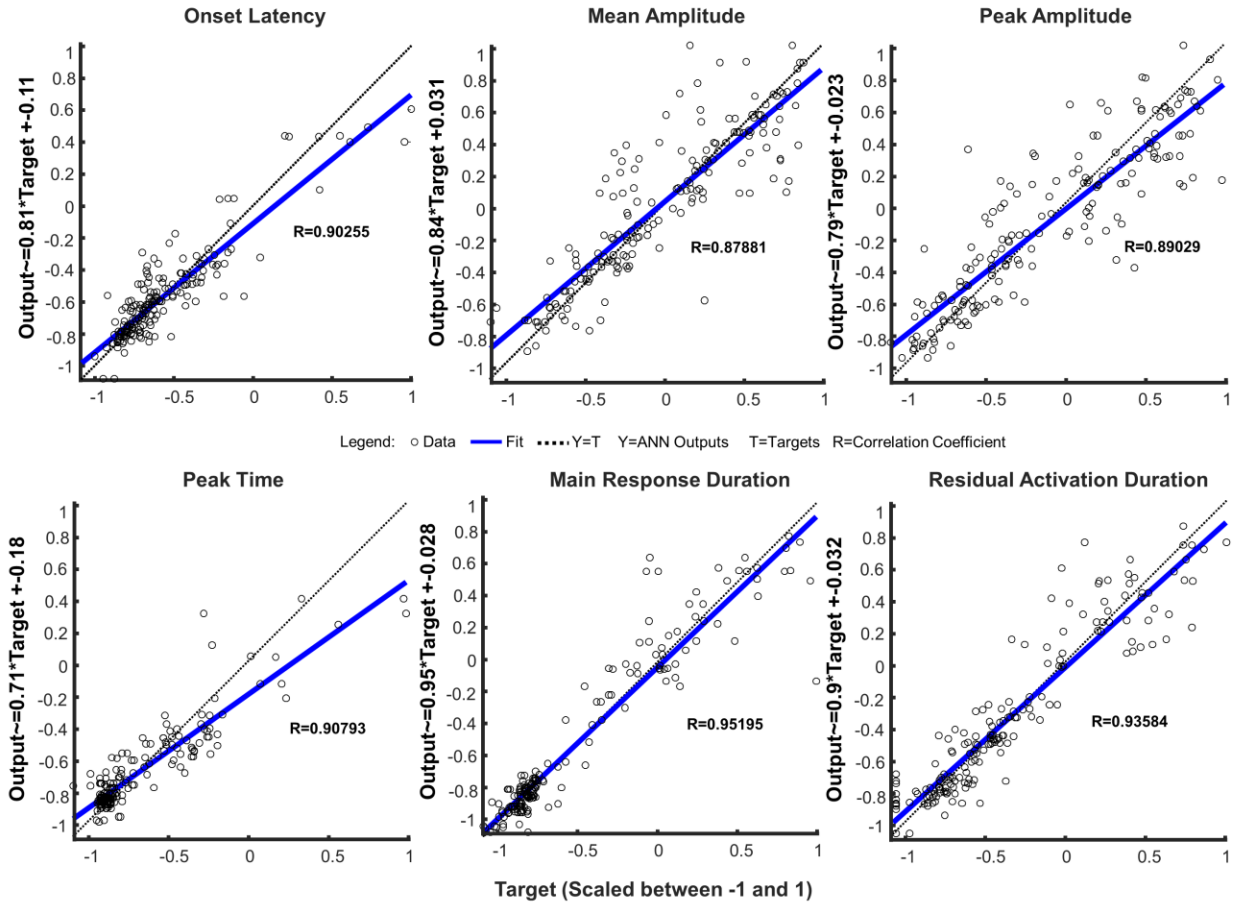

Figure 6-4: Network fit-correlation analysis. Each EMG metric was simulated by an independent neural network. The goodness of fit between the network outputs and target values is indicated with the best fit linear regression between the two parameters (blue), along with their correlation coefficients. Ideal conditions are represented by the dotted line.

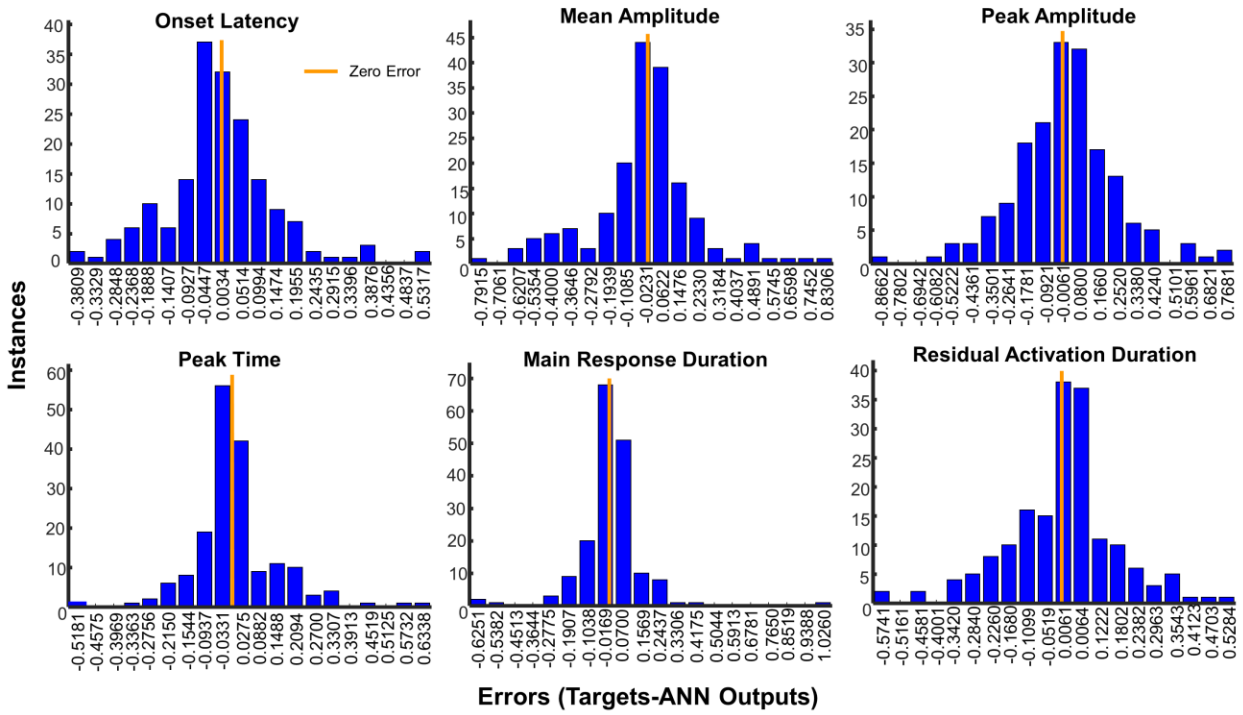

Figure 6-5: Network fit-error analysis. Discrepancies between targets and ANN outputs are depicted as error histograms for each network with 20 bins.

6.6 Discussion

A thorough understanding of input-output relationships in stimulation paradigms is not only essential to designing effective protocols but also provides insight into neural processes. Our goal was to provide a simple method for modeling the relationship between stimulation parameters and the responses they evoke. We chose to test this model on input-output data obtained from the rat motor system due to its simplicity and the abundance of knowledge pertaining to the structure and function of this particular system. We demonstrated that a two layer feed-forward ANN implemented with default settings using MATLAB's Neural Network Toolbox was capable of effectively simulating the EMG response metrics induced by stimulation. Here we discuss alternative implementation structures for the model, methods to improve performance, implications of this modeling technique, and provide detailed instruction for using this specific model or extending its principles to other applications.

6.6.1 Single vs. multi-target prediction structures

The process we modeled had four input variables (stimulation parameters: amplitude, frequency, pulse duration, train duration) and produced six outputs (EMG metrics: onset latency, peak amplitude, peak time, mean amplitude, main response duration, residual activation duration). We chose to employ target-wise decomposition of this multiple-input, multiple-output system and implemented six separate networks to predict each of the six outputs independently. This approach was taken since the relationship between the outputs is not often known prior to simulation, and is derived from the dataset during the training process. As such, we feel it does not add any inherent value to the model as it provides no additional information to the network. Arguably however, a model which performs multi-target prediction could be seen as simpler and preferable to the end user of the model. Multi-target prediction approaches will however, typically require more sophisticated implementation approaches and more extensive network training in order to produce adequate performance. Since both approaches are feasible and valid, the user must choose the structure of the model based on their goals.

6.6.2 Improving ANN performance

For the purpose of simplicity, our model was developed using standard procedures and design recommendations. For this particular dataset, this approach proved satisfactory; however this will not always be the case. To improve the performance, the user can modify the parameters of the network and different training algorithms can be selected. Similarly, removing outliers prior to training, retraining the network, adding more hidden layer neurons, or using additional training data can improve the performance. These approaches are conveniently detailed in MATLAB's help files for artificial neural networks.

6.6.3 Implications of the model

Recently, much effort has been devoted to optimizing a number of existing stimulation protocols for their specific purposes in clinical (Birdno et al., 2012; Foutz & McIntyre, 2010; Pulliam et al., 2015; Rajdev et al., 2011; Reich et al., 2015; Shigeto et al., 2013; Van Nieuwenhuyse et al., 2015) and research applications (Koivuniemi & Otto, 2011, 2012; Murasugi et al., 1993; Schiller et al., 2011; Tehovnik & Slocum, 2007; Van Acker et al., 2013). While these attempts are valuable and provide a wealth of knowledge, they do not facilitate the development of new

paradigms or explain the influence of stimulation parameters on neural activation in general. We propose a shift away from task-specific optimization and towards a black-box approach in which we define the generalized input-output relationship between the stimulation parameters and the effects they produce. The ANN modeling approach provides a simple implementation for simulating the effects of stimulation and as such is a valuable tool for developing and optimizing stimulation protocols, particularly those with known restrictions on the stimulus parameters.

Visual prosthetic devices seek to simulate vision by generating patterns with the visual percepts (phosphenes) produced by stimulation the visual cortex (Dobelle & Mladejovsky, 1974; Schmidt et al., 1996; Tehovnik & Slocum, 2007). The timing of this stimulation is essential to providing a real-time representation of the visual field. If the chosen stimulus induces long lasting activations the phosphenes it evokes will remain visible for longer than intended. Similarly, if the stimulus amplitude is too large the activation will spread within the cortex, producing phosphenes which blur together disrupting the intended spatial pattern. The ANN approach could be used design the ideal stimulus by simulating the effects of stimulus parameters on phosphene metrics such as size, duration, and brightness. In this case, the stimulation parameters would be taken as the input to the ANN, the ANN itself would model the response of the visual cortex to electrical stimulation, and the model outputs could be the qualitative phosphene metrics such as size, duration and brightness.

Applications which use deep brain stimulation for the treatment of epilepsy (Rajdev et al., 2011; Shigeto et al., 2013; Wyckhuys, Raedt, Vonck, Wadman, & Boon, 2010) may benefit from stimulation waveforms which produce responses with short onset latencies for seizure interruption applications or short duration responses to avoid kindling effects in sustained stimulation of target structures or epileptic focii. The ANN model approach can simulate the effects of stimulus parameters on the seizure metrics such the frequency or amplitude of interictal, kindling, and seizure-like events recorded intracranially or via electroencephalogram (EEG). In the case of seizure interruption applications, the parameters of the stimulus which interrupts the seizure activity is taken as the input to the ANN model. The ANN itself would model the effect of this electrical stimulus on the seizure activity, and the model outputs could be the duration for which the seizure activity persisted after stimulation, or the relative reduction in amplitude of seizure-like spiking activity occurring after the delivery of the interruption stimulus. In the case of seizure prevention through sustained stimulation of target structures or epileptic

foci, the seizure prevention stimulus would serve as the input to the ANN model. The ANN itself would model the ability of this particular stimulus to prevent the occurrence of seizure-like activity. The model outputs could be the frequency of occurrence of interictal spiking, preictal abnormalities or seizure-like events in a given time period.

Similarly, applications of deep brain stimulation for the treatment of Parkinson's (Benabid et al., 2009) may benefit from stimulation waveforms which produce long lasting responses in order to achieve the desired sustained effects with fewer stimulations. These applications are also known to have optimally effective frequencies. In the case of Parkinson's treatment, the ANN approach could be to simulate the influence of stimulation parameters on Parkinsonian symptom metrics such as tremor reduction or gait initiation. In this case, the parameters of the stimulus delivered by DBS would be taken as the input to the ANN model. The ANN itself would model the effect of this electrical stimulus on the Parkinsonian symptoms. The model outputs could be qualitative measures of tremor, bradykinesia or movement initiation times obtained with rating scales such as the Unified Parkinson's Disease Rating Scale (MDS-UPDRS), or quantitative measures obtained with motion sensors (Das et al., 2011; Pulliam et al., 2015). Using this modeling approach could improve DBS programming practices and reduce the time and expense of trial and error optimization approaches.

6.6.4 Using the model

Our forthcoming works detail the general effects of stimulation parameters on the responses they evoke (Watson et al., 2015a, 2015b; Watson et al., 2015), and this model provides a simple method for simulating these effects and exploring stimulus parameter combinations. We have included as supplementary material the complete input-output dataset for the rat motor cortex ANN simulation described in this work (Appendix A). We also provided a tutorial detailing its usage in an m-file format which includes sample code to run the simulation (Appendix B). This model can be used directly to design or optimize stimulus signals for use in rat motor cortex stimulation experiments. The user must simply load the appended data set, and follow the instructions in the appended tutorial. The user can either simulate the EMG responses to stimulation parameters which are fixed due to restrictions of their paradigm or they may use the model to select the stimulus parameters which produce the EMG metrics they wish to obtain (fast onset, long duration etc). Users with stimulus restrictions can achieve their desired EMG metrics

by varying the non-fixed parameters of their stimulus signal to compensate for the effects of a fixed parameter. Further details on the general relationships between stimulation inputs and the responses they evoke and methods for overcoming parameter restrictions can be found in our forthcoming works (Watson et al., 2015a, 2015b; Watson et al., 2015).

6.6.5 Extending the model principles to other applications

The ANN approach is a simple yet effective tool for modeling any input-output relationship. Detailed in the included tutorial are the steps required to modify this implementation for other uses including instructions for modifying the sample code. These modifications allow the user to implement the model on their own input-output data sets.

6.7 Conclusions

Since our knowledge of the brain is constantly evolving and new applications continue to be developed, more focus must be placed on developing methodologies to guide the design of new stimulation signals. These methodologies rely on an in-depth understanding of the influence that each parameter of a stimulation signal exerts on the brain. We propose a shift away from iterative testing approaches, replacing them with a design methodology in which we consider the desired physiological response and the neural activations necessary to achieve it. Understanding the role each stimulus parameter plays in neural activation is essential to this approach. The model presented here provides the framework for using artificial neural network models to simulate the input-output relationship between stimulation parameters and desired outcomes. This methodological approach not only allows for the optimization of existing paradigms but is an essential tool for the development of new applications.

6.8 Acknowledgements

The authors thank Boris Touvykine and Ian Moreau Debord for their contribution to data collection, Guillaume Elgbeili and Kelsey N. Dancause for consulting on statistical analysis procedures, and Philippe Drapeau for assistance with programming the stimulation equipment.

CHAPTER 7 GENERAL DISCUSSION

In the preceding chapters, we have demonstrated that the parameters of a stimulation signal greatly influence the responses they evoke and described the extent and nature of specific parameter effects. Electrical stimulation of the brain is the foundation of a number of state of the art technologies and the future of development in these fields relies heavily on the ability to design effective stimulation signals. The optimization of a signal for a specific goal can sometimes be achieved using iterative trial and error or computational methods; however these approaches have many limitations. We propose a shift in design principles in which the stimulation signal is crafted by first considering the neural activation necessary to achieve the stimulation goal and then determining the stimulation parameters required to induce the desired neural activation. This approach makes use of our knowledge of general parameter effects on neural circuits to provide a sound methodology for stimulus design. The computational model of input-output relationships developed in this work provides a tool to aid in the implementation of the proposed stimulus design methodology.

In this thesis, we tackled the issue of developing effective stimulus design principles. These principles are based on the knowledge of the input–output relationships between stimulus signals and the responses they evoke. In chapter 2, the review of the literature demonstrated that there are no precedents for this work as methodologies for informed stimulus design have not been developed previously. A few studies have explored the effects of some stimulus parameters through experimental testing (Dobelle & Mladejovsky, 1974; Koivuniemi & Otto, 2012; Koivuniemi & Otto, 2011; Schmidt et al., 1996; Semprini, Bennicelli, & Vato, 2012; Young, Vuong, Flynn, & Teskey, 2011) however these studies were not systematic and explored very limited parameter ranges. In this work we uncovered a number of parameter effects and relationships that only emerge in certain circumstances such as limits to the effects of certain parameters or the neural adaptation effects of stimulus train duration and amplitude which occur when certain stimuli are prevalent in an experimental session. The systematic approach to testing and the cross-comparisons we conducted were essential to these discoveries.

The design of our experiments relied heavily on insight derived from our review of many different stimulation studies conducted for vastly different purposes whose results were represented by various qualitative and quantitative measures. The comparison of the results was

however extremely difficult in the absence of standardized measurements. It is unrealistic to expect broad standards to be applied across such highly variable applications; however an improved method of comparison is required. The input-output model we implemented with an artificial network is a tool which allows for the comparison of results obtained in different studies, species, and applications. This approach uses the model to represent the cause and effect *relationships* between stimuli and the responses they evoke instead of focusing on the *absolute values* resulting from a particular study. When the focus is shifted to the relationships, we are able to make comparisons between studies conducted in different modalities.

For example, inducing a visual percept by stimulating the visual cortex surface with a macroelectrode uses different stimulus parameters than would be used to stimulate the input layers of the visual cortex with a microelectrode. Identical visual percepts can be produced by both modalities; however they will use different stimulation parameters in accordance with the differences in stimulation site and electrode size (Dobelle & Mladejovsky, 1974; Schmidt et al., 1996). Although the *absolute values* of the stimulus parameters vary between modalities, the *relationships* between the stimulus inputs and response outputs remain the same. In both systems, a brighter larger phosphene is produced by increasing the stimulus amplitude. Similarly, experiments conducted in different species tend to produce different *absolute values* of responses, similar to inter-subject variability. The current amplitude required to produce threshold forelimb movements in mice is smaller than that required for rats (Young et al., 2011), however the input-output *relationships* between stimulus parameters and evoked response metrics are preserved. When systems are modeled with this approach, the comparison between studies, subjects, species and modalities simply becomes a matter of data normalization.

With this approach, we could ensure that the vast supply of knowledge produced across the disciplines is accessible and readily comparable. Despite the identical goals and site of stimulation used for phosphene generation, the macrostimulation and microstimulation approaches were developed and validated independently. Similarly, the results of a study conducted in one animal model are not directly applicable to an identical study conducted in a different animal model. If the focus of data representation were to shift from absolute values to relationships then principles of one application could be more easily applied to another, and comparison between species could be facilitated.

Using this design approach, the principles of one application can be extended to others. This would be a particularly promising development in the field of visual prosthetics. The retinal approach to simulating vision has long surpassed the intracortical approach. Extensive testing has been conducted in both research and clinical trials (Horsager, Boynton, Greenberg, & Fine, 2011; Horsager, Greenberg, & Fine, 2010; Jepson et al., 2013; Nanduri et al., 2012; Savage, Grayden, Meffin, & Burkitt, 2013; Stronks, Barry, & Dagnelie, 2013; Weitz et al., 2014; Yanai et al., 2007) and truly remarkable modelling approaches (Jacobs et al., 2009; Joarder et al., 2007; Nirenberg & Pandarinath, 2012) have been taken to address the issue of stimulus design within the retinal prosthetic. If even some of the developments in retinal prosthetics could be interpreted and applied to intracortical prosthetics progress could be accelerated significantly.

Returning to the concept of stimulus design, we previously suggested that design be approached by a two step process: 1) the consideration of the *neural activity* required to achieve a *stimulation goal*, followed by 2) the consideration of the *stimulus parameters* required to induce the required *neural activation*. This approach requires an understanding of both the system in question and the general role of stimulation parameters in the excitation of tissue. For example, in the case of phosphene generation through visual cortex stimulation, the *stimulation goal* is to produce a small, punctate visual percept. The *neural activation* required to achieve this goal is the highly localized activation of a small region (hypercolumn) surrounding the electrode tip with minimal signal spread. The *stimulus parameters* required to achieve this activation consist of low amplitude, low frequency signals to limit the spread with extended pulse or train durations to improve the visibility of the percept. Although this approach is straightforward, it does require an extensive knowledge of the system in question as well as an understanding of the influence stimulus parameters exert on tissue excitation. The potential power behind this approach is however undeniable particularly for the development of new stimulation applications. Armed with an understanding of the neural circuitry in question and the goal of the stimulation an appropriate stimulus can be analytically designed. When combined with computational simulation methods, stimulus signals can be tested prior to validation with electrophysiology which could expedite the optimization process.

Recently, more studies are emerging seeking to optimize stimulation paradigms (Koivuniemi & Otto, 2012; Semprini et al., 2012; Young et al., 2011) or model stimulation effects on systems (Birdno et al., 2012; Birdno, Cooper, Rezai, & Grill, 2007; Chaturvedi, Luján, & McIntyre, 2013;

Foutz & McIntyre, 2010; Lempka et al., 2011; Lempka, Johnson, Miocinovic, Vitek, & McIntyre, 2010; McIntyre & Grill, 2001; McIntyre & Grill, 2002; McIntyre, Frankenmolle, Wu, Noecker, & Alberts, 2009; McIntyre & Grill, 2000; Reich et al., 2015) or neurons (Danziger & Grill, 2015; Joucla et al., 2012; Joucla & Yvert, 2009; Wongsarnpigoon & Grill, 2010). Some of these approaches are purely computational; however many choose to combine computational modeling with physiological data. We believe this combination is essential to producing truly beneficial works. Computational approaches must remain grounded in experimental data. Just as a prosthetic device requires the harmonious cooperation between engineering and neuroscience principles, so too does the model require a balance of computation and experimental data. Models based on theoretical principles which are not validated with physiological data are of limited value. Similarly, a model of exceeding complexity may be a marvel in its own right; however it is not accessible to the user. The model structure we have proposed here is an example of a simple yet powerful tool that can easily be used directly by physiologists studying the rat motor cortex or simply modified to represent any other input-output system. The resurgence of optimization and modeling studies in the field of electrophysiology could indicate discontent with current paradigms and optimization methods which could perhaps be mitigated with the use of the stimulus design methodology and modeling tools developed in this thesis.

The work presented in this thesis outlined the general effects of stimulus parameters on the responses they evoke in the rat motor system. We discovered that the standard ICMS signal used to evoke movements is currently not optimized and we outline changes which can be made to improve it. In the course of this study, we also identified a previously unexplored characteristic of the motor evoked potential response which we named “residual activation”. This activation can linger for extended durations after the stimulus and main response offsets and its characteristics are highly dependent on the parameters of stimulation. This component should be considered when designing stimulation protocols particularly when selecting adequate delays between trials, and it may be partially responsible for the influence of preceding trials which we describe in chapters 4 and 5. The model developed in this work can be used directly to design stimulus waveforms in the rat motor system to produce the desired response metrics as detailed in chapter 6. More importantly however, this model can be easily modified to represent other input-output data sets and could play a crucial role in the development of stimulation signals when restrictions are placed on certain stimulus parameter values. The model and methodology

together provide a sound framework for future research and their inherent structure facilitates the comparison of results derived from different subjects, species, systems and applications.

CHAPTER 8 CONCLUSION AND RECOMMENDATIONS

Effective signals are essential to all applications of stimulation, from probing neural function and connectivity to implementing a therapeutic treatment. Understanding the role each stimulus parameter plays in neural activation is essential to the design of effective stimulation signals. This approach not only allows for the optimization of existing paradigms but also facilitates the developments of new applications. The experiments conducted in this thesis used a simple circuit to demonstrate a powerful principle. The general effects of stimulus parameters on the responses they evoke were described and modelled computationally using an artificial neural network representing the input-output relationships of the system. A stimulus design methodology was proposed in which we first consider the neural activity required to achieve a stimulation goal and then determine the stimulus parameters required to induce the required neural activation. The stimulus design methodology and modelling approach developed in this work can easily be extended to other systems. To our knowledge, this thesis contains one of the first documented applications of input-output modeling applied to the relationships in intracortical microstimulation systems.

This thesis proposes several topics which should be addressed in future research. The standard ICMS signal for the rat motor cortex is not currently optimized and potential improvements are detailed in chapters 3-5. The neural mechanism and stimulus parameters responsible for producing residual activation require further study. Similarly, the influence of the residual activation and stimulus parameter effects on subsequent trials should be examined in more detail. The computational model described here is only capable of predicting responses to parameters within the test range of the data set, and the scope of the model could be extended by adding data outside this range. The model structure itself could be improved as described in chapter 6. It would also be beneficial to conduct more systematic studies such as those detailed in chapters 3-5 for different cortical areas, species and applications. It would also be beneficial to implement the input-output model for existing data sets and perhaps conduct meta-analysis to compare the effects across multiple studies. Of particular importance is the development of normalization procedures in order to improve ability to compare results between subjects, species, studies, and applications. The normalization procedure should preserve the general relationships between signal parameters and the response metrics while eliminating or controlling for the influence characteristics inherent to the data such as the influence of electrode size.

PUBLICATIONS

Watson M, Dancause N, and Sawan M. (2015a). Efficient microstimulation of the brain: A parametric approach. In Engineering in Medicine and Biology Society (EMBC), 2015 37th Annual International Conference of the IEEE. Milan, Italy.

Watson M, Dancause N, and Sawan M. (2015b). Intracortical microstimulation parameters dictate the amplitude and latency of evoked responses. Brain Stimulation (Accepted for Publication).

Watson M, Dancause N, and Sawan M. (2015c). Prediction of responses evoked by intracortical microstimulation using an artificial neural network model. Journal of Neural Engineering (Submitted).

Watson M, Sawan M, and Dancause N. (2015). Intracortical microstimulation parameters dictate the duration of evoked responses. Journal of Neurophysiology (Submitted).

BIBLIOGRAPHY

Abramian, M., Lovell, N. H., Morley, J. W., Suaning, G. J., & Dokos, S. (2012). Computational model of electrical stimulation of a retinal ganglion cell with hexagonally arranged electrodes. *Proceedings of the Annual International Conference of the IEEE Engineering in Medicine and Biology Society. IEEE Engineering in Medicine and Biology Society. Conference*, *2012*, San Diego, CA, August 28-September 1 (pp. 3029–3032) http://doi.org/10.1109/EMBC.2012.6346602

Agnew, W. F., McCreery, D. B., Yuen, T. G., & Bullara, L. A. (1989). Histologic and physiologic evaluation of electrically stimulated peripheral nerve: considerations for the selection of parameters. *Annals of Biomedical Engineering*, *17*(1), 39–60.

Andersen, P., Hagan, P. J., Phillips, C. G., & Powell, T. P. (1975). Mapping by microstimulation of overlapping projections from area 4 to motor units of the baboon's hand. *Proceedings of the Royal Society of London. Series B, Biological Sciences*, *188*(1090), 31–36.

Anderson, V. C., Burchiel, K. J., Hogarth, P., Favre, J., & Hammerstad, J. P. (2005). Pallidal vs subthalamic nucleus deep brain stimulation in Parkinson's disease. *Archives of Neurology*, *62*(4), 554–560. http://doi.org/10.1001/archneur.62.4.554

Archambeau, C., Delbeke, J., Veraart, C., & Verleysen, M. (2004). Prediction of visual perceptions with artificial neural networks in a visual prosthesis for the blind. *Artificial Intelligence in Medicine*, *32*(3), 183–194. http://doi.org/10.1016/j.artmed.2004.02.004

Armstrong, D. M., & Drew, T. (1984). Topographical localization in the motor cortex of the cat for somatic afferent responses and evoked movements. *The Journal of Physiology*, *350*, 33–54.

Asanuma, H., & Arnold, A. P. (1975). Noxious effects of excessive currents used for intracortical microstimulation. *Brain Research*, *96*(1), 103–107.

Asanuma, H., Arnold, A., & Zarzecki, P. (1976). Further study on the excitation of pyramidal tract cells by intracortical microstimulation. *Experimental Brain Research*, *26*(5), 443–461.

Asanuma, H., & Rosen, I. (1972). Topographical organization of cortical efferent zones projecting to distal forelimb muscles in the monkey. *Experimental Brain Research*, *14*(3), 243–256.

Bahmer, A., & Baumann, U. (2012). Application of triphasic pulses with adjustable phase amplitude ratio (PAR) for cochlear ECAP recording: I. Amplitude growth functions. *Journal of Neuroscience Methods*, *205*(1), 202–211. http://doi.org/10.1016/j.jneumeth.2011.12.005

Bahmer, A., Peter, O., & Baumann, U. (2010). Recording and analysis of electrically evoked compound action potentials (ECAPs) with MED-EL cochlear implants and different artifact reduction strategies in Matlab. *Journal of Neuroscience Methods*, *191*(1), 66–74. http://doi.org/10.1016/j.jneumeth.2010.06.008

Bak, M., Girvin, J. P., Hambrecht, F. T., Kufta, C. V., Loeb, G. E., & Schmidt, E. M. (1990). Visual sensations produced by intracortical microstimulation of the human occipital cortex. *Medical & Biological Engineering & Computing*, *28*(3), 257–259.

Bartlett, J. R., DeYoe, E. A., Doty, R. W., Lee, B. B., Lewine, J. D., Negrão, N., & Overman, W. H., Jr. (2005). Psychophysics of electrical stimulation of striate cortex in macaques. *Journal of Neurophysiology*, *94*(5), 3430–3442. http://doi.org/10.1152/jn.00406.2005

Benabid, A. L., Chabardes, S., Mitrofanis, J., & Pollak, P. (2009). Deep brain stimulation of the subthalamic nucleus for the treatment of Parkinson's disease. *The Lancet Neurology*, *8*(1), 67 – 81. http://doi.org/http://dx.doi.org/10.1016/S1474-4422(08)70291-6

Berg, J. A., Dammann, J. F., Tenore, F. V., Tabot, G. A., Boback, J. L., Manfredi, L. R., … Bensmaia, S. J. (2013). Behavioral demonstration of a somatosensory neuroprosthesis. *IEEE Transactions on Neural Systems and Rehabilitation Engineering*, *21*(3), 500–507. http://doi.org/10.1109/TNSRE.2013.2244616

Bierer, J. A., & Middlebrooks, J. C. (2002). Auditory cortical images of cochlear-implant stimuli: dependence on electrode configuration. *Journal of Neurophysiology*, *87*(1), 478–492.

Bierer, J. A., & Middlebrooks, J. C. (2004). Cortical responses to cochlear implant stimulation: channel interactions. *Journal of the Association for Research in Otolaryngology: JARO*, *5*(1), 32–48. http://doi.org/10.1007/s10162-003-3057-7

Birdno, M. J., Cooper, S. E., Rezai, A. R., & Grill, W. M. (2007). Pulse-to-pulse changes in the frequency of deep brain stimulation affect tremor and modeled neuronal activity. *Journal of Neurophysiology*, *98*(3), 1675–1684. http://doi.org/10.1152/jn.00547.2007

Birdno, M. J., Kuncel, A. M., Dorval, A. D., Turner, D. A., Gross, R. E., & Grill, W. M. (2012). Stimulus features underlying reduced tremor suppression with temporally patterned deep brain stimulation. *Journal of Neurophysiology*, *107*(1), 364–383. http://doi.org/10.1152/jn.00906.2010

Bonazzi, L., Viaro, R., Lodi, E., Canto, R., Bonifazzi, C., & Franchi, G. (2013). Complex movement topography and extrinsic space representation in the rat forelimb motor cortex as defined by long-duration intracortical microstimulation. *The Journal of Neuroscience: The Official Journal of the Society for Neuroscience*, *33*(5), 2097–2107. http://doi.org/10.1523/JNEUROSCI.3454-12.2013

Bradley, D. C., Troyk, P. R., Berg, J. A., Bak, M., Cogan, S., Erickson, R., … Xu, H. (2005). Visuotopic mapping through a multichannel stimulating implant in primate V1. *Journal of Neurophysiology*, *93*(3), 1659–1670. http://doi.org/10.1152/jn.01213.2003

Brecht, M., Schneider, M., Sakmann, B., & Margrie, T. W. (2004). Whisker movements evoked by stimulation of single pyramidal cells in rat motor cortex. *Nature*, *427*(6976), 704–710. http://doi.org/10.1038/nature02266

Brindley, G. S. (1973). Sensory effects of electrical stimulation of the visual and paravisual cortex in man. In G. Berlucchi, G. S. Brindley, B. Brooks, O. D. Creutzfeldt, E. Dodt, R. W. Doty, … D. Whitteridge, R. Jung (Ed.), *Visual Centers in the Brain* (Vol. 7 / 3 / 3 B, pp. 583–594). Berlin, Heidelberg: Springer Berlin Heidelberg. Retrieved from http://www.springerlink.com/index/10.1007/978-3-642-65495-4_14

Brindley, G. S. (1982). Effects of electrical stimulation of the visual cortex. *Human Neurobiology*, *1*(4), 281–283.

Brindley, G. S., & Lewin, W. S. (1968). The sensations produced by electrical stimulation of the visual cortex. *The Journal of Physiology*, *196*(2), 479–493.

Bronstein, J. M., Tagliati, M., Alterman, R. L., Lozano, A. M., Volkmann, J., Stefani, A., … DeLong, M. R. (2011). Deep brain stimulation for Parkinson disease: An expert consensus

and review of key issues. *Archives of Neurology*, *68*(2). http://doi.org/10.1001/archneurol.2010.260

Brown, A. R., & Teskey, G. C. (2014). Motor cortex is functionally organized as a set of spatially distinct representations for complex movements. *The Journal of Neuroscience: The Official Journal of the Society for Neuroscience*, *34*(41), 13574–13585. http://doi.org/10.1523/JNEUROSCI.2500-14.2014

Brus-Ramer, M., Carmel, J. B., & Martin, J. H. (2009). Motor cortex bilateral motor representation depends on subcortical and interhemispheric interactions. *The Journal of Neuroscience: The Official Journal of the Society for Neuroscience*, *29*(19), 6196–6206. http://doi.org/10.1523/JNEUROSCI.5852-08.2009

Butovas, S. (2003). Spatiotemporal effects of microstimulation in rat neocortex: A parametric study using multielectrode recordings. *Journal of Neurophysiology*, *90*(5), 3024–3039. http://doi.org/10.1152/jn.00245.2003

Butovas, S., & Schwarz, C. (2007). Detection psychophysics of intracortical microstimulation in rat primary somatosensory cortex. *European Journal of Neuroscience*, *25*(7), 2161–2169. http://doi.org/10.1111/j.1460-9568.2007.05449.x

Chakrabarty, S. (2005). Motor but not sensory representation in motor cortex depends on postsynaptic activity during development and in maturity. *Journal of Neurophysiology*, *94*(5), 3192–3198. http://doi.org/10.1152/jn.00424.2005

Chang, T. R., Chiu, T. W., Sun, X., & Poon, P. W. F. (2012). Modeling frequency modulated responses of midbrain auditory neurons based on trigger features and artificial neural networks. *Brain Research*, *1434*, 90–101. http://doi.org/10.1016/j.brainres.2011.09.042

Chaturvedi, A., Luján, J. L., & McIntyre, C. C. (2013). Artificial neural network based characterization of the volume of tissue activated during deep brain stimulation. *Journal of Neural Engineering*, *10*(5), 056023. http://doi.org/10.1088/1741-2560/10/5/056023

Cheney, P. D., Griffin, D. M., & Van Acker, G. M. (2013). Neural hijacking: Action of high-frequency electrical stimulation on cortical circuits. *The Neuroscientist*, *19*(5), 434–441. http://doi.org/10.1177/1073858412458368

Crist, R. E., & Lebedev, M. A. (2008). Multielectrode recording in behaving monkeys. In M. A. Nicolelis (Ed.), *Methods for Neural Ensemble Recordings* (2nd ed.). Boca Raton (FL): CRC Press. Retrieved from http://www.ncbi.nlm.nih.gov/books/NBK3891/

Dancause, N., Barbay, S., Frost, S. B., Mahnken, J. D., & Nudo, R. J. (2007). Interhemispheric connections of the ventral premotor cortex in a new world primate. *The Journal of Comparative Neurology*, *505*(6), 701–715. http://doi.org/10.1002/cne.21531

Danziger, Z., & Grill, W. M. (2015). A neuron model of stochastic resonance using rectangular pulse trains. *Journal of Computational Neuroscience*, *38*(1), 53–66. http://doi.org/10.1007/s10827-014-0526-4

Das, S., Trutoiu, L., Murai, A., Alcindor, D., Oh, M., De la Torre, F., & Hodgins, J. (2011). Quantitative measurement of motor symptoms in Parkinson's disease: A study with full-body motion capture data. *Conference Proceedings of the Annual International Conference of the IEEE Engineering in Medicine and Biology Society. IEEE Engineering in Medicine and Biology Society. Annual Conference*, *2011*, 6789–6792. http://doi.org/10.1109/IEMBS.2011.6091674

Davis, T. S., Parker, R. A., House, P. A., Bagley, E., Wendelken, S., Normann, R. A., & Greger, B. (2012). Spatial and temporal characteristics of V1 microstimulation during chronic implantation of a microelectrode array in a behaving macaque. *Journal of Neural Engineering*, *9*(6), 065003. http://doi.org/10.1088/1741-2560/9/6/065003

Del Rio-Oliva, C., Aviles-Olmos, I., Kefalopoulou, Z., Grover, T., Foltynie, T., & Zrinzo, L. (2012). Current controlled stimulation versus voltage controlled stimulation in patients with bilateral subthalamic nucleus deep brain stimulation for advanced Parkinson's disease. *Movement Disorders*, *27*, 485.

Deuschl, G., Schade-Brittinger, C., Krack, P., Volkmann, J., Schäfer, H., Bötzel, K., … Voges, J. (2006). A randomized trial of deep-brain stimulation for Parkinson's disease. *New England Journal of Medicine*, *355*(9), 896–908. http://doi.org/10.1056/NEJMoa060281

DeYoe, E. A., Lewine, J. D., & Doty, R. W. (2005). Laminar variation in threshold for detection of electrical excitation of striate cortex by macaques. *Journal of Neurophysiology*, *94*(5), 3443–3450. http://doi.org/10.1152/jn.00407.2005

Dobelle, W. H., & Mladejovsky, M. G. (1974). Phosphenes produced by electrical stimulation of human occipital cortex, and their application to the development of a prosthesis for the blind. *The Journal of Physiology*, *243*(2), 553–576.

Dobelle, W. H., Mladejovsky, M. G., & Girvin, J. P. (1974). Artifical vision for the blind: electrical stimulation of visual cortex offers hope for a functional prosthesis. *Science*, *183*(4123), 440–444.

Dokos, S., Suaning, G. J., & Lovell, N. H. (2005). A bidomain model of epiretinal stimulation. *IEEE Transactions on Neural Systems and Rehabilitation Engineering: A Publication of the IEEE Engineering in Medicine and Biology Society*, *13*(2), 137–146. http://doi.org/10.1109/TNSRE.2005.847390

Donoghue, J. P., Leibovic, S., & Sanes, J. N. (1992). Organization of the forelimb area in squirrel monkey motor cortex: representation of digit, wrist, and elbow muscles. *Experimental Brain Research*, *89*(1), 1–19.

Donoghue, J. P., & Wise, S. (1982). The motor cortex of the rat: Cytoarchitecture and microstimulation mapping. *The Journal of Comparative Neurology*, *212*(1), 76–88. http://doi.org/10.1002/cne.902120106

Ebrahimi, A., Pochet, R., & Roger, M. (1992). Topographical organization of the projections from physiologically identified areas of the motor cortex to the striatum in the rat. *Neuroscience Research*, *14*(1), 39–60.

Evans, JD. (1996). *Straightforward Statistics for the Behavioral Sciences*. Pacific Grove California: Brooks/Cole Publishing.

Fisher, R. S. (2012). Therapeutic devices for epilepsy. *Annals of Neurology*, *71*(2), 157–168. http://doi.org/10.1002/ana.22621

Fisher, R. S., Salanova, V., Witt, T., Worth, R., Henry, T., Gross, R., … SANTE Study Group. (2010). Electrical stimulation of the anterior nucleus of thalamus for treatment of refractory epilepsy. *Epilepsia*, *51*(5), 899–908. http://doi.org/10.1111/j.1528-1167.2010.02536.x

Foutz, T. J., & McIntyre, C. C. (2010). Evaluation of novel stimulus waveforms for deep brain stimulation. *Journal of Neural Engineering*, *7*(6), 066008. http://doi.org/10.1088/1741-2560/7/6/066008

Gerdle, B., Karlsson, S., Day, S., & Djupsjobacka, M. (1999). Acquisition, processing and analysis of the surface electromyogram. In *Modern techniques in neuroscience research* (pp. 705–753). Berlin ; New York: Springer.

Gharbawie, O. A., Stepniewska, I., & Kaas, J. H. (2011). Cortical connections of functional zones in posterior parietal cortex and frontal cortex motor regions in new world monkeys. *Cerebral Cortex*, *21*(9), 1981–2002. http://doi.org/10.1093/cercor/bhq260

Gioanni, Y., & Lamarche, M. (1985). A reappraisal of rat motor cortex organization by intracortical microstimulation. *Brain Research*, *344*(1).

Graziano, M. S. A., Taylor, C. S. R., & Moore, T. (2002). Complex movements evoked by microstimulation of precentral cortex. *Neuron*, *34*(5), 841–851.

Griffin, D. M., Hudson, H. M., Belhaj-Saïf, A., & Cheney, P. D. (2014). EMG activation patterns associated with high frequency, long-duration intracortical microstimulation of primary motor cortex. *The Journal of Neuroscience: The Official Journal of the Society for Neuroscience*, *34*(5), 1647–1656. http://doi.org/10.1523/JNEUROSCI.3643-13.2014

Griffin, D. M., Hudson, H. M., Belhaj-Saïf, A., McKiernan, B. J., & Cheney, P. D. (2008). Do corticomotoneuronal cells predict target muscle EMG activity? *Journal of Neurophysiology*, *99*(3), 1169–1986. http://doi.org/10.1152/jn.00906.2007

Habib, A. G., Cameron, M. A., Suaning, G. J., Lovell, N. H., & Morley, J. W. (2012). Efficacy of the hexpolar configuration in localizing the activation of retinal ganglion cells under electrical stimulation. *Conference Proceedings of the Annual International Conference of the IEEE Engineering in Medicine and Biology Society. IEEE Engineering in Medicine and Biology Society. Conference*, *2012*, 2776–2779. http://doi.org/10.1109/EMBC.2012.6346540

Haiss, F., & Schwarz, C. (2005). Spatial segregation of different modes of movement control in the whisker representation of rat primary motor cortex. *The Journal of Neuroscience: The Official Journal of the Society for Neuroscience*, *25*(6), 1579–1587. http://doi.org/10.1523/JNEUROSCI.3760-04.2005

Hall, R. D., & Lindholm, E. P. (1974). Organization of motor and somatosensory neocortex in the albino rat. *Brain Research*, *66*(1), 23–38. http://doi.org/10.1016/0006-8993(74)90076-6

Hanson, T., Fitzsimmons, N., & O'Doherty, J. E. (2008). Technology for multielectrode microstimulation of brain tissue. In M. A. Nicolelis (Ed.), *Methods for Neural Ensemble Recordings* (2nd ed.). Boca Raton (FL): CRC Press. Retrieved from http://www.ncbi.nlm.nih.gov/books/NBK3896/

Hill, A. V. (1936). Excitation and accommodation in nerve. *Proceedings of the Royal Society of London B: Biological Sciences*, *119*(814), 305–355. http://doi.org/10.1098/rspb.1936.0012

Horsager, A., Boynton, G. M., Greenberg, R. J., & Fine, I. (2011). Temporal interactions during paired-electrode stimulation in two retinal prosthesis subjects. *Investigative Ophthalmology & Visual Science*, *52*(1), 549–557. http://doi.org/10.1167/iovs.10-5282

Horsager, A., Greenberg, R. J., & Fine, I. (2010). Spatiotemporal interactions in retinal prosthesis subjects. *Investigative Ophthalmology & Visual Science*, *51*(2), 1223–1233. http://doi.org/10.1167/iovs.09-3746

Horwitz, G. D., & Newsome, W. T. (2001). Target selection for saccadic eye movements: direction-selective visual responses in the superior colliculus. *Journal of Neurophysiology*, *86*(5), 2527–2542.

Hubel, D. H., & Wiesel, T. N. (1977). Ferrier lecture. Functional architecture of macaque monkey visual cortex. *Proceedings of the Royal Society of London. Series B, Biological Sciences*, *198*(1130), 1–59.

Hyland, B. (1998). Neural activity related to reaching and grasping in rostral and caudal regions of rat motor cortex. *Behavioural Brain Research*, *94*(2), 255–269.

Jacobs, A. L., Fridman, G., Douglas, R. M., Alam, N. M., Latham, P. E., Prusky, G. T., & Nirenberg, S. (2009). Ruling out and ruling in neural codes. *Proceedings of the National Academy of Sciences*, *106*(14), 5936–5941. http://doi.org/10.1073/pnas.0900573106

Jepson, L. H., Hottowy, P., Mathieson, K., Gunning, D. E., Dabrowski, W., Litke, A. M., & Chichilnisky, E. J. (2013). Focal electrical stimulation of major ganglion cell types in the primate retina for the design of visual prostheses. *The Journal of Neuroscience: The Official Journal of the Society for Neuroscience*, *33*(17), 7194–7205. http://doi.org/10.1523/JNEUROSCI.4967-12.2013

Joarder, S. A., Dokos, S., Suaning, G. J., & Lovell, N. H. (2007). Finite element bidomain model of epiretinal stimulation. *Conference Proceedings of the Annual International Conference of the IEEE Engineering in Medicine and Biology Society. IEEE Engineering in Medicine and Biology Society. Conference*, *2007*, 1132–1135. http://doi.org/10.1109/IEMBS.2007.4352495

Joucla, S., Branchereau, P., Cattaert, D., & Yvert, B. (2012). Extracellular neural microstimulation may activate much larger regions than expected by simulations: A combined experimental and modeling study. *PLoS ONE*, *7*(8), e41324. http://doi.org/10.1371/journal.pone.0041324

Joucla, S., & Yvert, B. (2009). Improved focalization of electrical microstimulation using microelectrode arrays: a modeling study. *PloS One*, *4*(3), e4828. http://doi.org/10.1371/journal.pone.0004828

Kerrigan, J. F., Litt, B., Fisher, R. S., Cranstoun, S., French, J. A., Blum, D. E., … Graves, N. (2004). Electrical stimulation of the anterior nucleus of the thalamus for the treatment of intractable epilepsy. *Epilepsia*, *45*(4), 346–354. http://doi.org/10.1111/j.0013-9580.2004.01304.x

Kim, S., Callier, T., Tabot, G. A., Tenore, F. V., & Bensmaia, S. J. (2015). Sensitivity to microstimulation of somatosensory cortex distributed over multiple electrodes. *Frontiers in Systems Neuroscience*, *9*, 47. http://doi.org/10.3389/fnsys.2015.00047

Koivuniemi, A. S., & Otto, K. J. (2011). Asymmetric versus symmetric pulses for cortical microstimulation. *IEEE Transactions on Neural Systems and Rehabilitation Engineering*, *19*(5), 468–476. http://doi.org/10.1109/TNSRE.2011.2166563

Koivuniemi, A. S., & Otto, K. J. (2012). The depth, waveform and pulse rate for electrical microstimulation of the auditory cortex. *Conference Proceedings of the Annual International Conference of the IEEE Engineering in Medicine and Biology Society. IEEE Engineering in Medicine and Biology Society. Conference*, *2012*, 2489–2492. http://doi.org/10.1109/EMBC.2012.6346469

Koivuniemi, A. S., Regele, O. B., Brenner, J. H., & Otto, K. J. (2011). Rat behavioral model for high-throughput parametric studies of intracortical microstimulation. *Conference*

Proceedings: ... Annual International Conference of the IEEE Engineering in Medicine and Biology Society. IEEE Engineering in Medicine and Biology Society. Conference, *2011*, 7541–7544. http://doi.org/10.1109/IEMBS.2011.6091859

Kombos, T., Suess, O., Kern, B. C., Funk, T., Hoell, T., Kopetsch, O., & Brock, M. (1999). Comparison between monopolar and bipolar electrical stimulation of the motor cortex. *Acta Neurochirurgica*, *141*(12), 1295–1301.

Kral, A., Hartmann, R., Mortazavi, D., & Klinke, R. (1998). Spatial resolution of cochlear implants: the electrical field and excitation of auditory afferents. *Hearing Research*, *121*(1-2), 11–28.

Lau, B., Stanley, G. B., & Dan, Y. (2002). Computational subunits of visual cortical neurons revealed by artificial neural networks. *Proceedings of the National Academy of Sciences of the United States of America*, *99*(13), 8974–8979. http://doi.org/10.1073/pnas.122173799

Lee, K. J., Jang, K. S., & Shon, Y. M. (2006). Chronic deep brain stimulation of subthalamic and anterior thalamic nuclei for controlling refractory partial epilepsy. *Acta Neurochirurgica. Supplement*, *99*.

Lempka, S. F., Johnson, M. D., Miocinovic, S., Vitek, J. L., & McIntyre, C. C. (2010). Current-controlled deep brain stimulation reduces in vivo voltage fluctuations observed during voltage-controlled stimulation. *Clinical Neurophysiology: Official Journal of the International Federation of Clinical Neurophysiology*, *121*(12), 2128–2133. http://doi.org/10.1016/j.clinph.2010.04.026

Lempka, S. F., Johnson, M. D., Moffitt, M. A., Otto, K. J., Kipke, D. R., & McIntyre, C. C. (2011). Theoretical analysis of intracortical microelectrode recordings. *Journal of Neural Engineering*, *8*(4), 045006. http://doi.org/10.1088/1741-2560/8/4/045006

LeVay, S., Connolly, M., Houde, J., & Van Essen, D. C. (1985). The complete pattern of ocular dominance stripes in the striate cortex and visual field of the macaque monkey. *The Journal of Neuroscience: The Official Journal of the Society for Neuroscience*, *5*(2), 486–501.

Lilly, J. C. (1961). Injury and excitation by electric currents. A. The balanced pulse-pair waveform. In D. . Sheer (Ed.), *Electrical stimulation of the brain* (pp. 60–64). Austin Texas: University of Texas Press.

Lilly, J. C., Hughes, J. R., Alvord, E. C. J., & Galkin, T. W. (1955). Brief, noninjurious electric waveform for stimulation of the brain. *Science (New York, N.Y.)*, *121*(3144), 468–469.

Little, S., Pogosyan, A., Neal, S., Zavala, B., Zrinzo, L., Hariz, M., … Brown, P. (2013). Adaptive deep brain stimulation in advanced Parkinson disease: Adaptive DBS in PD. *Annals of Neurology*, n/a–n/a. http://doi.org/10.1002/ana.23951

Logothetis, N. K., Augath, M., Murayama, Y., Rauch, A., Sultan, F., Goense, J., … Merkle, H. (2010). The effects of electrical microstimulation on cortical signal propagation. *Nature Neuroscience*, *13*(10), 1283–1291. http://doi.org/10.1038/nn.2631

Lovell, N. H., Dokos, S., Cloherty, S. L., Preston, P. J., & Suaning, G. J. (2005). Current distribution during parallel stimulation: implications for an epiretinal neuroprosthesis. *Conference Proceedings: ... Annual International Conference of the IEEE Engineering in Medicine and Biology Society. IEEE Engineering in Medicine and Biology Society. Conference*, *5*, 5242–5245. http://doi.org/10.1109/IEMBS.2005.1615661

Lyons, M. K. (2011). Deep brain stimulation: current and future clinical applications. *Mayo Clinic Proceedings*, *86*(7), 662–672. http://doi.org/10.4065/mcp.2011.0045

Macherey, O., van Wieringen, A., Carlyon, R. P., Deeks, J. M., & Wouters, J. (2006). Asymmetric pulses in cochlear implants: effects of pulse shape, polarity, and rate. *Journal of the Association for Research in Otolaryngology: JARO*, *7*(3), 253–266. http://doi.org/10.1007/s10162-006-0040-0

Marple-Horvat, D. E., & Armstrong, D. M. (1999). Central regulation of motor cortex neuronal responses to forelimb nerve inputs during precision walking in the cat. *The Journal of Physiology*, *519*(1), 279–299. http://doi.org/10.1111/j.1469-7793.1999.0279o.x

Marzullo, T. C., Lehmkuhle, M. J., Gage, G. J., & Kipke, D. R. (2010). Development of closed-loop neural interface technology in a rat model: Combining motor cortex operant conditioning with visual cortex microstimulation. *IEEE Transactions on Neural Systems and Rehabilitation Engineering*, *18*(2), 117–126. http://doi.org/10.1109/TNSRE.2010.2041363

Masse, N. Y., & Cook, E. P. (2009). Behavioral time course of microstimulation in cortical area MT. *Journal of Neurophysiology*, *103*(1), 334–345. http://doi.org/10.1152/jn.91022.2008

Matteucci, P. B., Chen, S. C., Dodds, C., DokosNigel, S., Lovell, H., & Suaning, G. J. (2012). Threshold analysis of a quasimonopolar stimulation paradigm in visual prosthesis. *Conference Proceedings: ... Annual International Conference of the IEEE Engineering in Medicine and Biology Society. IEEE Engineering in Medicine and Biology Society. Conference*, *2012*, 2997–3000. http://doi.org/10.1109/EMBC.2012.6346594

McCarthy, P. T., Otto, K. J., & Rao, M. P. (2011). Robust penetrating microelectrodes for neural interfaces realized by titanium micromachining. *Biomedical Microdevices*, *13*(3), 503–515. http://doi.org/10.1007/s10544-011-9519-5

McCreery, D. B., Agnew, W. F., Yuen, T. G., & Bullara, L. A. (1990). Charge density and charge per phase as cofactors in neural injury induced by electrical stimulation. *IEEE Transactions on Bio-Medical Engineering*, *37*(10), 996–1001.

McCreery, D. B., Agnew, W. F., Yuen, T. G., & Bullara, L. A. (1992). Damage in peripheral nerve from continuous electrical stimulation: comparison of two stimulus waveforms. *Medical & Biological Engineering & Computing*, *30*(1), 109–114.

McCreery, D. B., Agnew, W. F., Yuen, T. G., & Bullara, L. A. (1995). Relationship between stimulus amplitude, stimulus frequency and neural damage during electrical stimulation of sciatic nerve of cat. *Medical & Biological Engineering & Computing*, *33*(3 Spec No), 426–429.

McCreery, D. B., Pikov, V., & Troyk, P. R. (2010). Neuronal loss due to prolonged controlled-current stimulation with chronically implanted microelectrodes in the cat cerebral cortex. *Journal of Neural Engineering*, *7*(3). http://doi.org/10.1088/1741-2560/7/3/036005

McIntyre, C. C., Frankenmolle, A. M., Wu, J., Noecker, A. M., & Alberts, J. L. (2009). Customizing deep brain stimulation to the patient using computational models. *Conference Proceedings: ... Annual International Conference of the IEEE Engineering in Medicine and Biology Society. IEEE Engineering in Medicine and Biology Society. Conference*, *2009*, 4228–4229. http://doi.org/10.1109/IEMBS.2009.5334592

McIntyre, C. C., & Grill, W. M. (2000). Selective microstimulation of central nervous system neurons. *Annals of Biomedical Engineering*, *28*(3), 219–233.

McIntyre, C. C., & Grill, W. M. (2001). Finite element analysis of the current-density and electric field generated by metal microelectrodes. *Annals of Biomedical Engineering*, *29*(3), 227–235. http://doi.org/10.1114/1.1352640

McIntyre, C. C., & Grill, W. M. (2002). Extracellular stimulation of central neurons: influence of stimulus waveform and frequency on neuronal output. *Journal of Neurophysiology*, *88*(4), 1592–1604.

Merrill, D. R., Bikson, M., & Jefferys, J. G. R. (2005). Electrical stimulation of excitable tissue: design of efficacious and safe protocols. *Journal of Neuroscience Methods*, *141*(2), 171–198. http://doi.org/10.1016/j.jneumeth.2004.10.020

Morrell, M. J. (2011). Responsive cortical stimulation for the treatment of medically intractable partial epilepsy. *Neurology*, *77*(13), 1295–1304. http://doi.org/10.1212/WNL.0b013e3182302056

Motamedi, G. K., Lesser, R. P., Miglioretti, D. L., Mizuno-Matsumoto, Y., Gordon, B., Webber, W. R. S., … Crone, N. E. (2002). Optimizing parameters for terminating cortical afterdischarges with pulse stimulation. *Epilepsia*, *43*(8), 836–846.

Murasugi, C. M., Salzman, C. D., & Newsome, W. T. (1993). Microstimulation in visual area MT: effects of varying pulse amplitude and frequency. *The Journal of Neuroscience: The Official Journal of the Society for Neuroscience*, *13*(4), 1719–1729.

Murphey, D. K., & Maunsell, J. H. R. (2007). Behavioral detection of electrical microstimulation in different cortical visual areas. *Current Biology: CB*, *17*(10), 862–867. http://doi.org/10.1016/j.cub.2007.03.066

Nanduri, D., Fine, I., Horsager, A., Boynton, G. M., Humayun, M. S., Greenberg, R. J., & Weiland, J. D. (2012). Frequency and amplitude modulation have different effects on the percepts elicited by retinal stimulation. *Investigative Ophthalmology & Visual Science*, *53*(1), 205–214. http://doi.org/10.1167/iovs.11-8401

Neafsey, E. J., Bold, E. L., Haas, G., Hurley-Gius, K. M., Quirk, G., Sievert, C. F., & Terreberry, R. R. (1986). The organization of the rat motor cortex: a microstimulation mapping study. *Brain Research*, *396*(1).

Neuman, M. R. (1998). Biopotential Electrodes. In J. G. Webster (Ed.), *Medical Instrumentation Application and Design* (3rd ed., pp. 183–230). Hoboken NJ: John Wiley and Sons.

Nirenberg, S., & Pandarinath, C. (2012). Retinal prosthetic strategy with the capacity to restore normal vision. *Proceedings of the National Academy of Sciences*, *109*(37), 15012–15017. http://doi.org/10.1073/pnas.1207035109

Nudo, R. J., Jenkins, W. M., & Merzenich, M. M. (1990). Repetitive microstimulation alters the cortical representation of movements in adult rats. *Somatosensory & Motor Research*, *7*(4), 463–483.

Nudo, R. J., Jenkins, W. M., Merzenich, M. M., Prejean, T., & Grenda, R. (1992). Neurophysiological correlates of hand preference in primary motor cortex of adult squirrel monkeys. *The Journal of Neuroscience : The Official Journal of the Society for Neuroscience*, *12*(8), 2918–2947.

Otto, K. J., Rousche, P. J., & Kipke, D. R. (2005). Cortical microstimulation in auditory cortex of rat elicits best-frequency dependent behaviors. *Journal of Neural Engineering*, *2*(2), 42–51. http://doi.org/10.1088/1741-2560/2/2/005

Overstreet, C. K., Klein, J. D., & Helms Tillery, S. I. (2013). Computational modeling of direct neuronal recruitment during intracortical microstimulation in somatosensory cortex. *Journal of Neural Engineering*, *10*(6), 066016. http://doi.org/10.1088/1741-2560/10/6/066016

Penfield, W., & Boldrey, E. (1937). Somatic motor and sensory representation in the cerebral cortex of man as studied by electrical stimulation. *Brain*, *60*(4), 389–443. http://doi.org/10.1093/brain/60.4.389

Penfield, W., & Perot, P. (1963). The brain's record of auditory and visual experience. A final summary and discussion. *Brain: A Journal of Neurology*, *86*, 595–696.

Penfield, W., & Welch, K. (1951). The supplementary motor area of the cerebral cortex; a clinical and experimental study. *A.M.A. Archives of Neurology and Psychiatry*, *66*(3), 289–317.

Polikov, V. S., Tresco, P. A., & Reichert, W. M. (2005). Response of brain tissue to chronically implanted neural electrodes. *Journal of Neuroscience Methods*, *148*(1), 1–18. http://doi.org/10.1016/j.jneumeth.2005.08.015

Prenger, R., Wu, M. C.-K., David, S. V., & Gallant, J. L. (2004). Nonlinear V1 responses to natural scenes revealed by neural network analysis. *Neural Networks: The Official Journal of the International Neural Network Society*, *17*(5-6), 663–679. http://doi.org/10.1016/j.neunet.2004.03.008

Pulliam, C. L., Heldman, D. A., Orcutt, T. H., Mera, T. O., Giuffrida, J. P., & Vitek, J. L. (2015). Motion sensor strategies for automated optimization of deep brain stimulation in Parkinson's disease. *Parkinsonism & Related Disorders*, *21*(4), 378–382. http://doi.org/10.1016/j.parkreldis.2015.01.018

Rajdev, P., Ward, M., & Irazoqui, P. (2011). Effect of stimulus parameters in the treatment of seizures by electrical stimulation in the kainate animal model. *International Journal of Neural Systems*, *21*(02), 151–162. http://doi.org/10.1142/S0129065711002730

Ranck, J. B., Jr. (1975). Which elements are excited in electrical stimulation of mammalian central nervous system: a review. *Brain Research*, *98*(3), 417–440.

Reich, M. M., Steigerwald, F., Sawalhe, A. D., Reese, R., Gunalan, K., Johannes, S., … Volkmann, J. (2015). Short pulse width widens the therapeutic window of subthalamic neurostimulation. *Annals of Clinical and Translational Neurology*, *2*(4), 427–432. http://doi.org/10.1002/acn3.168

Reilly, J. P. (2011a). Excitation Relationships. In *Electrostimulation: Theory, applications and computational model* (pp. 23–44). Boston: Artech House.

Reilly, J. P. (2011b). Waveform and Polarity Effects. In *Electrostimulation: Theory, applications and computational model* (pp. 77–99). Boston: Artech House.

Rouiller, E. M., Moret, V., & Liang, F. (1993). Comparison of the connectional properties of the two forelimb areas of the rat sensorimotor cortex: support for the presence of a premotor or supplementary motor cortical area. *Somatosensory & Motor Research*, *10*(3), 269–289.

Rousche, P. J., & Normann, R. A. (1999). Chronic intracortical microstimulation (ICMS) of cat sensory cortex using the Utah Intracortical Electrode Array. *IEEE Transactions on Rehabilitation Engineering: A Publication of the IEEE Engineering in Medicine and Biology Society*, *7*(1), 56–68.

Salzman, C. D., Britten, K. H., & Newsome, W. T. (1990). Cortical microstimulation influences perceptual judgements of motion direction. *Nature*, *346*(6280), 174–177. http://doi.org/10.1038/346174a0

Salzman, C. D., Murasugi, C. M., Britten, K. H., & Newsome, W. T. (1992). Microstimulation in visual area MT: effects on direction discrimination performance. *The Journal of Neuroscience: The Official Journal of the Society for Neuroscience*, *12*(6), 2331–2355.

Sanderson, K. J., Welker, W., & Shambes, G. M. (1984). Reevaluation of motor cortex and of sensorimotor overlap in cerebral cortex of albino rats. *Brain Research*, *292*(2), 251–260.

Savage, C. O., Grayden, D. B., Meffin, H., & Burkitt, A. N. (2013). Optimized single pulse stimulation strategy for retinal implants. *Journal of Neural Engineering*, *10*(1), 016003. http://doi.org/10.1088/1741-2560/10/1/016003

Savage, C. O., & Halpern, M. E. (2011). Phosphene brightness modelling for voltage driven waveforms (pp. 103–107). IEEE. http://doi.org/10.1109/ISSNIP.2011.6146575

Schieber, M. H. (2001). Constraints on somatotopic organization in the primary motor cortex. *Journal of Neurophysiology*, *86*(5), 2125–2143.

Schiller, P. H., Slocum, W. M., Kwak, M. C., Kendall, G. L., & Tehovnik, E. J. (2011). New methods devised specify the size and color of the spots monkeys see when striate cortex (area V1) is electrically stimulated. *Proceedings of the National Academy of Sciences*, *108*(43), 17809–17814. http://doi.org/10.1073/pnas.1108337108

Schiller, P. H., & Stryker, M. (1972). Single-unit recording and stimulation in superior colliculus of the alert rhesus monkey. *Journal of Neurophysiology*, *35*(6), 915–924.

Schmidt, E. M., Bak, M. J., Hambrecht, F. T., Kufta, C. V., O'Rourke, D. K., & Vallabhanath, P. (1996). Feasibility of a visual prosthesis for the blind based on intracortical microstimulation of the visual cortex. *Brain: A Journal of Neurology*, *119 (Pt 2)*, 507–522.

Schoesser, H., Zierhofer, C., & Hochmair, E.S. (2001). Measuring electrically evoked compound action potentials using triphasic pulses for the reduction of the residual stimulation artifact. *Presented at the Conference on Implantable Auditory Prosthesis 2001.*

Semprini, M., Bennicelli, L., & Vato, A. (2012). A parametric study of intracortical microstimulation in behaving rats for the development of artificial sensory channels. *Conference Proceedings: ... Annual International Conference of the IEEE Engineering in Medicine and Biology Society. IEEE Engineering in Medicine and Biology Society. Conference*, *2012*, 799–802. http://doi.org/10.1109/EMBC.2012.6346052

Shepherd, R. K., & Javel, E. (1999). Electrical stimulation of the auditory nerve: II. Effect of stimulus waveshape on single fibre response properties. *Hearing Research*, *130*(1-2), 171–188.

Shigeto, H., Boongird, A., Baker, K., Kellinghaus, C., Najm, I., & Lüders, H. (2013). Systematic study of the effects of stimulus parameters and stimulus location on afterdischarges elicited by electrical stimulation in the rat. *Epilepsy Research*, *104*(1-2), 17–25. http://doi.org/10.1016/j.eplepsyres.2012.10.002

Sironi, V. A. (2011). Origin and evolution of deep brain stimulation. *Frontiers in Integrative Neuroscience*, *5*. http://doi.org/10.3389/fnint.2011.00042

Snyder, R. L., Bierer, J. A., & Middlebrooks, J. C. (2004). Topographic spread of inferior colliculus activation in response to acoustic and intracochlear electric stimulation. *Journal of the Association for Research in Otolaryngology: JARO*, *5*(3), 305–322. http://doi.org/10.1007/s10162-004-4026-5

Stecker, M. M. (2004). Nerve stimulation with an electrode of finite size: differences between constant current and constant voltage stimulation. *Computers in Biology and Medicine*, *34*(1), 51–94.

Stoney, S. D., Jr, Thompson, W. D., & Asanuma, H. (1968). Excitation of pyramidal tract cells by intracortical microstimulation: effective extent of stimulating current. *Journal of Neurophysiology*, *31*(5), 659–669.

Stowe, A. M., Plautz, E. J., Eisner-Janowicz, I., Frost, S. B., Barbay, S., Zoubina, E. V., … Nudo, R. J. (2007). VEGF protein associates to neurons in remote regions following cortical infarct. *Journal of Cerebral Blood Flow and Metabolism: Official Journal of the International Society of Cerebral Blood Flow and Metabolism*, *27*(1), 76–85. http://doi.org/10.1038/sj.jcbfm.9600320

Stronks, H. C., Barry, M. P., & Dagnelie, G. (2013). Electrically elicited visual evoked potentials in Argus II retinal implant wearers. *Investigative Ophthalmology & Visual Science*, *54*(6), 3891–3901. http://doi.org/10.1167/iovs.13-11594

Sultan, F., Augath, M., & Logothetis, N. (2007). BOLD sensitivity to cortical activation induced by microstimulation: Comparison to visual stimulation. *Magnetic Resonance Imaging*, *25*(6), 754–759. http://doi.org/10.1016/j.mri.2007.03.014

Tabot, G. A., Dammann, J. F., Berg, J. A., Tenore, F. V., Boback, J. L., Vogelstein, R. J., & Bensmaia, S. J. (2013). Restoring the sense of touch with a prosthetic hand through a brain interface. *Proceedings of the National Academy of Sciences*, *110*(45), 18279–18284. http://doi.org/10.1073/pnas.1221113110

Tehovnik, E. J., & Slocum, W. M. (2007). Phosphene induction by microstimulation of macaque V1. *Brain Research Reviews*, *53*(2), 337–343. http://doi.org/10.1016/j.brainresrev.2006.11.001

Tehovnik, E. J., Slocum, W. M., Carvey, C. E., & Schiller, P. H. (2005). Phosphene induction and the generation of saccadic eye movements by striate cortex. *Journal of Neurophysiology*, *93*(1), 1–19. http://doi.org/10.1152/jn.00736.2004

Tehovnik, E. J., Slocum, W. M., & Schiller, P. H. (2003). Saccadic eye movements evoked by microstimulation of striate cortex. *The European Journal of Neuroscience*, *17*(4), 870–878.

Tehovnik, E. J., Slocum, W. M., Smirnakis, S. M., & Tolias, A. S. (2009). Microstimulation of visual cortex to restore vision. *Progress in Brain Research*, *175*, 347–375. http://doi.org/10.1016/S0079-6123(09)17524-6

Thomson, E. E., Carra, R., & Nicolelis, M. A. L. (2013). Perceiving invisible light through a somatosensory cortical prosthesis. *Nature Communications*, *4*, 1482. http://doi.org/10.1038/ncomms2497

Tolias, A. S., Sultan, F., Augath, M., Oeltermann, A., Tehovnik, E. J., Schiller, P. H., & Logothetis, N. K. (2005). Mapping cortical activity elicited with electrical microstimulation using fMRI in the macaque. *Neuron*, *48*(6), 901–911. http://doi.org/10.1016/j.neuron.2005.11.034

Torab, K., Davis, T. S., Warren, D. J., House, P. A., Normann, R. A., & Greger, B. (2011). Multiple factors may influence the performance of a visual prosthesis based on intracortical microstimulation: nonhuman primate behavioural experimentation. *Journal of Neural Engineering*, *8*(3), 035001. http://doi.org/10.1088/1741-2560/8/3/035001

Touvykine, B., Mansoori, B. K., Jean-Charles, L., Deffeyes, J., Quessy, S., & Dancause, N. (2015). The effect of lesion size on the organization of the ipsilesional and contralesional motor cortex. *Neurorehabilitation and Neural Repair*. http://doi.org/10.1177/1545968315585356

Van Acker, G. M., Amundsen, S. L., Messamore, W. G., Zhang, H. Y., Luchies, C. W., Kovac, A., & Cheney, P. D. (2013). Effective intracortical microstimulation parameters applied to primary motor cortex for evoking forelimb movements to stable spatial end points. *Journal of Neurophysiology*, *110*(5), 1180–1189. http://doi.org/10.1152/jn.00172.2012

Van Nieuwenhuyse, B., Raedt, R., Delbeke, J., Wadman, W. J., Boon, P., & Vonck, K. (2015). In search of optimal DBS paradigms to treat epilepsy: bilateral versus unilateral hippocampal stimulation in a rat model for temporal lobe epilepsy. *Brain Stimulation*, *8*(2), 192–199. http://doi.org/10.1016/j.brs.2014.11.016

van Wieringen, A., Macherey, O., Carlyon, R. P., Deeks, J. M., & Wouters, J. (2008). Alternative pulse shapes in electrical hearing. *Hearing Research*, *242*(1-2), 154–163. http://doi.org/10.1016/j.heares.2008.03.005

Wagenaar, D. A., Pine, J., & Potter, S. M. (2004). Effective parameters for stimulation of dissociated cultures using multi-electrode arrays. *Journal of Neuroscience Methods*, *138*(1-2), 27–37. http://doi.org/10.1016/j.jneumeth.2004.03.005

Wang, Y., & Kurata, K. (1998). Quantitative analyses of thalamic and cortical origins of neurons projecting to the rostral and caudal forelimb motor areas in the cerebral cortex of rats. *Brain Research*, *781*(1-2), 137–147.

Watson, M. C., Dancause, N., & Sawan, M. (2015a). Efficient microstimulation of the brain: A parametric approach. In *Engineering in Medicine and Biology Society (EMBC), 2015 37th Annual International Conference of the IEEE*. Milan, Italy.

Watson, M. C., Dancause, N., & Sawan, M. (2015b). Intracortical microstimulation parameters dictate the amplitude and latency of evoked responses. *Brain Stimulation*.

Watson, M. C., Dancause, N., & Sawan, M. (2015c). Prediction of responses evoked by intracortical microstimulation using an artificial neural network model.

Watson, M. C., Sawan, M., & Dancause, N. (2015). Intracortical microstimulation parameters dictate the duration of evoked responses.

Weaver, F. M., Follett, K. A., Stern, M., Luo, P., Harris, C. L., Hur, K., … Reda, D. J. (2012). Randomized trial of deep brain stimulation for Parkinson disease: thirty-six-month outcomes. *Neurology*, *79*(1). http://doi.org/10.1212/WNL.0b013e31825dcdc1

Weitz, A. C., Behrend, M. R., Ahuja, A. K., Christopher, P., Wei, J., Wuyyuru, V., … Weiland, J. D. (2014). Interphase gap as a means to reduce electrical stimulation thresholds for epiretinal prostheses. *Journal of Neural Engineering*, *11*(1), 016007. http://doi.org/10.1088/1741-2560/11/1/016007

Wongsarnpigoon, A., & Grill, W. M. (2010). Energy-efficient waveform shapes for neural stimulation revealed with a genetic algorithm. *Journal of Neural Engineering*, *7*(4), 046009. http://doi.org/10.1088/1741-2560/7/4/046009

Wurtz, R. H., & Mohler, C. W. (1976). Enhancement of visual responses in monkey striate cortex and frontal eye fields. *Journal of Neurophysiology*, *39*(4), 766–772.

Wyckhuys, T., Raedt, R., Vonck, K., Wadman, W., & Boon, P. (2010). Comparison of hippocampal deep brain stimulation with high (130Hz) and low frequency (5Hz) on afterdischarges in kindled rats. *Epilepsy Research*, *88*(2-3), 239–246. http://doi.org/10.1016/j.eplepsyres.2009.11.014

Yanai, D., Weiland, J. D., Mahadevappa, M., Greenberg, R. J., Fine, I., & Humayun, M. S. (2007). Visual performance using a retinal prosthesis in three subjects with retinitis pigmentosa. *American Journal of Ophthalmology*, *143*(5), 820–827. http://doi.org/10.1016/j.ajo.2007.01.027

Young, N. A., Vuong, J., Flynn, C., & Teskey, G. C. (2011). Optimal parameters for microstimulation derived forelimb movement thresholds and motor maps in rats and mice.

Journal of Neuroscience Methods, *196*(1), 60–69. http://doi.org/10.1016/j.jneumeth.2010.12.028

APPENDIX A – INPUT OUTPUT DATA ANN MODEL

```
%~~~~~~~~~~~~~~~~~~~~~~~~~~~~~~~~~~~~~~~~~~~~~~~~~~~~~~~~~~~~~~~~~~~~~~~~~~~~%
%~~~~~~~~~~~~~~~~~~~~~~~~~~DATA ORGANIZATION~~~~~~~~~~~~~~~~~~~~~~~~~~~~~~~~~%
%~~~~~~~~~~~~~~~~~~~~~~~~~~~~~~~~~~~~~~~~~~~~~~~~~~~~~~~~~~~~~~~~~~~~~~~~~~~~%

%load the workspace "inputsOutputsANN.mat" or run "InputOutputANN.m"
%contains two variables: 1)input, 2)output

%Inputs: each row contains one parameter of the stimulation signal (A,F,P,or T)
%        each column contains one complete stimulus (A,F,P,T combination)
%        parameters: A=amplitude,F=frequency,P=pulse duration, T=train duration
%        input organization: A(1,:), F(2,:), P(3,:), T(4,:)


%Outputs: each row contains one metric of the response signal
%         parameters: 1)onset latency, 2)mean, 3)peak, 4)peak time,
%                     5)main response duration, 6)residual activation duration
%         output organization: onset latency(1,:), mean(2,:),  peak(3,:), peak time(4,:),
%                              main response duration(5,:), residual activation duration(6,:)

input=[30,30,30,39,39,39,48,48,48,56,56,56,65,65,65,30,30,30,39,39,39,...
    48,48,48,56,56,56,65,65,65,30,30,30,39,39,39,48,48,48,56,56,56,65,...
    65,65,30,48,65,30,48,65,30,48,65,30,48,65,30,48,65,50,50,50,50,50,...
    50,50,50,50,50,50,50,50,50,50,50,50,50,50,50,50,50,50,50,50,50,50,...
    50,50,50,30,48,65,30,48,65,30,48,65,30,48,65,30,48,65,50,50,50,50,...
    50,50,50,50,50,50,50,50,50,50,50,50,50,50,50,50,50,50,50,50,50,50,...
    50,50,50,50,30,48,65,30,48,65,30,48,65,30,48,65,30,48,65,50,50,50,...
    50,50,50,50,50,50,50,50,50,50,50,50,50,50,50,50,50,50,50,50,50,50,...
    50,50,50,50,50;100,300,500,100,300,500,100,300,500,100,300,500,100,...
    300,500,303,303,303,303,303,303,303,303,303,303,303,303,303,303,303,...
    303,303,303,303,303,303,303,303,303,303,303,303,303,303,303,100,100,...
    100,200,200,200,300,300,300,400,400,400,500,500,500,100,100,100,200,...
    200,200,300,300,300,400,400,400,500,500,500,100,100,100,200,200,200,...
    300,300,300,400,400,400,500,500,500,303,303,303,303,303,303,303,303,...
    303,303,303,303,303,303,303,100,300,500,100,300,500,100,300,500,100,...
    300,500,100,300,500,303,303,303,303,303,303,303,303,303,303,303,303,...
    303,303,303,303,303,303,303,303,303,303,303,303,303,303,303,303,303,...
    303,100,300,500,100,300,500,100,300,500,100,300,500,100,300,500,303,...
    303,303,303,303,303,303,303,303,303,303,303,303,303,303,303;0.20,0.20,...
    0.20,0.20,0.20,0.20,0.20,0.20,0.20,0.20,0.20,0.20,0.20,0.20,0.20,...
    0.18,0.34,0.50,0.18,0.34,0.50,0.18,0.34,0.50,0.18,0.34,0.50,0.18,...
    0.34,0.50,0.20,0.20,0.20,0.20,0.20,0.20,0.20,0.20,0.20,0.20,0.20,...
    0.20,0.20,0.20,0.20,0.20,0.20,0.20,0.20,0.20,0.20,0.20,0.20,0.20,...
    0.20,0.20,0.20,0.20,0.20,0.20,0.18,0.34,0.50,0.18,0.34,0.50,0.18,...
    0.34,0.50,0.18,0.34,0.50,0.18,0.34,0.50,0.20,0.20,0.20,0.20,0.20,...
    0.20,0.20,0.20,0.20,0.20,0.20,0.20,0.20,0.20,0.20,0.18,0.18,0.18,...
    0.26,0.26,0.26,0.34,0.34,0.34,0.42,0.42,0.42,0.50,0.50,0.50,0.18,...
    0.18,0.18,0.26,0.26,0.26,0.34,0.34,0.34,0.42,0.42,0.42,0.50,0.50,...
    0.50,0.18,0.18,0.18,0.26,0.26,0.26,0.34,0.34,0.34,0.42,0.42,0.42,...
    0.50,0.50,0.50,0.20,0.20,0.20,0.20,0.20,0.20,0.20,0.20,0.20,0.20,...
    0.20,0.20,0.20,0.20,0.20,0.20,0.20,0.20,0.20,0.20,0.20,0.20,0.20,...
```

```
    0.20,0.20,0.20,0.20,0.20,0.20,0.20,0.18,0.34,0.50,0.18,0.34,0.50,...
    0.18,0.34,0.50,0.18,0.34,0.50,0.18,0.34,0.50;43,43,43,43,43,43,43,...
    43,43,43,43,43,43,43,43,43,43,43,43,43,43,43,43,43,43,43,43,43,43,...
    43,43,172,300,43,172,300,43,172,300,43,172,300,43,172,300,43,43,43,...
    43,43,43,43,43,43,43,43,43,43,43,43,43,43,43,43,43,43,43,43,43,43,...
    43,43,43,43,43,43,172,300,43,172,300,43,172,300,43,172,300,43,172,...
    300,43,43,43,43,43,43,43,43,43,43,43,43,43,43,43,43,43,43,43,43,43,...
    43,43,43,43,43,43,43,43,43,43,43,172,300,43,172,300,43,172,300,43,172,...
    300,43,172,300,43,43,43,107,107,107,172,172,172,236,236,236,300,300,...
    300,43,43,43,107,107,107,172,172,172,236,236,236,300,300,300,43,43,...
    43,107,107,107,172,172,172,236,236,236,300,300,300];


output=[NaN,44.4416000000000,29.5936000000000,NaN,33.5127272727273,...
    35.1641600000000,40.5504000000000,26.5609846153846,24.8180363636364,...
    39.4240000000000,23.6544000000000,20.0118857142857,38.1440000000000,...
    19.5584000000000,17.5274666666667,31.4368000000000,26.9482666666667,...
    28.0733538461538,32.5888000000000,23.9323428571429,22.1915428571429,...
    25.6512000000000,21.0944000000000,19.6900571428571,26.7027692307692,...
    19.2658285714286,17.4237538461538,18.0224000000000,16.4864000000000,...
    13.8386285714286,NaN,47.0016000000000,61.1181714285714,26.6922666666667,...
    46.2116571428571,43.4176000000000,28.7744000000000,24.9563428571429,...
    24.8393142857143,24.5602461538462,26.1120000000000,24.0201142857143,...
    21.5917714285714,21.4162285714286,18.9203692307692,NaN,46.4896,...
    38.9412571428571,37.5808000000000,31.5733333333333,21.4601142857143,...
    27.3066666666667,26.1851428571429,19.1049142857143,27.4432000000000,...
    25.3321846153846,18.4027428571429,30.4128000000000,25.3805714285714,...
    19.0610285714286,34.0650666666667,33.7042285714286,34.6624000000000,...
    30.0869818181818,23.9323428571429,23.1266461538462,27.3846857142857,...
    20.0265142857143,18.3149714285714,24.3273142857143,18.7785846153846,...
    11.7028571428571,25.2849230769231,18.2442666666667,14.6825846153846,...
    45.4656000000000,73.9958153846154,90.4045714285714,27.9722666666667,...
    32.1220923076923,30.6907428571429,21.6502857142857,25.3366857142857,...
    22.6450285714286,20.8164571428571,25.8486857142857,25.5122285714286,...
    24.1821538461538,25.5842461538462,23.5958857142857,14.9504000000000,...
    27.4432000000000,23.0478769230769,20.2342400000000,26.1986461538462,...
    17.8491076923077,31.1296000000000,22.9668571428571,16.2230857142857,...
    25.7675636363636,18.5197714285714,16.9196307692308,29.1446153846154,...
    17.7152000000000,16.5595428571429,26.8288000000000,28.1879272727273,...
    23.4154666666667,42.1888000000000,23.6544000000000,22.0745142857143,...
    33.4848000000000,20.6116571428571,20.9683692307692,38.7527111111111,...
    19.5291428571429,19.2219428571429,34.4064000000000,20.3093333333333,...
    17.5689142857143,27.0336000000000,25.1392000000000,27.8528000000000,...
    22.5910153846154,23.4349714285714,21.4893714285714,21.1090285714286,...
    18.3588571428571,20.9042285714286,20.9683692307692,19.8802285714286,...
    19.2984615384615,19.8948571428571,19.9241142857143,20.0704000000000,...
    NaN,37.4374400000000,25.4829714285714,37.4784000000000,42.80320,...
    24.1664000000000,45.5680000000000,34.9420307692308,24.3712000000000,...
    92.0576000000000,41.7004307692308,25.4098285714286,68.6080000000000,...
    39.2270769230769,25.9364571428571,23.8592000000000,34.7136000000000,...
    29.0816000000000,68.9356800000000,36.6299428571429,35.2628363636364,...
    60.0994909090909,29.0343384615385,38.7686400000000,81.1566545454545,...
    36.5961846153846,49.6810666666667,76.5952000000000,36.4071384615385,...
```

```
31.6322909090909,20.9920000000000,23.2999384615385,23.2684307692308,...
42.8819692307692,27.5017142857143,20.7725714285714,42.5984000000000,...
23.0107428571429,16.5741714285714,53.8065454545455,27.0043428571429,...
22.3524571428571,44.7658666666667,24.8539428571429,20.9334857142857;...
NaN,2.61274044532911,4.00316559989733,NaN,5.68997463481289,5.8809100,...
2.86457589027123,7.15978719129523,7.25671903777626,4.13278416999674,...
8.62738199560097,9.49309466185306,4.89650437884848,10.6314282999977,...
10.1942184431079,4.58008048553893,6.10550269660356,7.23701966113107,...
4.92105723992609,8.61742302861655,10.3748994726110,6.46834428152943,...
10.4286373893306,12.6762297765838,8.20563747895774,11.2142254887918,...
13.0712414504939,9.21539419453309,12.9383267254265,14.7131779613119,...
NaN,5.04608379969795,5.35767289225727,5.60758490387848,7.857914267,...
7.63221721302086,6.94454398139247,11.5161410576548,11.4798347437630,...
9.25697034810063,13.7596085940978,14.4181802690062,10.2767617136124,...
14.4582368843008,14.7978561082190,NaN,5.07992422171810,6.672050964,...
5.87084794322436,7.59498509716165,11.3588698237290,4.48313244094121,...
7.40284997325632,11.0238689660203,5.75945452292217,8.59169661026473,...
11.4153543008537,5.64820051132604,8.14930847253085,11.1433589042717,...
4.17201426895917,6.32815128977693,6.05678177459655,6.64031964597355,...
10.7782812491246,11.6938170761548,7.78187693635326,11.8042063114075,...
13.5812525647655,8.03916689172911,12.6124079303575,13.1682033737244,...
8.23634265741982,12.5653959120536,13.4059118976708,4.55578325745106,...
10.3855301450396,11.3265190756772,7.80892277936315,13.9022072839143,...
15.0725554960560,8.38849472272809,14.4521937880636,15.1863401415924,...
9.07047929087795,14.6931448640140,14.2570618632640,9.50997210656143,...
13.2126177506912,14.1844380242047,6.09413862228394,7.76439100713348,...
10.8208782266343,7.29566612543422,10.0586686037236,12.8760626657812,...
7.45372008502891,11.9114847926186,13.7613384120445,8.67114862483206,...
13.1456916060789,13.8489129810769,9.00977793488150,13.2459414824324,...
14.4319399329314,7.11127612966811,8.30824586578555,7.84117879934918,...
5.28164695355517,11.2739889792158,10.9757089887841,6.67835673034036,...
11.8043307034927,12.7771388555827,6.51931393098494,12.3517864396376,...
13.7721935091000,6.63354982528027,13.3088080466613,14.3241071017879,...
8.14343951399364,12.7838088408439,13.1914750317340,10.8614475642210,...
14.1662448262754,14.4275560729667,12.2200126662439,15.3798350850910,...
14.9308369656834,13.3787060549803,15.2623423237487,15.1456260663607,...
13.6567547479603,15.1517496736446,14.5636187219726,NaN,5.049934679,...
8.46707845474677,5.27185238752281,7.62913373364427,11.2962133178891,...
5.53566201233480,7.90678229979956,10.8627768245892,4.47615889243025,...
8.16516281842129,10.7889504761260,5.04296872350096,7.98155532230829,...
10.6682776147084,4.87117154079897,6.10705876624706,5.82257446997877,...
6.84384158375906,8.36186758793441,7.63314776784021,8.18714405878299,...
8.66753522971591,7.06277726294502,8.44637849116804,8.21402828968041,...
7.16026969863985,8.49700827529887,8.17024199652503,7.33376985160496,...
6.13704628449341,9.50266327820897,9.78550250303150,7.01766437207250,...
11.4047331538001,11.7206956734403,8.00045937956803,11.9736500242392,...
11.0885239662041,7.56314868037104,11.1922241298349,11.0259439419938,...
7.66912762628635,10.7727872611057,10.3286101875710;NaN,1.992306579,...
3.12564986870711,NaN,4.56287356924308,6.24334058391634,4.663762410,...
10.0146474393953,9.79366586761898,6.77849925523333,14.5650139659535,...
17.4773416412271,7.98806195234647,21.1762055317065,16.7673278416000,...
5.12729752699670,6.27013764642470,11.8508457295060,4.16434082239903,...
13.7839201345612,19.4075735830016,8.65017671003443,19.7397645089430,...
```

```
24.4649375937505,13.5339095257742,22.5262732718485,26.4954725415529,...
15.8268333052547,26.0441954326650,31.2763386643512,NaN,4.36878153,...
4.21541228336407,5.94396778473715,13.2107401051534,11.8714230958566,...
9.04123453437933,21.0547362777496,21.6525149231269,15.2195523891610,...
27.0142846992323,27.9314712575537,18.1198344892307,29.1558956502870,...
30.4041976570651,NaN,9.13853682504850,9.21049049511410,9.931687209,...
9.35892031383022,24.6477413887603,6.32104076480997,10.7196870507386,...
24.9502776251507,7.21283511870570,12.8892628831756,23.4370374927010,...
5.63471494510304,11.8694345846452,21.3931392846696,5.50392364248789,...
8.89950959869852,9.26494519392266,8.79692493933059,20.7914871340555,...
28.2451014629457,12.5798591861489,25.3839829074859,28.8782090838441,...
12.1190294688048,30.5370084583410,30.3032975144452,14.5728646540790,...
26.4438253992370,28.6735007081131,8.17679903873553,21.3360159119564,...
24.0422595320519,12.5433111034193,27.8622933898109,27.7309652892540,...
14.0191563584667,26.4521449865840,30.5525190222002,16.5213075362429,...
27.9852868578455,26.8677479172599,15.7516768705225,25.8010435338905,...
25.9005595136384,7.90739059448242,10.2783975206973,22.2814184365603,...
7.88894415222458,19.1378505056616,27.1538689315868,10.4945260452645,...
25.5313910025870,31.6402317554125,17.6864107989161,31.1843685478421,...
29.3159238749234,15.8393064951222,30.2249153950418,30.9017428785820,...
10.1243897802051,15.0381855704763,13.2383971961367,7.14552579895244,...
23.0333425881919,22.0450601826721,9.54116668608913,26.1696748978596,...
29.1943649511917,8.28243626865959,26.3924824947525,30.6598843025567,...
8.51416793097289,27.6436966447966,31.8328842832998,12.1276249949720,...
24.5069801993265,24.1048624087394,20.9136161496549,27.2525124364641,...
30.0487874021388,27.6908394570720,30.1306422441599,32.1958296047732,...
28.7511036822980,33.0759195201515,33.9027434389074,30.2222815420287,...
34.2451594839388,31.4144066656965,NaN,5.16494628755027,12.72488967,...
7.16785416443599,10.2903518950370,20.2973116886694,5.16772865921666,...
11.9602783832726,20.3062770651741,4.30974603204959,13.4921870609945,...
23.9306115677859,6.15436647422030,13.0341995477815,21.7131731525504,...
4.37262610830658,7.04063518242037,5.27567294739129,9.54272552462498,...
12.8227111417800,11.3005555704149,12.6958819402551,14.3452649144120,...
9.38855666845484,11.8206124749453,13.4770500433381,9.85906876849185,...
14.3820129096639,13.6409120246893,9.57786164690333,6.73273098072968,...
15.8912976425759,16.0998269750832,8.79183940364433,19.4710560858117,...
22.2106622719106,11.6330984383239,22.1613686984970,21.3002710032535,...
10.6961144676158,22.6776142621280,21.3149445309162,11.1833536493577,...
23.1584632664245,20.9869029796599;NaN,102.809600000000,96.66560000,...
NaN,101.785600000000,104.224581818182,106.291200000000,98.79236923,...
100.793107692308,105.369600000000,99.6644571428571,98.3186285714286,...
108.441600000000,95.8171428571429,98.0553142857143,90.5216000000000,...
101.393066666667,100.308114285714,100.684800000000,101.361371428571,...
101.361371428571,100.676266666667,97.9675428571429,98.4795428571429,...
98.6989714285714,94.9540571428571,96.2706285714286,99.2548571428572,...
96.7680000000000,95.7001142857143,NaN,160.512000000000,154.18514285,...
98.9411555555556,148.904228571429,158.866285714286,100.469028571429,...
148.406857142857,164.439771428571,101.419885714286,133.295542857143,...
119.954285714286,96.0365714285714,131.218285714286,156.203885714286,...
NaN,106.905600000000,110.913828571429,102.400000000000,105.318400,...
99.0793142857143,102.468266666667,99.3280000000000,96.6656000000000,...
97.9968000000000,101.405257142857,98.4941714285714,100.078933333333,...
98.1723428571429,95.8610285714286,107.724800000000,105.501257142857,...
```

```
106.274133333333,101.478400000000,102.765714285714,101.288228571429,...
105.252571428571,98.8745142857143,99.6937142857143,100.688457142857,...
98.2601142857143,94.2957714285714,99.6790857142857,99.3718857142857,...
93.5350857142857,107.929600000000,198.073107692308,266.459428571429,...
103.680000000000,156.789028571429,194.369828571429,100.454400000000,...
140.858514285714,133.163885714286,102.078171428571,138.898285714286,...
144.281600000000,96.7533714285714,136.309028571429,154.521600000000,...
80.4864000000000,101.085866666667,95.6123428571428,101.867520000000,...
96.7972571428571,95.7732571428572,96.0307200000000,95.8610285714286,...
98.3917714285714,101.673890909091,96.3291428571428,94.0324571428571,...
99.2334769230769,95.0857142857143,97.9529142857143,105.062400000000,...
97.5965090909091,98.6348307692308,110.510080000000,96.7826285714286,...
99.3572571428571,110.080000000000,99.6498285714286,96.3437714285714,...
108.157155555556,97.4555428571429,95.3782857142857,107.337955555556,...
97.0313142857143,98.2747428571428,98.3970909090909,131.686400000000,...
132.206276923077,96.1457230769231,123.801600000000,132.783542857143,...
100.117942857143,120.597942857143,121.548800000000,98.5380571428572,...
122.221714285714,136.294400000000,96.7387428571429,114.863542857143,...
115.068342857143,NaN,103.792640000000,103.306971428571,161.79200000,...
143.462400000000,128.424228571429,200.396800000000,147.408738461538,...
131.291428571429,180.428800000000,147.219692307692,140.112457142857,...
267.673600000000,152.891076923077,135.021714285714,90.5216000000000,...
102.912000000000,108.270933333333,162.017280000000,140.960914285714,...
136.992581818182,186.014254545455,158.152861538462,156.078080000000,...
229.711127272727,147.566276923077,157.440000000000,209.285120000000,...
152.481476923077,138.928872727273,103.628800000000,102.006153846154,...
97.0898285714286,136.318030769231,126.127542857143,111.659885714286,...
148.590276923077,120.861257142857,113.854171428571,151.705600000000,...
121.168457142857,114.527085714286,157.661866666667,124.138057142857,...
113.532342857143;NaN,33.5872000000000,44.1344000000000,NaN,45.8193,...
49.4796800000000,36.2496000000000,62.3222153846154,62.9666909090909,...
27.3408000000000,64.4388571428571,68.0082285714286,44.6976000000000,...
72.6454857142857,75.3493333333333,40.8576000000000,52.1386666666667,...
62.5427692307692,44.2624000000000,64.5705142857143,66.8525714285714,...
61.2181333333333,70.1203692307692,71.0802285714286,58.9036307692308,...
73.8011428571429,72.4046769230769,70.4658285714286,75.3078857142857,...
77.3412571428572,NaN,150.835200000000,209.042285714286,41.2103111,...
167.599542857143,260.637257142857,59.8601142857143,207.345371428571,...
328.089600000000,59.0454153846154,228.761600000000,343.493485714286,...
68.1106285714286,246.842514285714,353.185476923077,NaN,24.8832000,...
61.8788571428571,66.6624000000000,50.4320000000000,70.4950857142857,...
61.4400000000000,64.0877714285714,75.8930285714286,63.1808000000000,...
62.9523692307692,78.1750857142857,63.6928000000000,70.0269714285714,...
75.0592000000000,32.6314666666667,63.3124571428572,61.9349333333333,...
56.2082909090909,70.7145142857143,74.4211692307692,66.3552000000000,...
76.0246857142857,76.7707428571429,70.3195428571429,80.6754461538462,...
85.2553142857143,62.6688000000000,78.3018666666667,84.7872000000000,...
45.3973333333333,139.295507692308,245.920914285714,63.2490666666667,...
202.688984615385,300.163657142857,68.9737142857143,217.936457142857,...
287.963428571429,72.2212571428571,210.139428571429,300.544000000000,...
62.5112615384615,222.286769230769,277.577142857143,100.556800000000,...
56.1834666666667,64.6852923076923,75.0387200000000,59.6598153846154,...
77.6664615384615,49.9916800000000,62.6102857142857,74.5764571428572,...
```

```
77.8240000000000,73.7133714285714,75.2403692307692,54.7761230769231,...
74.6203428571429,75.0592000000000,70.2464000000000,53.6576000000000,...
66.7648000000000,56.0332800000000,62.5078857142857,61.4400000000000,...
66.5941333333333,68.4909714285714,73.9643076923077,49.6981333333333,...
73.4208000000000,78.1458285714286,53.1797333333333,67.8400000000000,...
77.9410285714286,51.3024000000000,201.489066666667,289.776246153846,...
62.3537230769231,204.741485714286,328.996571428571,66.8525714285714,...
202.766628571429,300.119771428571,70.1833846153846,218.521600000000,...
332.012307692308,69.8221714285714,205.604571428571,333.677714285714,...
NaN,51.2000000000000,59.8016000000000,144.588800000000,100.6762666,...
131.145142857143,153.600000000000,155.584984615385,191.566769230769,...
107.929600000000,191.992123076923,239.235657142857,359.116800000000,...
188.794092307692,270.321371428571,38.6048000000000,57.4464000000000,...
69.0176000000000,81.2032000000000,108.295314285714,103.684654545455,...
143.136581818182,168.203815384615,127.139840000000,180.577745454545,...
211.747446153846,173.038933333333,231.731200000000,192.653784615385,...
238.945745454545,90.7264000000000,62.2119384615385,77.8240000000000,...
90.1750153846154,127.458742857143,134.509714285714,150.827323076923,...
179.097600000000,198.524342857143,182.234763636364,220.160000000000,...
238.431085714286,201.352533333333,260.988342857143,281.921828571429;...
NaN,0,0,NaN,35.9889454545455,43.6019200000000,0,51.5938461538462,...
60.8442181818182,16.2816000000000,87.1424000000000,93.4180571428571,...
23.8592000000000,109.070628571429,138.274133333333,0,36.5568000000000,...
67.3634461538462,0,61.4692571428571,80.7497142857143,46.8480000000000,...
116.956553846154,113.356800000000,46.2690461538462,113.459200000000,...
121.950523076923,98.6258285714286,101.844114285714,134.758400000000,...
NaN,94.3616000000000,190.581028571429,52.4743111111111,197.617371428571,...
238.299428571429,58.4557714285714,272.106057142857,275.031771428571,...
67.1744000000000,252.328228571429,273.963885714286,111.455085714286,...
242.146742857143,297.369600000000,NaN,33.5872000000000,58.9824000000000,...
75.4688000000000,52.4629333333333,86.2939428571429,56.9344000000000,...
50.9805714285714,93.8276571428571,0,82.4556307692308,123.904000000000,...
16.7594666666667,56.7588571428571,94.5298285714286,0,37.5661714285714,...
25.4293333333333,51.4420363636364,111.381942857143,83.5111384615385,...
70.0854857142857,114.600228571429,114.848914285714,68.0228571428571,...
103.187692307692,122.645942857143,90.5058461538462,143.155200000000,...
171.764184615385,0,155.506215384615,236.397714285714,69.4954666666667,...
278.827323076923,348.657371428571,92.4233142857143,288.256000000000,...
350.281142857143,80.8667428571429,304.303542857143,339.017142857143,...
85.5433846153846,319.251692307692,389.105371428571,129.843200000000,...
66.4746666666667,89.4976000000000,63.4880000000000,92.8531692307692,...
141.233230769231,43.9500800000000,84.9334857142857,149.357714285714,...
47.4391272727273,122.806857142857,157.995323076923,53.2795076923077,...
131.130514285714,160.358400000000,99.5328000000000,59.6712727272727,...
64.5632000000000,57.9993600000000,94.9540571428571,96.0950857142857,...
78.0629333333333,111.162514285714,132.600123076923,40.0497777777778,...
126.902857142857,126.946742857143,59.6423111111111,119.876266666667,...
158.281142857143,45.5065600000000,302.882133333333,339.999507692308,...
90.7579076923077,278.966857142857,328.265142857143,113.269028571429,...
321.799314285714,349.447314285714,125.243076923077,289.557942857143,...
363.330953846154,115.463314285714,297.047771428571,341.708800000000,...
NaN,41.0828800000000,80.9252571428572,169.984000000000,80.1621333333333,...
195.627885714286,139.161600000000,195.993600000000,197.679261538462,...
```

```
    181.452800000000,204.768492307692,249.812114285714,109.260800000000,...
    239.300923076923,290.962285714286,37.4784000000000,51.8656000000000,...
    0,65.9251200000000,110.533485714286,124.146036363636,133.995054545455,...
    178.191753846154,136.908800000000,179.330327272727,246.232615384615,...
    195.635200000000,244.224000000000,239.663261538462,222.561745454545,...
    0,51.2000000000000,61.9283692307692,69.6320000000000,192.541257142857,...
    193.536000000000,152.276676923077,220.350171428571,272.661942857143,...
    183.389090909091,281.790171428571,270.613942857143,249.992533333333,...
    339.090285714286,276.567771428571];
```

Published with MATLAB® R2015a

APPENDIX B – ANN MATLAB TUTORIAL

```
%~~~~~~~~~~~~~~~~~~~~~~~~~~~~~~~~~~~~~~~~~~~~~~~~~~~~~~~~~~~~~~~~~~~~~~~~~~~~%
%~~~~~~~~~~~~~~~~~~~~~~~~~1)DATA ORGANIZATION~~~~~~~~~~~~~~~~~~~~~~~~~~~~~~~%
%~~~~~~~~~~~~~~~~~~~~~~~~~~~~~~~~~~~~~~~~~~~~~~~~~~~~~~~~~~~~~~~~~~~~~~~~~~~~%

%load the workspace "inputsOutputsANN.mat"
%contains two variables: 1)input, 2)output

%Inputs: each row contains one parameter of the stimulation signal (A,F,P,or T)
%        each column contains one complete stimulus (A,F,P,T combination)
%        parameters: A=amplitude,F=frequency,P=pulse duration, T=train duration
%        input organization: A(1,:), F(2,:), P(3,:), T(4,:)


%Outputs: each row contains one metric of the response signal
%         parameters: 1)onset latency, 2)mean, 3)peak, 4)peak time,
%                     5)main response duration, 6)residual activation duration
%         output organization: onset latency(1,:), mean(2,:),  peak(3,:), peak time(4,:),
%                              main response duration(5,:), residual activation duration(6,:)

%Use: this ANN takes 4 input parameters (A,F,P,T) and one output metric(ex. mean)
%     look for "USER ACTION REQUIRED" (section 2 & 3)and make changes based on your goals

%Nomenclature: input=stimulus parameters, input to ANN
%              output=response metrics, target for ANN
%              y=ANN output from simulating trained network(scaled (-1,1))
%              yF=ANN output (y) converted back to units of original data
%              PS=process settings scale units between (-1,1)
%              TS=process settings to convert ANN results to units of original data

%~~~~~~~~~~~~~~~~~~~~~~~~~~~~~~~~~~~~~~~~~~~~~~~~~~~~~~~~~~~~~~~~~~~~~~~~~~~~%
%~~~~~~~~~~~~~~~~~~~~~~~~~~2)PREPROCESS DATA~~~~~~~~~~~~~~~~~~~~~~~~~~~~~~~~~%
%~~~~~~~~~~~~~~~~~~~~~~~~~~~~~~~~~~~~~~~~~~~~~~~~~~~~~~~~~~~~~~~~~~~~~~~~~~~~%

%data must be preprocessed to suit the functions used within the ANN
%function used in ANN hidden layer (tansig) requires inputs between (-1,1)
%mapminmax function converts data into distribution between (-1,1)


%preprocess ANN inputs
[PNin,PSin]=mapminmax(input,-1,1);

%USER ACTION REQUIRED: uncomment whichever output you are interested in
%choose one row of "output" to address one metric at a time in the ANN

%preprocess ANN output targets
[TNout1,TSout1]=mapminmax(output(1,:),-1,1);   %onset latency
%[TNout2,TSout2]=mapminmax(output(2,:),-1,1);   %mean
%[TNout3,TSout3]=mapminmax(output(3,:),-1,1);   %peak
%[TNout4,TSout4]=mapminmax(output(4,:),-1,1);   %peak time
%[TNout5,TSout5]=mapminmax(output(5,:),-1,1);   %main response duration
```

```
%[TNout6,TSout6]=mapminmax(output(6,:),-1,1);   %residual activation duration

%~~~~~~~~~~~~~~~~~~~~~~~~~~~~~~~~~~~~~~~~~~~~~~~~~~~~~~~~~~~~~~~~~~~~~~~~~~~~%
%~~~~~~~~~~~~~~~~~~~~~~~~~3)TRAIN, VALIDATE ANN~~~~~~~~~~~~~~~~~~~~~~~~~~~~~%
%~~~~~~~~~~~~~~~~~~~~~~~~~~~~~~~~~~~~~~~~~~~~~~~~~~~~~~~~~~~~~~~~~~~~~~~~~~~~%

%1)Define preprocessed input and output(target) variables for ANN
x=PNin;
PS=PSin;
%USER ACTION REQUIRED: change number to match output choice in section 2
t=TNout1;
TS=TSout1;

%2) Choose training function
trainFcn='trainlm';  % Levenberg-Marquardt backpropagation.

%3) Create a Fitting Network
hiddenLayerSize=20;
net=fitnet(hiddenLayerSize,trainFcn);

%4)Setup Division of Data for Training, Validation, Testing
net.divideParam.trainRatio=70/100;
net.divideParam.valRatio=15/100;
net.divideParam.testRatio=15/100;

%5)Train the Network
[net,tr]=train(net,x,t);

%6)Test the Network
y=net(x); %simulates the network
e=gsubtract(t,y);
performance=perform(net,t,y)

%7)Visualize Performance
view(net)
figure, plotperform(tr)
figure, ploterrhist(e)
figure, plotregression(t,y) %use button on nftool to get all plots

%8)Convert ANN output "y" to original data scale (undo -1,1 scaling)
yF=mapminmax('reverse',y,TS);

%~~~~~~~~~~~~~~~~~~~~~~~~~~~~~~~~~~~~~~~~~~~~~~~~~~~~~~~~~~~~~~~~~~~~~~~~~~~~%
%~~~~~~~~~~~~~~~~~~~~~~~~4)TEST NEW DATA USING ANN~~~~~~~~~~~~~~~~~~~~~~~~~~~%
%~~~~~~~~~~~~~~~~~~~~~~~~~~~~~~~~~~~~~~~~~~~~~~~~~~~~~~~~~~~~~~~~~~~~~~~~~~~~%
%Use the ANN established in section 3 to test new data inputs (predict outputs)

%1)format a test input by choosing values between the range restrictions
%Range restrictions for this ANN: A:30-65,F:100-500,P:0.18-0.5,T:43-300

test=[45;350;0.3;200]; %sample test data

%2)preprocess test input
```

```
%you **MUST** use the process settings structure "PS" that were developed
%when the original ANN inputs were preprocessed

PNinTest=mapminmax('apply',test,PS);

%3)simulate the network using the test data
z=sim(net,PNinTest);

%4)convert simulation output from -1 to 1 scale into original data units
%you **MUST** use the process settings structure "TS" that were developed
%when the original ANN output(targets) were preprocessed
zF=mapminmax('reverse',z,TS);

%~~~~~~~~~~~~~~~~~~~~~~~~~~~~~~~~~~~~~~~~~~~~~~~~~~~~~~~~~~~~~~~~~~~~~~~~~~~~%
%~~~~~~~~~~~~~~~~~~~~~~~~~~HELP WITH NEURAL NETWORKS~~~~~~~~~~~~~~~~~~~~~~~~~%
%~~~~~~~~~~~~~~~~~~~~~~~~~~~~~~~~~~~~~~~~~~~~~~~~~~~~~~~~~~~~~~~~~~~~~~~~~~~~%
% MATLAB help documentation under Neural Network Toolbox-->Neural Network
% Toolbox Examples-->Function Fitting and Approximation see the "House
% Price Estimation" example

%If you are uncomfortable with MATLAB programming, begin by explore the
%house fitting example in the built-in GUI application nftool
%1)type "nftool" in the command window
%2)use the GUI to "load example data set" choosing "house fitting"
%3)follow default settings and prompts to train, simulate and view the ANN

%Once comfortable with the GUI, choose the option to produce an m file
%based on work done in the GUI. Compare it with this m file to further your
%undertanding of ANN implementation

%~~~~~~~~~~~~~~~~~~~~~~~~~~~~~~~~~~~~~~~~~~~~~~~~~~~~~~~~~~~~~~~~~~~~~~~~~~~~%
%~~~~~~~~~~~~~~~~~~~~USING THE ANN TO TEST YOUR OWN DATA~~~~~~~~~~~~~~~~~~~~%
%~~~~~~~~~~~~~~~~~~~~~~~~~~~~~~~~~~~~~~~~~~~~~~~~~~~~~~~~~~~~~~~~~~~~~~~~~~~~%

%1)look for USER ACTION REQUIRED sections and make changed appropriate to
%your goals

%2)follow instructions of section 4 above

%~~~~~~~~~~~~~~~~~~~~~~~~~~~~~~~~~~~~~~~~~~~~~~~~~~~~~~~~~~~~~~~~~~~~~~~~~~~~%
%~~~~~~~~~~~~~~~~~HOW TO MODIFY FOR YOUR OWN INPUTS AND OUTPUTS~~~~~~~~~~~~~%
%~~~~~~~~~~~~~~~~~~~~~~~~~~~~~~~~~~~~~~~~~~~~~~~~~~~~~~~~~~~~~~~~~~~~~~~~~~~~%

%create variables "input" and "output" following the same organization
%principles demonstrated here:

%1)each row of "input" represents one stimulus parameter,

%2)each row of "output" represents one response metric

%3)trials are organized into columns
%each column of input represents one stimulus, each column of output
%represents one complete set of metrics for the response signal evoked by
```

```
%the stimulus during the trial represented by that column


%If building your own ANN from your own data set, learn how to process your
%data, which is generally done with the function "mapminmax". Understand
%the help documentation for how to implement this function for the
%following processes:
%1)preprocess inputs and outputs(targets) fed to the ANN
%2)convert ANN output "y" from scaled (-1,1) to original data type
%3)use settings obtained by mapmaxmin "PS" to preprocess new test inputs
%4)use settings obtained by mapmaxmin "TS" to convert ANN test results

%to improve performance of ANN
%1)increase number of nodes
%2)change distribution of training, validation and test data
%3)retrain network (available in nftool)
```

Published with MATLAB® R2015a